

1stAsia Oceania Workshop of Pulmonary Functional Imaging
combined with
8thJapanese Society of Pulmonary Functional Imaging

1stAOWPFI & 8thJSPFI

**Advancement of Pulmonary Functional Imaging:
From Basics to Clinical Medicine**

Date

January 29 (Fri) - 31 (Sun), 2016

Venue

**Awaji Yumebutai International Conference Center,
Hyogo, Japan**

1 Yumebutai, Awaji City, Hyogo, 656-2306, Japan
Phone: +81-799-74-1020 Fax: +81-799-74-1021

President

Yoshiharu Ohno, M.D., Ph.D.

Secretariat Chair

Hisanobu Koyama, M.D., Ph.D.

Secretariat

**Department of Radiology,
Kobe University Graduate School of Medicine**

Department of Radiology, Kobe University Graduate School of Medicine
7-5-2 Kusunoki-cho, Chuo-ku, Kobe, 650-0017, Japan
Phone : +81-78-382-6104 Fax : +81-78-382-6129
E-mail : aowpfi@med.kobe-u.ac.jp

Congress Secretariat Office

FUKUDA AD Agency

Hiranomachi Chuo Bldg. 4F, 3-2-13, Hirano-machi,
Chuo-ku, Osaka, 541-0046, Japan

Awaji Island

<http://aowpfi-jspfi2016.umin.jp>

INDEX

Welcome Message	1
Access & Map	2
Floor Guide	4
Information for Participants	6
Instruction for Speakers and Moderators/Discussers	8
Time Table	10
Program	
January 29, 2016 [Fri]	21
January 30, 2016 [Sat]	35
January 31, 2016 [Sun]	49
Abstracts	
Special Lecture	55
Morning Lecture	61
Luncheon Lecture	65
Evening Lecture	75
Core Session (Includes Scientific Presentation)	81
Poster Session	109

Welcome Message from President

Dear Colleagues and Friends,

It is our great pleasure to invite you to a joint meeting, combining the 1st Asia Oceania Workshop of Pulmonary Functional Imaging (1st AOWPFI) and 8th meeting of the Japanese Society of Pulmonary Functional Imaging (8th JSPFI), scheduled for January 29-31, 2016. This joint meeting aims to serve emerging clinical needs for improved imaging diagnostics for various lung diseases by bringing together a multidisciplinary group of researchers and clinicians working at the forefront of image-based approaches to lung function analysis. AOWPFI and JSPFI will offer an attractive scientific program consisting of invited keynote lectures, selected scientific papers and poster presentations on several specific topics.



The inaugural meeting of the JSPFI in Kyoto in 2009 was followed by meetings in Okinawa in 2010, in Awaji in 2011, in Otsu in 2012, in Tokushima in 2013, in Sapporo in 2014 and in Tokyo in 2015. JSPFI has cooperative societies such as the International Workshop of Pulmonary Functional Imaging, which was started in Philadelphia in 2002 and followed up with meetings in Awaji in 2004, in Heidelberg in 2006, in Boston in 2009, in Awaji in 2011, in Madison in 2013 and in Edinburgh in 2015, and the Korean Workshop of Pulmonary Functional Imaging (KWPF), which has been continuously held in Seoul since 2011, and other domestic and international societies. Since we held the 1st joint meeting combining the 3rd JSPFI and 5th IWPF in 2011, this research field has been continuously growing, encouraging younger researchers and clinicians and will continue to attract more and more attention in not only Japan, but also in Asia and Oceania.

This time, we plan to hold the 1st joint meeting combining 1st AOWPFI and 8th JSPFI under cooperation with IWPF and KWPF at the Awaji Yumebutai International Conference Center and Westin Hotel, where the 2nd IWPF and 1st Joint meeting combining 3rd JSPFI and 5th IWPF were held in 2004 and 2011. As you may know, Awaji Island is located just off the coast of Honshu about 20 kilometers west of Kobe, 40 kilometers west of Osaka and 60 kilometers west of Kyoto.

We cordially invite you to join us on this beautiful island where you will experience warm hospitality as well as both modern and traditional Japanese culture while sharing and adding to your knowledge of Pulmonary Functional Imaging. We are expecting a large number of researchers, physicians and students at this exciting meeting. We look forward to seeing you on Awaji Island in January, 2016.

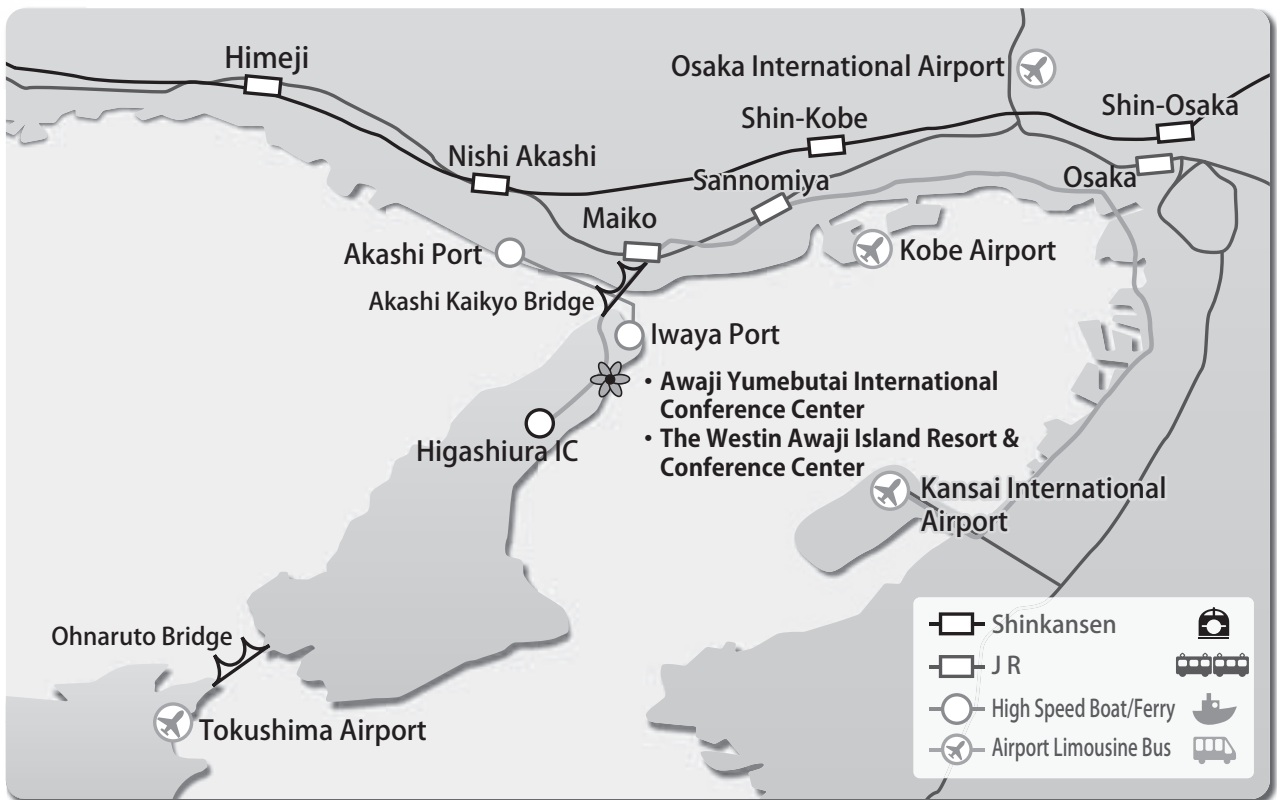
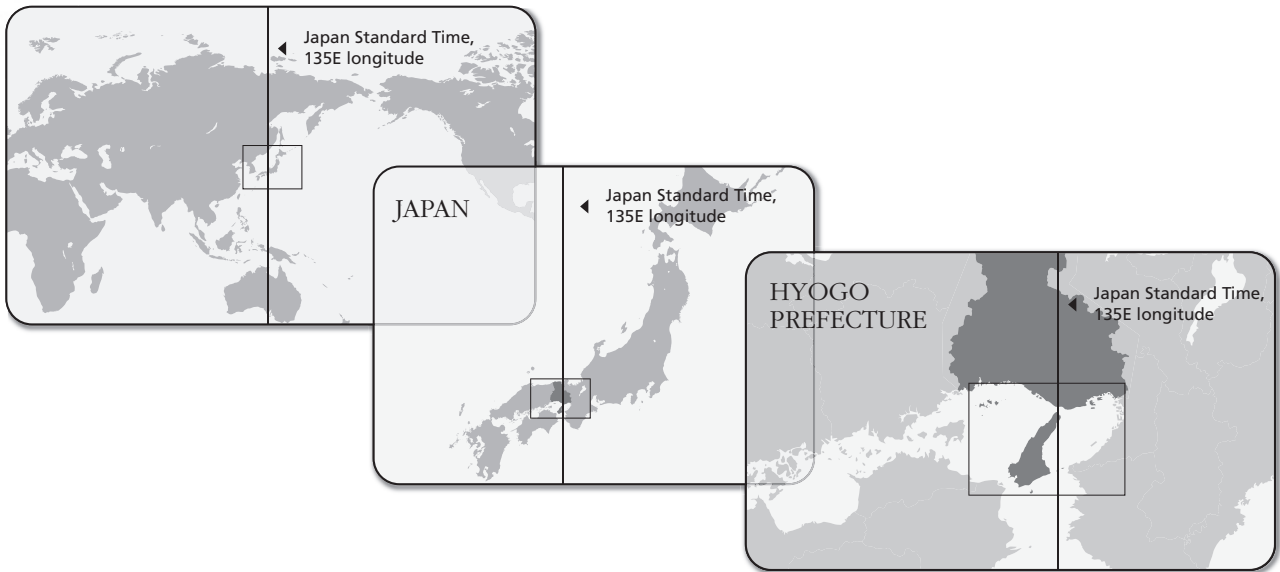
A handwritten signature in black ink, appearing to read 'Yoshiharu Ohno'.

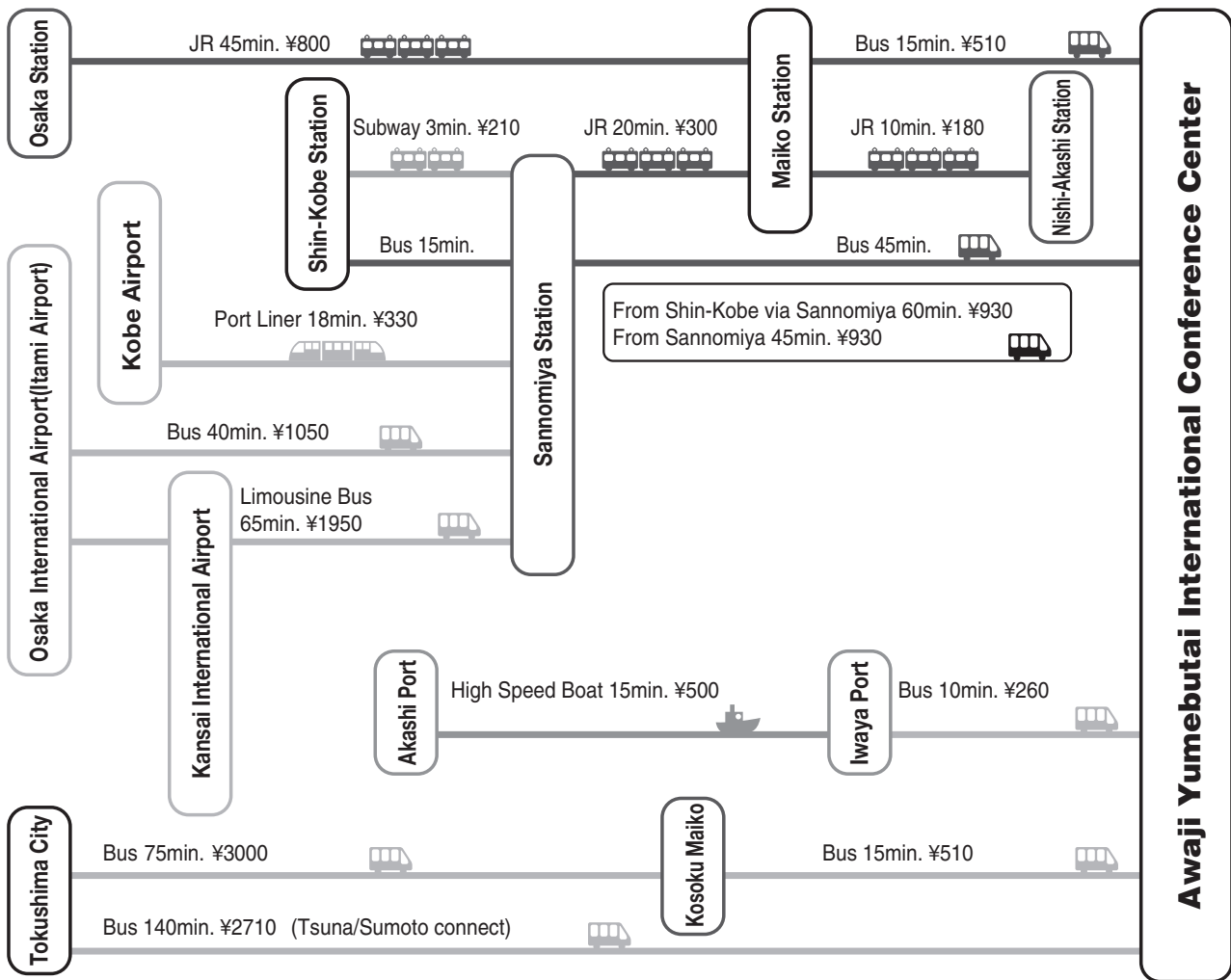
Yoshiharu Ohno, M.D., Ph.D.

President of the Organizing Committee

Joint Meeting combining the 1st Asia Oceania Workshop of Pulmonary Functional Imaging (AOWPFI) and the 8th meeting of the Japanese Society of Pulmonary Functional Imaging (JSPFI)

Access & Map





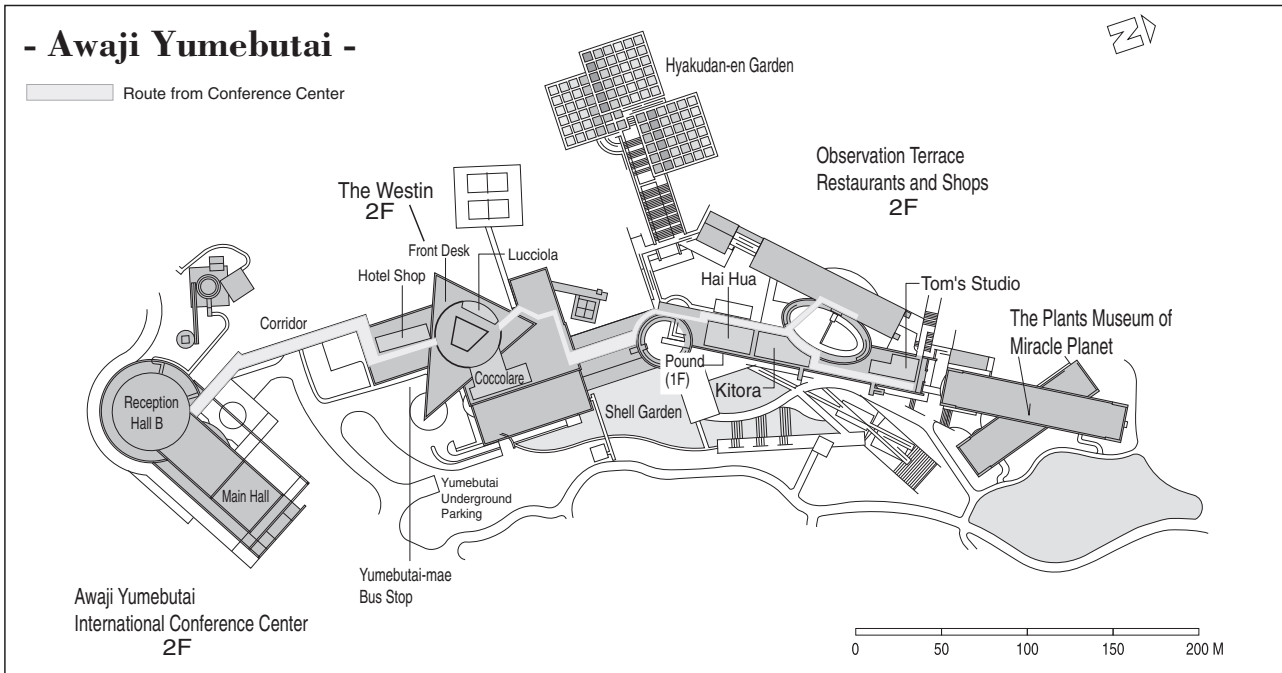
By Car

You can access Awaji Yumebutai in :

- 30 min. from Kobe (Sannomiya) - 30 km
- 60 min. from Osaka (Umeda) - 60 km
- 90 min. from Kansai International Airport (via the Hanshin Highway Wangan Line and Akashi Kaikyo Bridge) - 100 km
- 50 min. from Osaka International Airport (via the Chugoku Expressway, Hanshin Highway Kitakobe Line, and Akashi Kaikyo Bridge) - 75km
- 45 min. from Kobe Airport - 45 km
- 70 min. from Tokushima Airport - 85 km
- 5 min. along Route 28 from Awaji IC exit or Higashiura IC exit on Kobe Awaji Naruto Expressway.

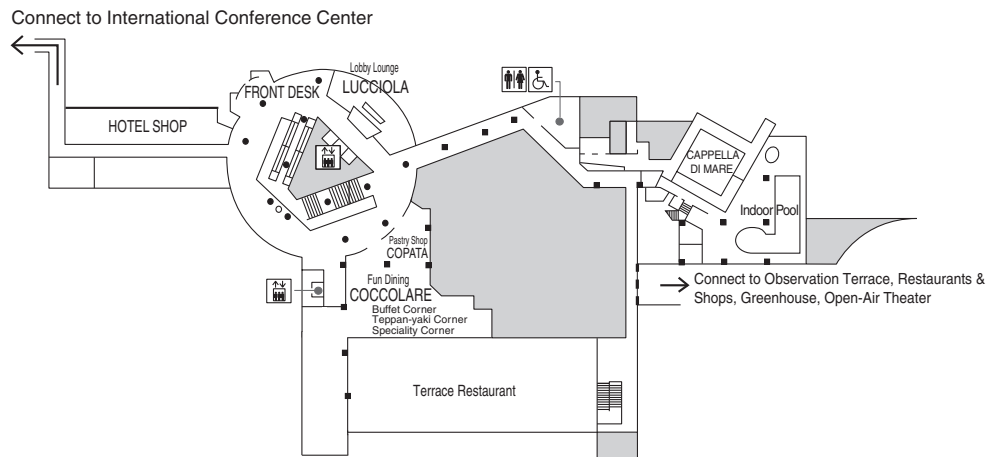
Floor Guide

- Awaji Yumebutai -

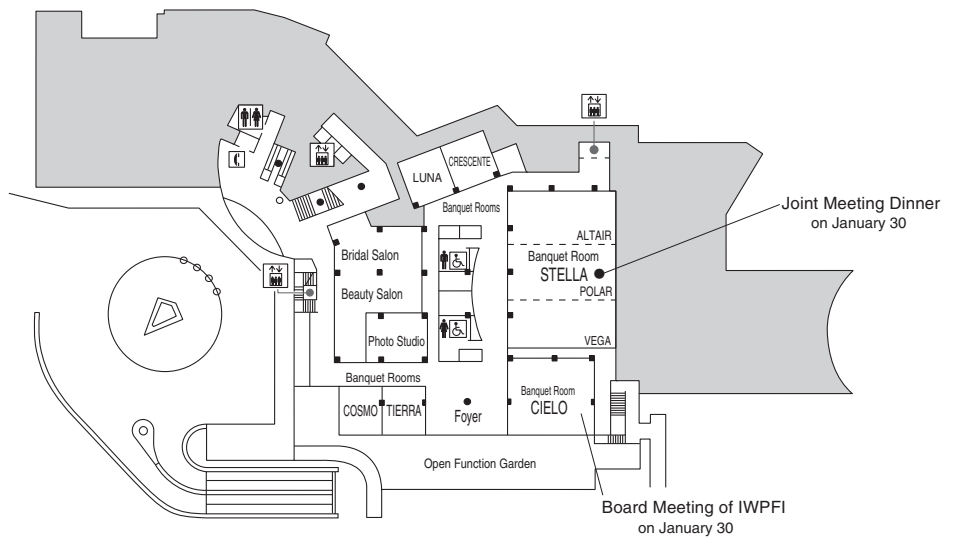


- The Westin Awaji Island -

2F

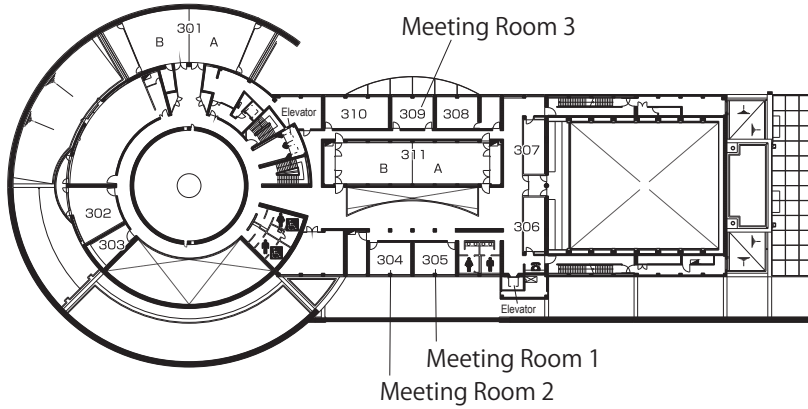


1F

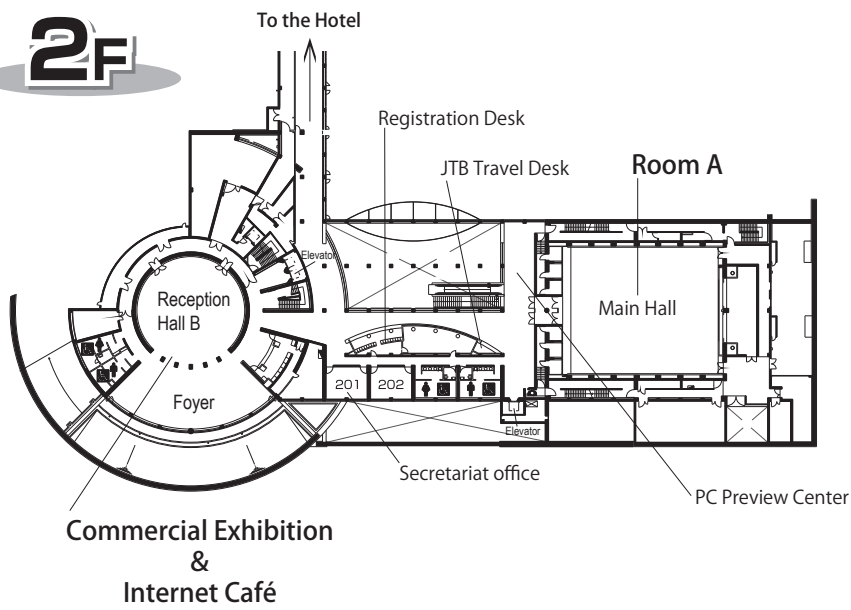


- Awaji Yumebutai International Conference Center -

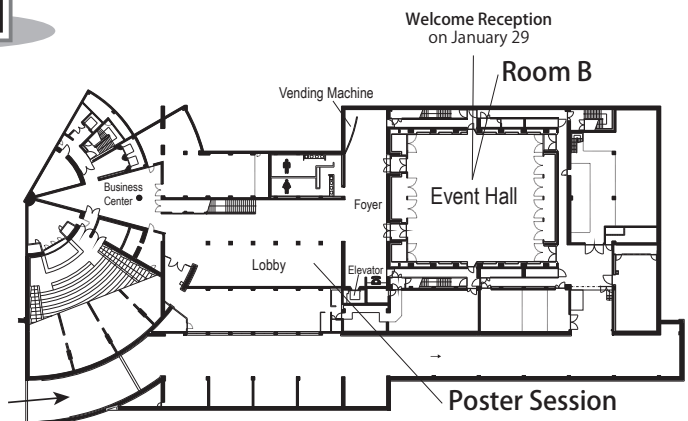
3F



2F



B1



Information for Participants

1. Registration

On-site Registration

Registration Desk

Registration Desk will be opened the following hours at the meeting venue.

---Open Hours---

17:00-18:30 Thursday, January 28, 2016
8:15-18:30 Friday, January 29, 2016
8:15-18:30 Saturday, January 30, 2016
9:30-14:00 Sunday, January 31, 2016

1) Registration fee (Only Japanese Yen)

	Early Registration (Before 17:00 on Oct 30)	Late Registration (17:01, Oct 30 - 17:00, Dec 25)	On-Site Registration
Doctor (JSPFI Member)	JPY15,000	JPY20,000	JPY22,000
Doctor (JSPFI Non-Member)	JPY17,000	JPY22,000	JPY24,000
Non-Doctor (JSPFI Member)	JPY12,000	JPY17,000	JPY19,000
Non-Doctor (JSPFI Non-Member)	JPY14,000	JPY19,000	JPY21,000
Student*	JPY5,000	JPY10,000	JPY12,000

JSPFI: Japanese Society for Pulmonary Functional Imaging

*Student(Includes Graduate student) : Student participants are required to present a valid student ID upon the Registration Desk.

The all type of registration fee includes: 1. Admission to scientific programs
2. Admission to the exhibition
3. Documentation including a book of abstracts.

2) Payment Method (Only Japanese Yen)

Payment must be made in Japanese Yen, by cash or with a credit card at Registration Desk. Please note that neither personal checks nor any other currencies will be accepted.

Credit card: American Express, Visa, MasterCard, Diners Club, and JCB are acceptable.

2. Name Badges

Please wear your name badges at all times during the meeting for identification and security purposes. Only registered participants wearing a name badges will be allowed access to the session rooms, exhibition and social programs.

3. Commercial Exhibition

Commercial Exhibition will be held at the “Reception Hall B” during the meeting. Exhibitors will be eager to demonstrate and explain their latest products, and answer your question.

4. Internet Access Service & Drink Service

Internet access service and drink service are available at the “Reception Hall B Foyer”.

5. Travel Desk

Travel Desk will be opened at the venue operated by JTB.

6. Mobile Phone

During the session, you are prohibited from using a mobile phone. Please turn off or switch to the silent mode.

7. Message Board

To prevent from interrupting the sessions, we do not call up anyone in the meeting venue. Please use message board. Leave your message for your friends and colleagues and look for messages left for you.

8. Cloakroom

The Cloakroom is on 2F near by Front Desk of The Westin.

9. Be warned against pickpockets or stolen

Please keep valuables in your possession at all times. The meeting cannot responsible for lost or stolen items.

10. Social Events

The organizing committee takes pleasure in presenting the following social events that offer all participants and accompanying persons.

Welcome Reception

18:40-20:30, Friday, January 29, 2016 at Event Hall (B1F) Room B

※Entrance fee JPY5,000

Joint Meeting Dinner at The Westin

19:10-21:00, Saturday, January 30, 2016 at The Westin Awaji Island (1F) “STELLA”

※Entrance fee JPY5,000

※The Best Poster Award will be announced.

Instruction for Speakers and Moderators / Discussers

Instruction for Speakers

Presentation Time (except Invited Speakers)

Session	Presentation(min.)	Discussion(min.)	Method
Core Session Scientific Presentation	7	3	PC
Poster Session	3	5	-

For Invited Speakers: Please follow the instruction for presentation and discussion time from secretariat and moderators.

Oral Presentation Information

(Special Lecture, Morning Lecture, Luncheon Lecture, Evening Lecture, Core Session)

Equipment: Computers

OS	Software for Presentation
Windows	PowerPoint ver. 2003 - 2013

All meeting rooms are equipped with the following audio - visual equipment:
1 - Video Projector, 1 - Screen, 1 - Windows-based PC, 1 - Laser Pointer

PC Preview Center (2F, Front of "Room A")

---Open Hours---

17:00-18:30	Thursday, January 28, 2016
8:15-18:30	Friday, January 29, 2016
8:15-18:30	Saturday, January 30, 2016
9:30-14:00	Sunday, January 31, 2016

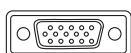
- All Speakers (except Poster Session) are requested to come to the PC Preview Center at least **30 minutes** in advance of their presentations to verify that the data functions properly on the equipment provided.
- ※ If you bring your own laptop PC, after checking-in at the PC Preview Center, please come to the PC operation desk in front of the podium located at the left-front in the session room by **15 minutes prior** to your presentation and hand your PC to the staff. (You can come to the PC operation desk while the previous session is proceeding.)

PowerPoint Presenters

- Bring your presentation in a USB flash Drive or CD-ROM. **In case you use animation, you should to bring your own laptop PC.**
- If you have prepared the presentation data on a **Macintosh**, you are requested to bring your own computer.
- Make sure that you close or "finalize" your presentation file when create a CD. If you omit this step, you cannot access the CD from any other computers.
- Only the standard font (e.g., Times New Roman, Arial, Century) will be available. Unusual fonts may not be displayed properly on the computers in session rooms.
- Please name the file as:
"Date of presentation_presenter's name,ppt(x)"e.g., 0128_TaroAWAJI. pptx
- In order to avoid virus infection, please scan your data with updated anti-virus software beforehand.
- Please note that you cannot make any modification at the PC Preview Center and session room.
- After the meeting, all presentation data will be erased by secretariat.

Laptops

- Speakers using their own laptops must have a **Mini D-sub 15pin female output**. Special video output cable is required for some laptops to use Mini D-sub 15pin to connect to external monitors and data projectors. Please note that we are not equipped with that special cable and you must bring it in case it is necessary.



Mini D-sub 15pin

- Please be sure to bring the power adapter.

Poster Presentation Information

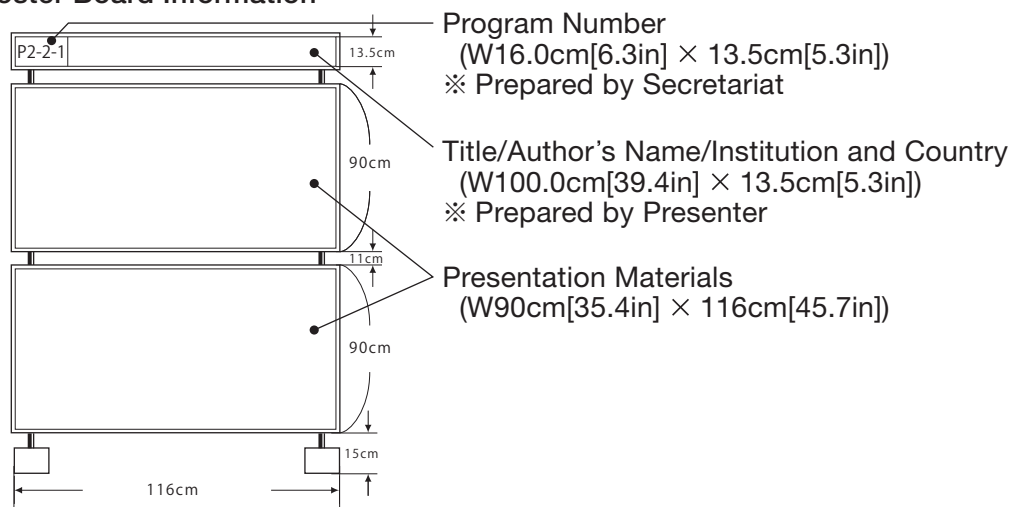
Guidelines for Poster Presenters:

Presenters are requested to follow the schedule below in mounting poster on their assigned board. The poster number for your presentation can be found in the program book. Please follow the instructions provided. The organizers will be forced to remove and discard any posters that remain displayed after this period.

•Schedule

Date	Mounting	Presentation	Removal
Thursday January 28, 2016	17:00-18:30	-	-
Friday January 29, 2016	8:15-11:00	17:40-18:40	-
Saturday January 30, 2016	-	17:40-18:40	-
Sunday January 31, 2016	-	-	9:00-14:00

Poster Board Information



- Your poster number will already be on your assigned board.
- Please prepare a label showing the title, institution(includes country) and the auhtor's name. You cannot use pins or adhesive tape.
- Hook - and - loop fastener for mounting will be available from the Poster Reception Desk at the Poster Session Area.
- Poster should be brought by yourself to the meeting and not mailed, as the organizing committee cannot be responsible for loss or mishandling.
- Presenters are responsible for posting and removing their own materials.
- Audio-visual equipment may not be used. Please refer to the poster image for your poster.

The Best Poster Award

This award will be established committee of the meeting to encourage the high performance of the presentation in the poster session. The winner will be selected during the poster presentation time by the moderators.

For the winner

Acommendation ceremony by the president of the meeting during the Joint Meeting Dinner at The Westin, 19:10-, January 30.

Instructions for Moderators and Discussers

All moderators and discussers are asked to ensure that each sessions start on time and finish punctually as scheduled.

Oral Sessions

- Please come to the "Next moderator"'s seat of the session room (the front row on your right side) no later than **15 minutes** prior to the beginning of the session and identify yourself to the staff.

Poster Sessions

- All moderators for poster session are requested to come to the "Poster Reception Desk" near by Poster Session Area no later than **15 minutes** prior to the beginning of the session.
- Please select the best poster presentation of the session (one person per session), and tell the staff of "Poster Reception Desk".

Time Table

January 28, 2016 [Thu]				
	ROOM A	ROOM B	Poster Exhibition	Commercial Exhibition & Internet Café
	Main Hall (2F)	Event Hall (B1F)	Lobby (B1F)	Reception Hall B (2F)
17:00			17:00-18:30	
18:00			Poster Mounting	
19:00				
January 29, 2016 [Fri]				
	ROOM A	ROOM B	Poster Exhibition	Commercial Exhibition & Internet Café
	Main Hall (2F)	Event Hall (B1F)	Lobby (B1F)	Reception Hall B (2F)
8:00				
8:45-9:00	Opening Remark		8:15-11:00	
9:00-11:00	Core Session 1: Pulmonary Thromboembolism <i>Lecture</i> <i>Oral Presentation</i>		Poster Mounting	9:00-17:40
10:00				9:00-18:30
11:00	11:00-11:20	Break		Commercial Exhibition Internet Café
11:20-12:00	Organizer Meeting of JSPFI			
12:00	12:00-12:20	Break		
12:20-13:20	Luncheon Lecture 1	12:20-13:20 Luncheon Lecture 2		
13:20-13:40	Break			
13:40-16:00	Core Session 2: Thoracic Malignancy: Diagnosis and Treatment Response Assessment <i>Lecture</i> <i>Oral Presentation</i>			
15:00				
16:00	16:00-16:20	Break		
16:20-17:20	Evening Lecture 1			
17:00	17:20-17:40			
18:00			17:40-18:40 Poster Session	
19:00		18:40-20:30 Welcome Reception	P1, P2-1, P2-2 P3-1, P3-2, P4-1 P5, P6-1, P7-1	
20:00				

January 30, 2016 [Sat]					
	ROOM A	ROOM B	Poster Exhibition	Commercial Exhibition & Internet Café	
	Main Hall (2F)	Event Hall (B1F)	Lobby (B1F)	Reception Hall B (2F)	
8:00	8:00-8:30 Board Meeting of IWPFI at The Westin "CIELO", 1F			Commercial Exhibition	
	8:30-8:45 Break				
9:00	8:45-9:45 Morning Lecture				Internet Café
	9:45-10:00 Break				
10:00	10:00-12:10 Core Session 3: COPD, Asthma and Airway Disease Lecture Oral Presentation				
11:00	12:10-12:30 Break				
12:00	12:30-13:30 Luncheon Lecture 3	12:30-13:30 Luncheon Lecture 4			
13:00	13:30-14:00 Break				
14:00	14:00-15:00 Special Lecture 1				
15:00	15:00-15:10 Break				
16:00	15:10-16:15 Core session 4: Basics of Computational Analysis for Pulmonary Imaging Lecture / Oral Presentation				
	16:15-16:25 Break				
17:00	16:25-17:25 Evening Lecture 2				
	17:25-17:40 Break				
18:00			17:40-18:40 Poster Session		
19:00	18:40-19:10 Break			P2-3, P2-4, P3-3 P3-4, P4-2, P6-2 P7-2, P7-3, P7-4	
20:00	19:10-21:00 Joint Meeting Dinner at The Westin "STELLA", 1F				
21:00	January 31, 2016 [Sun]				
	ROOM A	ROOM B	Poster Exhibition	Commercial Exhibition & Internet Café	
	Main Hall (2F)	Event Hall (B1F)	Lobby (B1F)	Reception Hall B (2F)	
8:00				Commercial Exhibition	
9:00			9:00-14:00		Internet Café
10:00	9:30-10:00 General Meeting of JSPFI				
	10:00-10:15 Break				
11:00	10:15-12:15 Core Session 5: Interstitial Lung Disease Lecture Oral Presentation		Poster Removal		
12:00	12:15-12:30 Break				
13:00	12:30-13:30 Luncheon Lecture 5	12:30-13:30 Luncheon Lecture 6			
	13:30-13:50 Break				
14:00	13:50-14:50 Special Lecture 2				
15:00	14:50-15:00 Closing Remark				

Special Lecture

January 30 [Sat] 14:00-15:00

1. From Morphology to Function and Metabolism

Moderator : **Masaharu Nishimura** Hokkaido University
Mayuki Uchiyama The Jikei University School of Medicine
Yeun-Chung Ray Chang National Taiwan University

14:00-14:20 **Lung 3D Micro Analysis using Synchrotron Radiation CT**

Invited Speaker 1 : **Noboru Niki** Tokushima University

14:20-14:40 **From Morphology to Function and Metabolism
Radiology Aspect**

Invited Speaker 2 : **Hiroto Hatabu** Brigham and Women's Hospital, Harvard Medical School

14:40-15:00 **From Physician side**

Invited Speaker 3 : **Toyohiro Hirai** Kyoto University

January 31 [Sun] 13:50-14:50

2. New Techniques for Pulmonary Functional Imaging

Moderator : **Michiaki Mishima** Kyoto University
Kiyoshi Murata Shiga University of Medical Science
Jai Soung Park Soonchunhyang University Hospital

13:50-14:10 **Computer-aided diagnosis and assessment for pulmonary functional imaging**

Invited Speaker 1 : **Eric Hoffman** University of Iowa

14:10-14:30 **New MR Applications for Morpho-Functional Pulmonary Imaging**

Invited Speaker 2 : **Hans-Ulrich Kauczor** Heidelberg University Medical Center

14:30-14:50 **New CT applications for pulmonary functional imaging**

Invited Speaker 3 : **Joon Beom Seo** University of Ulsan College of Medicine, Asan Medical Center

Morning Lecture

January 30 [Sat] 8:45-9:45

Sponsored by Nihon Medi-Physics Co.,Ltd.

1. PET/CT and PET/MRI for the chest and lung disease: review of the current literature and clinical perspective

Moderator : Tsuyoshi Komori Osaka Medical College

8:45-9:45

PET/CT and PET/MRI for the chest and lung disease: review of the current literature and clinical perspective

Invited Speaker : Munenobu Nogami Hyogo Cancer Center

Luncheon Lecture

January 29 [Fri] 12:20-13:20

Sponsored by TOSHIBA MEDICAL SYSTEMS CORPORATION

1. New Techniques for Pulmonary Functional Imaging

Moderator : Koichiro Tatsumi Chiba University

12:20-12:50

New Techniques for Pulmonary Functional Imaging: CT-based functional imaging

Invited Speaker 1 : Edwin J.R. van Beek Edinburgh University

12:50-13:20

MR-Based Functional and Metabolic Imaging at 3T System

Invited Speaker 2 : Yoshiharu Ohno Kobe University

Sponsored by FUJIFILM Medical Co., Ltd.

2. New analysis using SYNAPSE VINCENT[®] for the evaluation of respiratory function

Moderator : Noriyuki Tomiyama Osaka University

12:20-12:50

Regional lung assessment using lobe segmentation methods and nonrigid multimodality image registration techniques by SYNAPSE VINCENT[®]

Invited Speaker 1 : Shigeo Muro Kyoto University

12:50-13:20

Bronchial dimension analysis of asthmatic patients using automatic route matching technique by SYNAPSE VINCENT[®]

Invited Speaker 2 : Tsuyoshi Oguma Kyoto University

January 30 [Sat] 12:30-13:30

Sponsored by Nippon Boehringer Ingelheim Co., Ltd.

3. The latest topics of COPD treatment

Moderator : Masaharu Nishimura Hokkaido University

12:30-13:00

Importance of symptom improvement for COPD treatment

Invited Speaker 1 : Yasutaka Nakano Shiga University of Medical Science

13:00-13:30

Importance of inhalational device for COPD treatment

Invited Speaker 2 : Yuko Komase St. Marianna University School of Medicine, Yokohama-City Seibu Hospital

January 30 [Sat] 12:30-13:30

Sponsored by Philips Electronics Japan, Ltd.

4. Cardiopulmonary Functional Imaging

Moderator : Hiroshi Kimura Nara Medical University School of Medicine

12:30-13:00 **Balloon pulmonary angioplasty for chronic thromboembolic pulmonary hypertension: Assessment of CT angiography, MRI, and perfusion scintigraphy**

Invited Speaker 1 : Michinobu Nagao Kyushu University Hospital

13:00-13:30 **MR Application for Cardiopulmonary Diseases**

Invited Speaker 2 : Ichizo Tsujino Hokkaido University

January 31 [Sun] 12:30-13:30

Sponsored by GE Healthcare Japan Corporation

5.

Moderator : Noriyuki Tomiyama Osaka University

12:30-12:40 **Gemstone Spectral Imaging Technology**

Invited Speaker 1 : Kousuke Sasaki GE Healthcare Japan Corporation

12:40-13:30 **Update of Thoracic Imaging: new iterative reconstruction and gemstone spectral imaging**

Invited Speaker 2 : Masahiro Yanagawa Osaka University

Sponsored by Accuray Japan K.K./CHIYODA TECHNOL CORPORATION

6. CyberKnife: Real Time Image Guided Radiation Therapy for Lung Cancer

Moderator : Ryohei Sasaki Kobe University Hospital

12:30-13:30 **CyberKnife: Real Time Image Guided Radiation Therapy for Lung Cancer**

Invited Speaker : Hideki Nishimura Kobe Minimally Invasive Cancer Center

Evening Lecture

January 29 [Fri] 16:20-17:20

Sponsored by FUJIFILM RI Pharma Co., Ltd.

1. Imaging Biomarker for Pulmonary Diseases

Moderator : **Hiroto Hatabu** Brigham and Women's Hospital, Harvard Medical School

16:20-16:50 **CT-Based Imaging Biomarkers**

Invited Speaker 1 : **David A. Lynch** National Jewish Health

16:50-17:20 **MR Based Imaging Biomarkers**

Invited Speaker 2 : **David L. Levin** Mayo Clinic, University of California

January 30 [Sat] 16:25-17:25

Sponsored by Bayer Yakuhin, Ltd.

2. Pulmonary Hypertension: Clinical and Functional Assessments

Moderator : **Minoru Kanazawa** Saitama Medical University

16:25-16:55 **CT assessment of pulmonary hypertension**

Invited Speaker 1 : **Sang Min Lee** Asan Medical Center

16:55-17:25 **Pulmonary Hypertension: Clinical presentation and Functional Assessment Using Imaging**

Invited Speaker 2 : **Mark L. Schiebler** University of Wisconsin

Core Session

January 29 [Fri] 9:00-11:00

1. Pulmonary Thromboembolism

Moderator : **Koichiro Tatsumi** Chiba University
Sadayuki Murayama University of the Ryukyus
Discussor : **Ki Yeol Lee** Korea University Medical Center Ansan Hospital

- 9:00-9:15 **Distal lesions of chronic thromboembolic pulmonary hypertension and balloon pulmonary angioplasty**
Invited Speaker 1 : **Takeshi Ogo** National Cerebral and Cardiovascular Center
- 9:15-9:35 **Update for Treatment for Pulmonary Thromboembolic Disease**
Invited Speaker 2 : **Nobuhiro Tanabe** Chiba University
- 9:35-9:50 **Assessment of pulmonary thromboembolic disease in nuclear medicine**
Invited Speaker 3 : **Norinari Honda** Saitama Medical University
- 9:50-10:05 **CT Assessment for Pulmonary Thromboembolism**
Invited Speaker 4 : **Jin Hur** Severance Hospital, Yonsei University College of Medicine
- 10:05-10:20 **MR Assessment for Pulmonary Thromboembolic Disease**
Invited Speaker 5 : **David L. Levin** Mayo Clinic, University of California
- 10:20-10:30 **Assessment of Cross-Sectional Lung Ventilation-Perfusion Imbalance in Primary and Passive Pulmonary Hypertension with Automated V/Q Quotient SPECT**
Scientific Presentation 1 : **Kazuyoshi Suga** St. Hill Hospital
- 10:30-10:40 **Utility of computed tomography-derived measurements of the pulmonary vasculature in the diagnosis and hemodynamic assessment of pulmonary arterial hypertension**
Scientific Presentation 2 : **Kaoruko Shimizu** Hokkaido University
- 10:40-10:50 **Diagnostic Performance of the Combined Pulmonary Arterial MRI and Indirect Magnetic Resonance Venography Using Unenhanced and Contrast-Enhanced Techniques in the Diagnosis of Venous Thromboembolism**
Scientific Presentation 3 : **Nevzat Karabulut** Pamukkale University Medical Center
- 10:50-11:00 **Further Discussion time in this session**

January 29 [Fri] 13:40-16:00

2. Thoracic Malignancy: Diagnosis and Treatment Response Assessment

Moderator : **Nevzat Karabulut** Pamukkale University Medical Center

Noriyuki Tomiyama Osaka University

Discussor : **Yung-Liang Wan** Chang Gung Memorial Hospital

13:40-13:55 **An Update on the Management of Lung Nodules**

Invited Speaker 1 : **Jin Mo Goo** Seoul National University Hospital

13:55-14:10 **Update of Medical Therapy for Advanced Lung Cancer**

Invited Speaker 2 : **Koichi Takayama** Kyoto Prefectural University of Medicine

14:10-14:25 **Lung cancer treatment assessment in the era of precision medicine: RECIST and beyond**

Invited Speaker 3 : **Mizuki Nishino** Harvard Medical School

14:25-14:35 **PET Imaging for Prognosis and Treatment Response Assessment in Lung Cancer**

Invited Speaker 4 : **Tae Jung Kim** Samsung Medical Center

14:35-14:50 **CAD for Prognosis and Treatment Response Assessment in Lung Cancer**

Invited Speaker 5 : **Masahiro Yanagawa** Osaka University

14:50-15:05 **New MR Techniques for Prognosis and Treatment Response Assessment**

Invited Speaker 6 : **Hidetake Yabuuchi** Kyushu University

15:05-15:20 **Radiomics and Radiogenomics in Lung Cancer: Clinical Perspectives**

Invited Speaker 7 : **Ho Yun Lee** Samsung Medical Center, Sungkyunkwan University School of Medicine

15:20-15:30 **Prediction of therapeutic effect of chemotherapy for non-small-cell lung cancer using perfusion CT: comparison between regimens with and without anti-angiogenic agent**

Scientific Presentation 1 : **Hidetake Yabuuchi** Kyushu University

15:30-15:40 **MR evaluation of the treatment response of HCC827 to erlotinib alone or combination with bevacizumab in mice model**

Scientific Presentation 2 : **Yi-Fang Chen** National Taiwan University

15:40-15:50 **Dynamic Contrast-Enhanced Integrated PET/MR of Non-Small Cell Lung Cancer: Assessment of Response to Stereotactic Body Radiation Therapy**

Scientific Presentation 3 : **Yu-Sen Huang** National Taiwan University Hospital

15:50-16:00 **Further Discussion time in this session**

January 30 [Sat] 10:00-12:10

3. COPD, Asthma and Airway Disease

Moderator : **Shu Hashimoto** Nihon University

Yasuo Nakajima St. Marianna University School of Medicine

Discusser : **Sang Do Lee** University of Ulsan College of Medicine, Asan Medical Center

10:00-10:15 **COPD Phenotype and Treatment**

Invited Speaker 1 : **Shigeo Muro** Kyoto University

10:15-10:30 **VENTILATION/PERFUSION TOGRAPHY (V/P SPECT) – THE FUNCTIONAL IMAGING FOR COPD PHENOTYPING**

Invited Speaker 2 : **Marika Bajc** Skåne University Hospital

10:30-10:45 **Quantitative CT for COPD phenotyping**

Invited Speaker 3 : **Yasutaka Nakano** Shiga University of Medical Science

10:45-11:00 **New Quantitative CT Techniques for COPD Phenotyping**

Invited Speaker 4 : **Joon Beom Seo** University of Ulsan College of Medicine, Asan Medical Center

11:00-11:15 **Magnetic Resonance Imaging for Chronic obstructive lung disease phenotyping**

Invited Speaker 5 : **Tae Iwasawa** Kanagawa Cardiovascular and Respiratory Center

11:15-11:30 **Phenotyping lung disease using optical coherence tomography (OCT)**

Invited Speaker 6 : **Harvey O Coxson** University of British Columbia, St Paul's Hospital

11:30-11:40 **Transfer Factor and Blood Gases in the V/P SPECT Emphysema Phenotype of COPD**

Scientific Presentation 1 : **Marika Bajc** Skåne University Hospital

11:40-11:50 **Continuous quantitative measurements of proximal airway dimensions and lung density on dynamic-ventilation CT in smokers: a novel imaging approach using a 320-row detector CT scanner**

Scientific Presentation 2 : **Tsuneo Yamashiro** University of the Ryukyus

11:50-12:00 **Morpho-functional 1H-MRI of the lung in COPD: Short-term test-retest reliability**

Scientific Presentation 3 : **Mark O Wielpuetz** University of Heidelberg

12:00-12:10 **Further Discussion time in this session**

January 30 [Sat] 15:10-16:15

4. Basics of Computational Analysis for Pulmonary Imaging

Moderator : **Toyohiro Hirai** Kyoto University

Kenya Murase Osaka University

Discusser : **Jong Hyo Kim** Seoul National University

15:10-15:25 **Basics of Computational Analysis for Pulmonary Imaging**

Invited Speaker 1 : **Namkug Kim** University of Ulsan College of Medicine, Asan Medical Center

- 15:25-15:40 **Basics of Computational Assessment for Diffuse Lung Diseases (DLDs)**
Invited Speaker 2 : **Shoji Kido** Yamaguchi University
- 15:40-15:55 **Lung CAD**
Invited Speaker 3 : **Noboru Niki** Tokushima University
- 15:55-16:05 **Computer aided detection system for lung cancer, COPD, and osteoporosis in low-dose CT screening**
Scientific Presentation 1 : **Hidenobu Suzuki** Tokushima University
- 16:05-16:15 **Further Discussion time in this session**

January 31 [Sun] 10:15-12:15

5. Interstitial Lung Disease

- Moderator : **Arata Azuma** Nippon Medical School
Takeshi Johkoh Kinki Central Hospital of Mutual Aid Association of Public School Teachers
Discusser : **Jae-Woo Song** University of Ulsan College of Medicine, Asan Medical Center

- 10:15-10:35 **Update for Diagnosis of Interstitial Lung disease**
Invited Speaker 1 : **Gong Yong Jin** Chonbuk National University Medical School and Hospital
- 10:35-10:50 **Recent advances in the treatment of idiopathic pulmonary fibrosis**
Invited Speaker 2 : **Noboru Hattori** Hiroshima University
- 10:50-11:05 **Quantitative CT Assessment for ILD**
Invited Speaker 3 : **David A. Lynch** National Jewish Health
- 11:05-11:20 **Quantitative MRI Assessment for ILD**
Invited Speaker 4 : **Yoshiharu Ohno** Kobe University
- 11:20-11:30 **Evaluation of Drug efficacy of Ethyl Pyruvate on the Pulmonary Fibrosis in mice with Hyperpolarized ¹²⁹Xe MRI Pulmonary Function Diagnosis**
Scientific Presentation 1 : **Shota Hodono** Osaka University
- 11:30-11:40 **The association between pulmonary hemodynamics measured by phase-contrast MRI and acute exacerbations of interstitial lung diseases**
Scientific Presentation 2 : **Nanae Tsuchiya** University of the Ryukyus
- 11:40-12:15 **Further Discussion time in this session**

Program

January 29, 2016 [Fri]

Room A Jan, 29 [Fri]
Main Hall (2F)

January 29 [Fri]
2016

8:45-9:00 **Opennig Remark**

9:00-11:00 **Core Session 1**

Pulmonary Thromboembolism

Moderator : **Koichiro Tatsumi** Chiba University

Sadayuki Murayama University of the Ryukyus

Discussor : **Ki Yeol Lee** Korea University Medical Center Ansan Hospital

Invited Speaker

9:00-9:15

1. Distal lesions of chronic thromboembolic pulmonary hypertension and balloon pulmonary angioplasty

Takeshi Ogo

National Cerebral and Cardiovascular Center

9:15-9:35

2. Update for Treatment for Pulmonary Thromboembolic Disease

Nobuhiro Tanabe

Chiba University

9:35-9:50

3. Assessment of pulmonary thromboembolic disease in nuclear medicine

Norinari Honda

Saitama Medical University

9:50-10:05

4. CT Assessment for Pulmonary Thromboembolism

Jin Hur

Severance Hospital, Yonsei University College of Medicine

10:05-10:20

5. MR Assessment for Pulmonary Thromboembolic Disease

David L. Levin

Mayo Clinic, University of California

Scientific Presentation

10:20-10:30

1. Assessment of Cross-Sectional Lung Ventilation-Perfusion Imbalance in Primary and Passive Pulmonary Hypertension with Automated V/Q Quotient SPECT

Kazuyoshi Suga

St. Hill Hospital

10:30-10:40

2. Utility of computed tomography-derived measurements of the pulmonary vasculature in the diagnosis and hemodynamic assessment of pulmonary arterial hypertension

Kaoruko Shimizu

Hokkaido University

10:40-10:50

3. Diagnostic Performance of the Combined Pulmonary Arterial MRI and Indirect Magnetic Resonance Venography Using Unenhanced and Contrast-Enhanced Techniques in the Diagnosis of Venous Thromboembolism

Nevzat Karabulut
Pamukkale University Medical Center

10:50-11:00 **Further Discussion time in this session**

11:20-12:00 **Organizer Meeting of JSPFI**

12:20-13:20 **Luncheon Lecture 1** Sponsored by **TOSHIBA MEDICAL SYSTEMS CORPORATION**

New Techniques for Pulmonary Functional Imaging

Moderator : **Koichiro Tatsumi** Chiba University

Invited Speaker

12:20-12:50

1. New Techniques for Pulmonary Functional Imaging: CT-based functional imaging

Edwin J.R. van Beek
Edinburgh University

12:50-13:20

2. MR-Based Functional and Metabolic Imaging at 3T System

Yoshiharu Ohno
Kobe University

13:40-16:00 **Core Session 2**

Thoracic Malignancy: Diagnosis and Treatment Response Assessment

Moderator : **Nevzat Karabulut** Pamukkale University Medical Center

Noriyuki Tomiyama Osaka University

Discussor : **Yung-Liang Wan** Chang Gung Memorial Hospital

Invited Speaker

13:40-13:55

1. An Update on the Management of Lung Nodules

Jin Mo Goo
Seoul National University Hospital

13:55-14:10

2. Update of Medical Therapy for Advanced Lung Cancer

Koichi Takayama
Kyoto Prefectural University of Medicine

14:10-14:25

3. Lung cancer treatment assessment in the era of precision medicine: RECIST and beyond

Mizuki Nishino
Harvard Medical School

14:25-14:35

4. PET Imaging for Prognosis and Treatment Response Assessment in Lung Cancer

Tae Jung Kim
Samsung Medical Center

14:35-14:50

5. CAD for Prognosis and Treatment Response Assessment in Lung Cancer

Masahiro Yanagawa
Osaka University

14:50-15:05

6. New MR Techniques for Prognosis and Treatment Response Assessment

Hidetake Yabuuchi
Kyushu University

15:05-15:20

7. Radiomics and Radiogenomics in Lung Cancer: Clinical Perspectives

Ho Yun Lee
Samsung Medical Center, Sungkyunkwan University School of Medicine

Scientific Presentation

15:20-15:30

1. Prediction of therapeutic effect of chemotherapy for non-small-cell lung cancer using perfusion CT: comparison between regimens with and without anti-angiogenic agent

Hidetake Yabuuchi
Kyushu University

15:30-15:40

2. MR evaluation of the treatment response of HCC827 to erlotinib alone or combination with bevacizumab in mice model

Yi-Fang Chen
National Taiwan University

15:40-15:50

3. Dynamic Contrast-Enhanced Integrated PET/MR of Non-Small Cell Lung Cancer: Assessment of Response to Stereotactic Body Radiation Therapy

Yu-Sen Huang
National Taiwan University Hospital

15:50-16:00

Further Discussion time in this session

16:20-17:20 **Evening Lecture 1**

Sponsored by **FUJIFILM RI Pharma Co., Ltd.**

Imaging Biomarker for Pulmonary Diseases

Moderator : **Hiroto Hatabu** Brigham and Women's Hospital, Harvard Medical School

Invited Speaker

16:20-16:50

1. CT-Based Imaging Biomarkers

David A. Lynch
National Jewish Health

16:50-17:20

2. MR Based Imaging Biomarkers

David L. Levin
Mayo Clinic, University of California

Room B Jan, 29 [Fri]
Event Hall (B1F)

January 29 [Fri]
2016

12:20-13:20 **Luncheon Lecture 2** Sponsored by FUJIFILM Medical Co., Ltd.

New analysis using SYNAPSE VINCENT[®] for the evaluation of respiratory function

Moderator : **Noriyuki Tomiyama** Osaka University

Invited Speaker

12:20-12:50

1. Regional lung assessment using lobe segmentation methods and nonrigid multimodality image registration techniques by SYNAPSE VINCENT[®]

Shigeo Muro
Kyoto University

12:50-13:20

2. Bronchial dimension analysis of asthmatic patients using automatic route matching technique by SYNAPSE VINCENT[®]

Tsuyoshi Oguma
Kyoto University

18:40-20:30 **Welcome Reception**

Poster Session Jan, 29 [Fri]
Lobby (B1F)

17:40-18:40 **Poster Session**

1. Pulmonary Thromboembolism
Pulmonary vascular disease

Moderator : **Shuichi Ono** Hirosaki University
Takeshi Ogo National Cerebral and Cardiovascular Center

- P1-1. Potential role of CT metrics in chronic obstructive pulmonary disease with pulmonary hypertension
Katsutoshi Ando
Juntendo University
- P1-2. Ratio of pulmonary arterial to aortic diameter and right to left ventricular diameter associate with poor outcome in medically-treated chronic thromboembolic pulmonary hypertension
Ryogo Ema
Chiba University
- P1-3. Mean Pulmonary Artery Pressure by echocardiography in chronic thromboembolic pulmonary hypertension
Hajime Kasai
Chiba University
- P1-4. Quantitative analysis of thrombosis using CT images
Kaori Fujisawa
Tokushima University
- P1-5. Energy efficiency after balloon pulmonary angioplasty in chronic thromboembolic pulmonary hypertension: Assessment by phase-contrast MRI
Michinobu Nagao
Kyushu University
- P1-6. Relationship between Improved Pulmonary Arterial Pressure and Changes in the Wall Thickness of Right Ventricle Myocardium by 320-slice CT in Patients Under Pulmonary Endarterectomy
Toshihiko Sugiura
Chiba University

17:40-18:40 **Poster Session**

2. Thoracic Malignancy

2-1. Lung cancer: Therapeutic effect assessment

Moderator : **Masahiro Endo** Shizuoka Cancer Center Hospital
Hiroaki Sakai Hyogo Prefectural Amagasaki General Medical Center

P2-1-1. Correlation of early PET findings with tumor response to sensitive molecular targeted agents in patients with advanced non-small cell lung cancer

Tomonobu Koizumi
Shinshu University

P2-1-2. Stereotactic radiotherapy with Cyberknife for stage I non-small-cell lung cancer at our institute: Radiation pneumonitis

Masaki Nakamura
Kobe Minimally Invasive Cancer Center

P2-1-3. A case of acute arterial thrombosis in patient with postoperative adjuvant cisplatin-based chemotherapy for completely resected lung adenocarcinoma

Kenichi Okuda
The University of Tokyo

P2-1-4. Characterization of F-18-FDG Uptake in Irradiated Lung on Dual-Time-Point PET/CT Scan

Kazuyoshi Suga
St. Hill Hospital

P2-1-5. Initial Experience of Trans Pulmonary Arterial Marker Placement for Respiratory Gated Lung Stereotactic Radiotherapy

Yumiko Onishi
Kobe Minimally Invasive Cancer Center

17:40-18:40 **Poster Session**

2. Thoracic Malignancy

2-2. Lung nodule: CT

Moderator : **Masahiko Kusumoto** National Cancer Center Hospital East
Takashi Hirose NHO Tokyo National Hospital

P2-2-1. Radiology's Role in Lung Cancer Screening Programs

Fuldem Mutlu
Sakarya University Education and Research Hospital

P2-2-2. Ground Glass Nodule (GGN) Detection by Chest Digital Tomosynthesis (CDT) with Iterative Reconstruction (IR): a phantom study using simulated nodules and clinical evaluation in 79 cases

Yukihiro Nagatani
Shiga University of Medical Science

- P2-2-3. Atypical Adenomatous Hyperplasia of Lung Presenting as Pure Ground Glass Nodules or Part Solid Nodules: A Retrospective Study
 Yung Liang Wan
 Chang Gung Memorial Hospital, Chang Gung University
- P2-2-4. Incidental nodular lesion in anterior mediastinum on chest CT screening: incidence and characteristics
 Soon Ho Yoon
 Seoul National University College of Medicine
- P2-2-5. Comparison of Thin-section CT Features of T1 Invasive Adenocarcinomas of Lungs According to the sub-classification Diagnosed by using New WHO Classification
 Daisuke Takenaka
 Hyogo Cancer Center

17:40-18:40 **Poster Session**
3. COPD, Asthma and Airway Disease
3-1. COPD CT 1

Moderator : **Shingo Iwano** Nagoya University
Susumu Sato Kyoto University Hospital

- P3-1-1. Quantitative and qualitative analysis for chest CT with statistical or model-based iterative reconstruction: a chest phantom study
 Satoshi Kawanami
 Kyushu University
- P3-1-2. The impact of iterative reconstruction onto quantitative evaluation of COPD using fully automated lobar segmentation
 Hyun-ju Lim
 University Hospital of Heidelberg
- P3-1-3. Assessment of regional xenon-ventilation, perfusion and ventilation-perfusion mismatch Using Dual-Energy Computed Tomography in COPD Patients
 Hye Jeon Hwang
 Hallym University College of Medicine, Hallym University Sacred Heart Hospital,
 University of Ulsan College of Medicine, Asan Medical Center
- P3-1-4. Longitudinal Follow-up Study of Smoking-induced Emphysema Progressing using Low-dose CT Screening
 Kohji Shimada
 Tokushima University
- P3-1-5. Correlation of clinical characteristics by the grade of pulmonary emphysema in combined pulmonary fibrosis and emphysema
 Keishi Sugino
 Toho University Omori Medical Center

17:40-18:40 **Poster Session**

3. COPD, Asthma and Airway Disease

3-2. COPD Therapeutic effect and physiologic assessment

Moderator : **Tuneo Yamashiro** University of the Ryukyus
Kazuhisa Asai Osaka City University

- P3-2-1. Evaluation of pharmacological volume reduction effect induced by tiotropium via 3D-CT image analysis
Kazuya Tanimura
Kyoto University
- P3-2-2. Morphologic and Functional change after bronchoscopic lung volume reduction in COPD assessed with combined xenon ventilation and iodine perfusion dual energy CT
Joon Beom Seo
University of Ulsan College of Medicine, Asan Medical Center
- P3-2-3. Exertional dyspnoea and cortical oxygenation in patients with COPD
Yuji Higashimoto
Kinki University
- P3-2-4. Assessment of CT-derived airway wall area in COPD patients with indacaterol therapy
Ruriko Seto
Shiga University of Medical Science
- P3-2-5. Computer tomography (CT)-assessed bronchodilation induced by inhaled indacaterol and glycopyrronium /indacaterol combination in COPD
Kaoruko Shimizu
Hokkaido University

17:40-18:40 **Poster Session**

4. Basics of Computational Analysis for Pulmonary Imaging

4-1. CAD: clinical application

Moderator : **Hiroshi Fujita** Gifu University
Takatoshi Aoki University of Occupational and Environmental Health

- P4-1-1. Classifying regional texture patterns of diffuse lung disease at HRCT with deep convolutional neural networks : Comparison with support vector machine
Guk Bae Kim
University of Ulsan College of Medicine, Asan Medical Center
- P4-1-2. Comparison of skeleton based- and offset surfaces methods on pulmonary artery and veins: Validation with artificial vessel phantom and normal 3D volumetric CT
Jang Pyo Bae
University of Ulsan College of Medicine, Asan Medical Center

P4-1-3. Three-dimensional morphological analysis of spiculated pulmonary nodules in thoracic CT images

Yoshiki Kawata
Tokushima University

P4-1-4. Computer-aided diagnosis for osteoporosis using chest 3D CT images

Kazuya Yoneda
University of Tokushima

17:40-18:40 **Poster Session**

5. Interstitial Lung Disease

ILD : CT and MRI

Moderator : **Nobuyuki Tanaka** Saiseikai Yamaguchi General Hospital
Takashi Ogura Kanagawa Cardiovascular and Respiratory Center

P5-1. Survival analysis with quantified regional disease patterns at thin section CT in patients with idiopathic pulmonary fibrosis

Sang Min Lee
Asan Medical Center

P5-2. Composite CT indices derived from texture-based disease patterns for physiologic parameters in patients with idiopathic pulmonary fibrosis

Soyeoun Lim
Asan Medical Center

P5-3. Enhancement of Classification Accuracy in Automated Lung Quantification for Diffuse Interstitial Lung Disease in HRCT with Ensemble Methods

Sanghoon Jun
Asan Medical Center

P5-4. Six cases of unilateral upper-lung field pulmonary fibrosis

Akimasa Sekine
Kanagawa Cardiovascular and Respiratory Center

17:40-18:40 **Poster Session**

6. Motion Analysis and Biomechanical Imaging

6-1. Motion analysis and biomechanical imaging

Moderator : **Tae Iwasawa** Kanagawa Cardiovascular and Respiratory Center
Koji Chihara Shizuoka City Hospital

P6-1-1. Direct evidence of airflow limitation at the intra-mediastinal airway in emphysema patients by the use of maximum forced expiratory 4D-CT images

Takashi Kijima
Osaka University

P6-1-2. Dynamic change of airway in a patient with bronchial stenosis by ultra-low dose 4D-CT
Osamu Honda
Osaka University

P6-1-3. Pleural sliding mapping derived for detecting pleural adhesions
Ryo Sakamoto
Kyoto University

P6-1-4. New developed motion imaging to evaluate the effect of bronchodilator on human bronchial ciliary movement using bronchoscopic sample
Toshiyuki Sawa
Gifu Municipal Hospital

17:40-18:40 **Poster Session**

7. Others

7-1. Infection disease

Moderator : **Fumito Okada** Oita University
Makoto Osawa Shiga University

P7-1-1. Computed tomography findings in 749 patients with pulmonary infection
Fumito Okada
Oita University

P7-1-2. TYPICAL CT AND RADIOGRAFIC FINDINGS OF PULMONARY ECHINOCOCCOSIS
Esra Bilgi
Dresra Bilgi

P7-1-3. Correlation of HRCT findings with pulmonary function test and immunologic diagnostic test of tuberculosis: Comparison interferon-gamma release assay[IGRA] and tuberculosis skin test[TST]
Do Hyung Lee
Korea University Medical Center

P7-1-4. Bacteriological etiology in pneumonia patients with pulmonary emphysema using the clone library analysis of 16S rRNA gene in BALF
Keisuke Naito
University of Occupational and Environmental Health

Program

January 30, 2016 [Sat]

Room A Jan, 30 [Sat]
Main Hall (2F)

January 30 [Sat]
2016

8:00-8:30 **Board Meeting of IWPFJ at The Westin**

8:45-9:45 **Morning Lecture 1** Sponsored by **Nihon Medi-Physics Co., Ltd.**
PET/CT and PET/MRI for the chest and lung disease: review of the current literature and clinical perspective
Moderator : **Tsuyoshi Komori** Osaka Medical College

Invited Speaker

8:45-9:45
PET/CT and PET/MRI for the chest and lung disease: review of the current literature and clinical perspective
Munenobu Nogami
Hyogo Cancer Center

10:00-12:10 **Core Session 3**
COPD, Asthma and Airway Disease
Moderator : **Shu Hashimoto** Nihon University
Yasuo Nakajima St. Marianna University School of Medicine
Discussor : **Sang Do Lee** University of Ulsan College of Medicine, Asan Medical Center

Invited Speaker

10:00-10:15
1. COPD Phenotype and Treatment
Shigeo Muro
Kyoto University

10:15-10:30
2. VENTILATION/PERFUSION TOGRAPHY (V/P SPECT) – THE FUNCTIONAL IMAGING FOR COPD PHENOTYPING
Marika Bajc
Skåne University Hospital

10:30-10:45
3. Quantitative CT for COPD phenotyping
Yasutaka Nakano
Shiga University of Medical Science

10:45-11:00
4. New Quantitative CT Techniques for COPD Phenotyping
Joon Beom Seo
University of Ulsan College of Medicine, Asan Medical Center

11:00-11:15
5. Magnetic Resonance Imaging for Chronic obstructive lung disease phenotyping
Tae Iwasawa
Kanagawa Cardiovascular and Respiratory Center

11:15-11:30

6. Phenotyping lung disease using optical coherence tomography (OCT)

Harvey O Coxson

University of British Columbia, St Paul's Hospital

Scientific Presentation

11:30-11:40

1. Transfer Factor and Blood Gases in the V/P SPECT Emphysema Phenotype of COPD

Marika Bajc

Skåne University Hospital

11:40-11:50

2. Continuous quantitative measurements of proximal airway dimensions and lung density on dynamic-ventilation CT in smokers: a novel imaging approach using a 320-row detector CT scanner

Tsuneo Yamashiro

University of the Ryukyus

11:50-12:00

3. Morpho-functional 1H-MRI of the lung in COPD: Short-term test- retest reliability

Mark O Wielpuetz

University of Heidelberg

12:00-12:10

Further Discussion time in this session

12:30-13:30

Luncheon Lecture 3

Sponsored by **Nippon Boehringer Ingelheim Co., Ltd.**

The latest topics of COPD treatment

Moderator : **Masaharu Nishimura** Hokkaido University

12:30-13:00

1. Importance of symptom improvement for COPD treatment

Yasutaka Nakano

Shiga University of Medical Science

13:00-13:30

2. Importance of inhalational device for COPD treatment

Yuko Komase

St. Marianna University School of Medicine, Yokohama-City Seibu Hospital

14:00-15:00

Special Lecture 1

From Morphology to Function and Metabolism

Moderator : **Masaharu Nishimura** Hokkaido University

Mayuki Uchiyama The Jikei University School of Medicine

Yeun-Chung Ray Chang National Taiwan University

14:00-14:20

1. Lung 3D Micro Analysis using Synchrotron Radiation CT

Noboru Niki

Tokushima University

14:20-14:40
2. From Morphology to Function and Metabolism
Radiology Aspect

Hiroto Hatabu
Brigham and Women's Hospital, Harvard Medical School

14:40-15:00
3. From Physician side

Toyohiro Hirai
Kyoto University

15:10-16:15 **Core Session 4**
Basics of Computational Analysis for Pulmonary Imaging

Moderator : **Toyohiro Hirai** Kyoto University
 Kenya Murase Osaka University
Discussor : **Jong Hyo Kim** Seoul National University

Invited Speaker

15:10-15:25
1. Basics of Computational Analysis for Pulmonary Imaging

Namkug Kim
University of Ulsan College of Medicine, Asan Medical Center

15:25-15:40
2. Basics of Computational Assessment for Diffuse Lung Diseases (DLDs)

Shoji Kido
Yamaguchi University

15:40-15:55
3. Lung CAD

Noboru Niki
Tokushima University

Scientific Presentation

15:55-16:05
1. Computer aided detection system for lung cancer, COPD, and osteoporosis in low-dose CT screening

Hidenobu Suzuki
Tokushima University

16:05-16:15 **Further Discussion time in this session**

16:25-17:25 **Evening Lecture 2**

Sponsored by **Bayer Yakuhin, Ltd.**

Pulmonary Hypertension: Clinical and Functional Assessments

Moderator : **Minoru Kanazawa** Saitama Medical University

Invited Speaker

16:25-16:55

1. CT assessment of pulmonary hypertension

Sang Min Lee
Asan Medical Center

16:55-17:25

2. Pulmonary Hypertension: Clinical presentation and Functional Assessment Using Imaging

Mark L. Schiebler
University of Wisconsin

19:10-21:00 **Joint Meeting Dinner at The Westin**

Room B Jan, 30 [Sat]
Event Hall (B1F)

12:30-13:30 **Luncheon Lecture 4**

Sponsored by **Philips Electronics Japan, Ltd.**

Cardiopulmonary Functional Imaging

Moderator : **Hiroshi Kimura** Nara Medical University School of Medicine

Invited Speaker

12:30-13:00

1. Balloon pulmonary angioplasty for chronic thromboembolic pulmonary hypertension:
Assessment of CT angiography, MRI, and perfusion scintigraphy

Michinobu Nagao
Kyushu University Hospital

13:00-13:30

2. MR Application for Cardiopulmonary Diseases

Ichizo Tsujino
Hokkaido University

Poster Session Jan, 30 [Sat]
Lobby (B1F)

17:40-18:40 **Poster Session**

2. Thoracic Malignancy

2-3. Thoracic Malignancy: PET, PET/CT and MRI

Moderator : **Koji Murakami** Keio University
Shigeru Kosuda Kouseikai Clinic and Hospital

P2-3-1. Diffusion-Weighted MRI vs. FDG-PET/CT: Utility for the Management of Thymic Epithelial Tumors

Hisanobu Koyama
Kobe University

P2-3-2. Appropriate b Value Selection at Chest Computed Diffusion-Weighted Imaging for Improving Pulmonary Nodule/Mass Differentiation

Hisanobu Koyama
Kobe University

P2-3-3. Evaluation of the detectability of pulmonary micrometastases of 5 mm and smaller in dual time point TOF FDG PET/CT

Tsuyoshi Komori
Osaka Medical College

P2-3-4. FDG-PET/CT findings of primary lung cancer arising from the cyst wall or cavity

Maki Otomo
Tokushima University Hospital

P2-3-5. Value of 4 dimensional PET/CT in the diagnosis for primary lung cancer to compare with 3D PET/CT

Jun Sato
Iwata City Hospital

17:40-18:40 **Poster Session**

2. Thoracic Malignancy

2-4. Lung cancer: CT

Moderator : **Koji Takahashi** Asahikawa Medical University
Yasuhiko Nishioka Tokushima University

P2-4-1. Clinical features of lung cancer and effect of its resection on pulmonary function in patients with combined pulmonary fibrosis and emphysema

Katsutoshi Ando
Juntendo University

- P2-4-2. Evaluation of lung cancer by enhanced dual-energy CT: Association between three-dimensional iodine concentration and tumor differentiation
 Shingo Iwano
 Nagoya University
- P2-4-3. Classifications and Measurements in Subsolid Nodules: Which Window Setting is Better?
 Roh-Eul Yoo
 Seoul National University Hospital
- P2-4-4. Utility of Dual-Energy CT for Differentiation of Pulmonary Nodules: Comparison of Dual-Energy CT and FDG-PET/CT
 Sachiko Miura
 Nara Medical University

17:40-18:40 **Poster Session**
3. COPD, Asthma and Airway Disease
3-3. COPD CT 2

Moderator : **Shin Matsuoka** St.Marianna University School of Medicine
Keisaku Fujimoto Shinshu University

- P3-3-1. Quantitative analysis of combined pulmonary fibrosis and emphysema (CPFE): correlation with impairment of lung function
 Kum Ju Chae
 Chonbuk National University Hospital
- P3-3-2. Association of Epicardial Adipose Tissue with Airway Lesion of Chronic Obstructive Pulmonary Disease in Vietnamese
 Yuichi Higami
 Shiga University of Medical Science
- P3-3-3. Robustness of the power law analysis of emphysema hole size distribution to the variation of lung inflation level and correlation with clinical parameters in KOLD cohort
 Jeogneun Hwang
 University of Ulsan College of Medicine, Asan Medical Center
- P3-3-4. Automatic evaluation on fissure integrity for target lobe selection of endobronchial valve volume reduction procedure using volumetric chest CT: Validation with radiologic visual evaluation
 Minho Lee
 University of Ulsan College of Medicine, Asan Medical Center
- P3-3-5. Estimated postoperative pulmonary function calculated with lung volume in 3D-CT for lung cancer patients with and without COPD
 Masanori Yokoba
 Kitasato University Hospital, Kitasato University

17:40-18:40 **Poster Session**

3. COPD, Asthma and Airway Disease
3-4. COPD Others

Moderator : **Munenobu Nogami** Hyogo Cancer Center
Takashi Iwanaga Kinki University

- P3-4-1. Verification of Co-Morbidities: an Additional Value of V/P SPECT in COPD
Marika Bajc
Skåne University Hospital
- P3-4-2. Obstructive Bronchitis and Emphysema Phenotypes by V/P SPECT Co- Exist in Severe COPD
Marika Bajc
Skåne University Hospital
- P3-4-3. Relationship between Brain and Pulmonary Function Studied by Hyperpolarized ^{129}Xe MRI/MRS
Akihiro Shimokawa
Osaka University
- P3-4-4. Analysis of the microstructure of the secondary pulmonary lobulus by a synchrotron radiation CT
Kohichi Minami
Tokushima University
- P3-4-5. Quantitative study of airway changes in murine asthma models on micro-CT: comparison with pathologic findings
Sanghyun Paik
Soon Chun Hyang University Hospital

17:40-18:40 **Poster Session**

4. Basics of Computational Analysis for Pulmonary Imaging
4-2. Image informatics: registration and segmentation

Moderator : **Yoshiki Kawata** Tokushima University
Kensaku Mori Nagoya University

- P4-2-1. Novel Airway Segmentation Technique in Low-dose CT Images: Global Validation with EXACT09
Sang Joon Park
Seoul National University Hospital
- P4-2-2. Blood Flow Contribution Analysis for Pulmonary Artery and Aorta using Contrast Enhanced Images
Tomoki Saka
Yokohama National University

P4-2-3. 3D Partial Rigid Registration with ICP for airways using point classification
 Leonardo Ishida-Abe
 Yokohama National University

P4-2-4. Extraction algorithm of bronchi and pulmonary artery and vein using anatomical features based on multi-slice CT images
 Mikio Matsuhiro
 Tokushima University

P4-2-5. A Temporal Subtraction Technique from Thoracic MDCT Images Based on Image Registration Technique
 Masashi Kondo
 Kyushu Institute of Technology

17:40-18:40 **Poster Session**
6. Motion Analysis and Biomechanical Imaging
6-2. Airway and parenchyma

Moderator : **Hiromitsu Sumikawa** Osaka Rosai Hospital
Takashi Kijima Osaka University

P6-2-1. Quantification of mucociliary function in murine lungs using magnetic particle imaging
 Kohei Nishimoto
 Osaka University

P6-2-2. Simulation study of inhaled gas imaging by the use of a 4D lung model and computational fluid dynamics
 Hiroko Kitaoka
 JSOL Corporation

P6-2-3. A combinatory simulator of ventilation, diffusion, and perfusion in the human pulmonary subacinus
 Hiroko Kitaoka
 JSOL Corporation

P6-2-4. Procaterol-stimulated increases in ciliary bend amplitude and ciliary beat frequency in mouse bronchioles
 Nobuyo Tamiya
 Kyoto Prefectural University of Medicine

17:40-18:40 **Poster Session**

7. Others

7-2. Others: CT and MRI

Moderator : **Hidetake Yabuuchi** Kyusyu University
Atsuomi Kimura Osaka University

P7-2-1. Fat Suppression Capabilities at Chest 3T MRI: Utilities of Two-point TSE-Dixon Technique in Comparison with SPAIR Technique

Yuji Kishida
Kobe University

P7-2-2. Anatomic and functional evaluation of central lymphatics with noninvasive MR lymphangiography

Eun Young Kim
Samsung Medical Center

P7-2-3. Reproducibility of pulmonary blood flow measurements by phase-contrast MRI using two different MR scanners

Rin Iraha
University of the Ryukyus

P7-2-4. Automatic bone of torso segmentation using contrast enhanced CT

Ahmed S. Maklad
Tokushima University

17:40-18:40 **Poster Session**

7. Others

7-3. Others

Moderator : **Takeshi Kubo** Kyoto University
Yoshinobu Iwasaki North Medical Center, Kyoto Prefectural University of Medicine

P7-3-1. Accuracy of Narrow Band Imaging in Conjunction with White Light by Thoracoscopy for Detection of Disseminated Thoracic Endometriosis in Patients of Catamenial Pneumothorax

Teruaki Mizobuchi
Nissan Kohseikai Tamagawa Hospital

P7-3-2. A CASE PULMONARY ARTERIOVENOUS MALFORMATION

Mehmet Oncu
Dresra Bilgi

P7-3-3. Pulmonary Agenesis Diagnosed in mid-age

Cagatay Bolgen
Murat Gedikoglu

P7-3-4. Effects of weight loss therapy on respiratory system impedance in obese adults

Etsuhiro Nikkuni
Tohoku University

17:40-18:40 **Poster Session**

7. Others

7-4. Case reports

Moderator : **Yuichiro Maruyama** Komoro Kousei General Hospital
Tamotsu Ishizuka University of Fukui

P7-4-1. Long-term pulmonary complications of sulfur mustard exposure in former workers of poison gas factory

Yoshifumi Nishimura
Hiroshima University, Tadanoumi Hospital

P7-4-2. Experience of IgG4-related thoracic diseases on F-18-FDG PET/CT in our institute

Kazuyoshi Suga
St. Hill Hospital

P7-4-3. A case with rheumatoid arthritis who presented wheezes and methotrexate-associated lymphoproliferative disorder

Mariko Kinoshita
Teikyo University

P7-4-4. IgG4-related thoracic disease: report of two cases

Fumiyasu Tsushima
Hirosaki University

Program

January 31, 2016 [Sun]

Room A Jan, 31 [Sun]
Main Hall (2F)

9:30-10:00 **General Meeting of JSPFI**

10:15-12:15 **Core Session 5**

Interstitial Lung Disease

Moderator : **Arata Azuma** Nippon Medical School

Takeshi Johkoh Kinki Central Hospital of Mutual Aid Association of Public School
Teachers

Discussor : **Jae-Woo Song** University of Ulsan College of Medicine, Asan Medical Center

Invited Speaker

10:15-10:35

1. Update for Diagnosis of Interstitial Lung disease

Gong Yong Jin

Chonbuk National University Medical School and Hospital

10:35-10:50

2. Recent advances in the treatment of idiopathic pulmonary fibrosis

Noboru Hattori

Hiroshima University

10:50-11:05

3. Quantitative CT Assessment for ILD

David A. Lynch

National Jewish Health

11:05-11:20

4. Quantitative MRI Assessment for ILD

Yoshiharu Ohno

Kobe University

Scientific Presentation

11:20-11:30

1. Evaluation of Drug efficacy of Ethyl Pyruvate on the Pulmonary Fibrosis in mice with
Hyperpolarized ^{129}Xe MRI Pulmonary Function Diagnosis

Shota Hodono

Osaka University

11:30-11:40

2. The association between pulmonary hemodynamics measured by phase-contrast MRI and
acute exacerbations of interstitial lung diseases

Nanae Tsuchiya

University of the Ryukyus

11:40-12:15

Further Discussion time in this session

12:30-13:30 **Luncheon Lecture 5** Sponsored by **GE Healthcare Japan Corporation**
Moderator : **Noriyuki Tomiyama** Osaka University

Invited Speaker

12:30-12:40
1. Gemstone Spectral Imaging Technology
Kousuke Sasaki
GE Healthcare Japan Corporation

12:40-13:30
2. Update of Thoracic Imaging: new iterative reconstruction and gemstone spectral imaging
Masahiro Yanagawa
Osaka University

13:50-14:50 **Special Lecture 2**
New Techniques for Pulmonary Functional Imaging
Moderator : **Michiaki Mishima** Kyoto University
Kiyoshi Murata Shiga University of Medical Science
Jai Soung Park Soonchunhyang University Hospital

Invited Speaker

13:50-14:10
1. Computer-aided diagnosis and assessment for pulmonary functional imaging
Eric Hoffman
University of Iowa

14:10-14:30
2. New MR Applications for Morpho-Functional Pulmonary Imaging
Hans-Ulrich Kauczor
Heidelberg University Medical Center

14:30-14:50
3. New CT applications for pulmonary functional imaging
Joon Beom Seo
University of Ulsan College of Medicine, Asan Medical Center

14:50-15:00 **Closing Remark**

Room B Jan, 31 [Sun]
Event Hall (B1F)

12:30-13:30 **Luncheon Lecture 6** Sponsored by **Accuray Japan K.K./CHIYODA TECHNOLOGICAL CORPORATION**

CyberKnife: Real Time Image Guided Radiation Therapy for Lung Cancer

Moderator : **Ryohei Sasaki** Kobe University Hospital

Invited Speaker

12:30-13:30

CyberKnife: Real Time Image Guided Radiation Therapy for Lung Cancer

Hideki Nishimura
Kobe Minimally Invasive Cancer Center

January 31 [Sun]
2016

Abstracts

Special Lecture

| Special Lecture 1-1

Lung 3D Micro Analysis using Synchrotron Radiation CT

Noboru Niki

Tokushima University, Japan

The lung consists of numerous anatomic units smaller than a lobe or segment. Secondary pulmonary lobule and lung acinus are considered to be fundamental units of these subsegmental lung units. At the level of the pulmonary secondary lobule, airways, pulmonary arteries, veins, lymphatics, and lung interstitium are observed. The recognition of abnormalities relative to the lobular anatomy has become increasingly important in the diagnosis of lung abnormalities at clinical routines of CT examinations. The secondary pulmonary lobule consists of several acini which represent terminal units of the respiratory airways comprising the terminal bronchiole and all the air spaces distal to the terminal bronchiole. The alveolated structure in the acinus plays an important role in gas exchange function. Three-dimensional (3D) analysis of the acinus region is fundamental in understanding the structure-function relationship. The purpose of this study is to analyze microstructures of acinus region with isotropic spatial resolution in the range of several micrometers using synchrotron radiation micro CT (SR μ CT). Previously, we demonstrated the ability of SR μ CT using offset scan mode in microstructural analysis of the secondary pulmonary lobule. The main focus of this presentation is to develop a semi-automatic acinar airspace segmentation method from the 3D SR μ CT image of the secondary pulmonary lobule. Our experiments demonstrate the potential usefulness of the method to extract pulmonary acini from the 3D SR μ CT image of the secondary pulmonary lobule.

| Special Lecture 1-2

From Morphology to Function and Metabolism Radiology Aspect

Hiroto Hatabu

Center for Pulmonary Functional Imaging
Department of Radiology, Brigham and Women's Hospital
Professor of Radiology, Harvard Medical School, USA

Lung is an evolutionary product of the organ, which made humans and animals live in the air atmosphere on the earth. It is essential to life from the moment of our birth to the moment of the death. In the lung, the morphology of the alveolar structure is uniquely designed for its essential function of gas exchange. Its anatomical structure of secondary pulmonary lobule is designed for the effective distribution of air with oxygen and deoxygenized blood as well as collection of air with carbon dioxide and the oxygenized blood. High-resolution CT scan provides insight to physiological and pathological process at the level of secondary pulmonary lobule. MRI can acquire information or images of pulmonary functions including blood flow, airflow, gas exchange, motion, and biomechanics. The metabolism and genetics of the lung are still largely unknown. Image-based phenotyping is an approach to use a large scale CT scan data of thousands or tens of thousands subjects in correlation with the human genetic data. The use of computational approaches including machine learning and "big data" are becoming unavoidable. Our radiologic approaches toward morphology, function, and metabolism of the lung will continue to evolve.

From Physician side

Toyohiro Hirai

Department of Respiratory Medicine, Graduate School of Medicine, Kyoto University, Japan

Image diagnosis including Chest X-ray examination and computed tomography (CT) has been widely used for the morphological assessment of respiratory diseases in a clinical setting. Not only visual assessment but also quantitative evaluation of lesion is important and useful for clinical researches. For example, numerous studies using CT images in chronic obstructive pulmonary disease have used the ratio of low attenuation area to total lung area as a useful parameter to quantitatively evaluate the extent of emphysema. On the other hand, functional assessment is able to provide additional information to the morphology, though some functional parameters are related with the structural parameters. For example, several reports have presented pulmonary function tests as better prognostic factors in interstitial lung disease than histopathological diagnosis. Moreover, functional imaging such as magnetic resonance imaging and the nuclear medicine techniques can provide visual information of regional function. All these quantitative parameters have contributed to differential diagnosis, evaluation of disease severity and effects of treatment, and understanding of pathophysiology in lung diseases. However, there may be some variations among medical devices and also limitations in accurate quantitative evaluation. It is necessary to understand these differences and variations to interpret the measurements data in a clinical setting, especially in multicenter studies. The clinical application of quantitative parameters derived from morphological and functional assessments and the standardization of the measurements using different devices are warranted.

Computer-aided diagnosis and assessment for pulmonary functional imaging

Eric Hoffman

Department of Radiology, Medicine and Biomedical Engineering University of Iowa, USA

Imaging has increased importance in defining phenotypes to sub-categorize a growing number of lung diseases including COPD and Asthma. Computer-based methods for objective quantitation of multi-detector-row computed tomography (MDCT) data sets to compare normal and diseased lung parenchyma are increasingly used in multi-center studies searching for phenotype-genotype linkages and seeking intermediary outcome measures. A cornerstone of lung assessment for emphysema by MDCT scanning is known as the density mask. By empirically defining emphysematous lung as a given lung density at full inspiration, one can set a CT density threshold (HU) below which all voxels are defined as emphysema. The density mask is particularly useful in classifying mild/moderate and severe emphysema and has been used to identify subgroups of patients who show benefit from lung volume reduction surgery and endo-bronchial interventions. A wealth of literature in the last several years has provided a roadmap to the standardization and customization of density metrics for numerous large scale studies. These measures have identified correspondence of quantitative CT measures of emphysema and air trapping to: genotypes, LV filling, physiologic measures, environmental smoke exposure in childhood as a risk factor for emphysema, predictors of bronchoreversibility, association of cigarette smoking with sub-clinical disease, and trapped gas in severe asthma.

Using MDCT to quantitate parenchymal characteristics has its challenges, however. Scanner mis-calibration and inconsistent use of reconstruction kernels can cause variations in measurements and accuracy in QCT requires consistency. Furthermore, the growing concern of radiation dose significantly limits the ability to apply CT imaging longitudinally, especially in populations younger than 40-50 years. Because of the interest in both airway and parenchymal pathologies, the quest for airway wall characterization has largely driven the dose decision, with little information with which to evaluate the true limits of the technology at a given dose.

Despite considerable successes using quantitative CT to assess the presence and distribution of emphysema and airway wall remodeling, critical underlying differences exist among disease sub-populations that have yet to be characterized with quantitative MDCT. We strongly believe that an assessment of functional phenotypes such as pulmonary perfusion and ventilation parameters, indices of inflammation, and an objective basis characterizing relationships between structure and function are critical to advance insights into the etiology of the disease. Perfusion heterogeneity via CT has recently supported a biologic hypothesis regarding emphysema etiology rather than simply providing a report of the destruction. However, the methods used to assess first pass kinetics would be cumbersome to implement at multiple clinical centers. Multi-spectral CT imaging (Dual Energy CT: DECT) provides the path to interrogate regional perfusion and ventilation parameters via CT at spatial resolution of a pulmonary acinus. To use DECT for full lung coverage, we must resort to lower dose, single breath-hold methods. Furthermore, we must limit the volume of iodinated contrast agent and limit the percentage of xenon gas for ventilation because of anesthetic effects.

While tools for assessing airway structure linking to measures of ventilation are fairly mature, the tools for extracting the geometry of the pulmonary arterial and venous trees, especially in non-contrast images are in their infancy. The airways and vessel trees not only are important for providing further understanding of the physiology associated with the disease, but are critical for sub-dividing the lung into its functional parts to include the boundaries of the sub-lobar segments.

| Special Lecture 2-2

New MR Applications for Morpho-Functional Pulmonary Imaging

Hans-Ulrich Kauczor

Heidelberg University Medical Center, Germany

MRI of the lung has successfully entered the clinical arena as significant progress has been made in addressing its major challenges, i.e. low proton density, susceptibility artifacts as well as respiratory and cardiac motion. For routine clinical use standardized protocols have been implemented on MR scanners of all major vendors. In the last years morphological imaging was limited with regard to spatial resolution and clearly inferior to CT. Only recently new promising techniques for high resolution MRI, mainly based on ultra short TE sequences, have been introduced. These are especially promising for the visualization of reticular and fibrotic changes. Beyond visualization of lung morphology functional imaging has become an integral part of the routine protocols. This mainly comprises perfusion and diffusion MRI. Ventilation MRI based on gases is only available in dedicated centers.

Considering the recent progress in approved specific therapies imaging biomarkers are required for therapy response imaging in different lung diseases. MRI is in the pole position to provide answers to these urgent questions. Dynamic contrast-enhanced MRI has the potential to assess the inflammatory activity of interstitial lung disease. T2w imaging will help to differentiate between mucus and airway remodeling. Diffusion-weighted MRI demonstrates changes of cellularity in lung cancer early in treatment as well as involvement of mediastinal lymph nodes challenging PET/CT. Multidirectional flow measurements are promising for the assessment of pulmonary arterial hypertension challenging echocardiography. Measurements of regional lung compliance as well as the generation of nomograms for image based 4D pulmonary function are also warranted.

| Special Lecture 2-3

New CT applications for pulmonary functional imaging

Joon Beom Seo

Department of Radiology, University of Ulsan College of Medicine, Asan Medical Center, Korea

Dual-energy CT is a new, emerging, imaging technique which can differentiate such materials as iodine, xenon, bone, and air, based on their specific attenuation differences at high and low x-ray energies. This technology has opened a new field of direct visualization of pulmonary perfusion and ventilation. One of typical applications is perfusion or blood volume imaging, which is based on the ability of extraction of iodine content from contrast enhanced CT images. Typical indication of DECT perfusion imaging is the diagnosis and severity assessment of acute embolism. Perfusion imaging is also useful in the assessment of chronic embolism and other vascular diseases. In addition, the simultaneous assessment of anatomy and perfusion may open new fields of functional imaging of various diffuse lung diseases including COPD, smoker's lung, interstitial lung diseases, and so on. Another potential application of DECT is xenon ventilation imaging for the simultaneous assessment of anatomy and ventilation. Possible clinical indications of this new approach include the assessment of COPD, asthma and various airway diseases. By combining perfusion and ventilation imaging, assessment of V-Q mismatch can be assessed in various diseases.

Abstracts

Morning Lecture

PET/CT and PET/MRI for the chest and lung disease: review of the current literature and clinical perspective

Munenobu Nogami

Department of Diagnostic Radiology, Hyogo Cancer Center, Japan

Since more than ten years ago, PET/CT using 2-Deoxy-2-[18F] fluoroglucose (FDG) has been developed and is now widely employed in a clinical setting especially for oncological purposes. In the field of chest imaging, PET/CT is one of the current standards for assessment of lung cancer and applied to its staging, therapeutic evaluation and prediction of prognosis. Because PET is one of the functional-imaging modalities, FDG PET can evaluate the glucose metabolism of the targeted lesion and useful for assessment of the biological behavior of several diseases. Combination of PET and CT produces anatomically fused images of function and morphology, yielding more accurate and comprehensive understanding of characteristics of the malignancies including lung cancer than by respective modality alone.

PET/MRI, on the other hand, is a recently introduced modality which enables not only anatomically-precise fusions of PET and MRI but also a simultaneous image-acquisition of both modalities. Because the history of PET/MRI is far shorter than that of PET/CT, the clinical utility and role of PET/MRI has yet to be confirmed and is now under investigation by several researchers and clinicians. Especially for assessment in the lung, many researches are skeptical about the additional value of PET/MRI over PET/CT because of the difficulties in lung imaging by MRI; however, currently there exists too limited evidences to draw a conclusion of clinical utility of PET/MRI in the chest.

Based on the above backgrounds of PET/CT and PET/MRI, this presentation will review the recent literature regarding both modalities targeting the lesions in the chest and summarize the current direction of clinical utility of PET/CT and PET/MRI for the chest and lung disease.

Abstracts

Luncheon Lecture

| Luncheon Lecture 1-1

New Techniques for Pulmonary Functional Imaging: CT-based functional imaging

Edwin J.R. van Beek

Edinburgh University, UK

The use of CT for imaging of morphological diseases in the chest has been applied for many decades. Until relatively recently, protocols were used to minimize radiation dose, which effectively limited the scale of investigations that could be performed.

With the advent of low-dose applications, such as dose modulation and iterative reconstruction methods, the radiation dose has been dramatically reduced. This in turn has allowed development of comprehensive cardiothoracic imaging protocols, which not only assess morphological characteristics, but also address functional states of the heart, lungs and vascular systems.

In addition to the dose reduction techniques, CT systems have become faster in effective rotation times or have been enabled to perform volumetric assessment in a single rotation. This has allowed an increasingly integrated CT approach to combined cardiothoracic imaging.

This lecture will summarize a number of applications that are of importance and will likely be of routine use for the future of CT investigations. These include:

- Volumetric inspiratory and expiratory isotropic voxel imaging
- CT perfusion methods and their potential applications
- CT ventilation methods using Xenon gas
- Dynamic inspiratory and expiratory methods for evaluation of airways disease
- Dual energy methods to assess pulmonary blood volume
- Integrated approach to cardiothoracic CT

| Luncheon Lecture 1-2

MR-Based Functional and Metabolic Imaging at 3T System

Yoshiharu Ohno

Division of Functional and Diagnostic Imaging Research, Department of Radiology, Kobe University School of Medicine, Japan

Advanced Biomedical Imaging Research Center, Kobe University Graduate School of Medicine, Japan

Since clinical installation of MR imaging in routine clinical practice, pulmonary magnetic resonance imaging (MRI) has been studied at mainly 1.5T MR system in various pulmonary diseases including lung cancer, COPD, asthma, and pulmonary vascular diseases. Currently, pulmonary MR imaging at 1.5T MR system is considered as a new research and diagnostic tool as well as CT and nuclear medicine study in these diseases.

In the last decade, the 3T MR system has been clinically applied to body MRI in various organs. In this time point, pulmonary MRI at 3T MR system is suggested as more challenging and difficult than that at 1.5T system. Because the 3T MR system is suggested as having increased susceptibility, chemical shift, motion and distortion artifacts, relatively prolonged T1 relaxation time and higher SAR levels, which makes the limitations of sequence parameter setting. Therefore, various technical advances have been reported for overcoming the drawbacks of pulmonary MRI at 3T MR system. In addition, pulmonary MRI at 3T system is tried to demonstrate the potential for providing not only morphological, but also function and metabolic information.

This lecture covers 1) recent technical advances for pulmonary MRI as well as whole-body MRI at a 3T system, 2) new applications for solving academic and clinical questions in patients with pulmonary diseases including thoracic malignancies, and 3) future direction of pulmonary MRI by means of Vantage Titan 3T.

Regional lung assessment using lobe segmentation methods and nonrigid multimodality image registration techniques by SYNAPSE VINCENT®

Shigeo Muro

Department of Respiratory medicine, Graduate School of Medicine, Kyoto University, Japan

COPD is a heterogeneous disease defined by the airflow limitation and their "persistent airflow limitation is usually progressive (Global Strategy for Diagnosis, Management and Prevention of COPD (GOLD))". Emphysema is an important and major pathological change in COPD, however, the change or the progression of emphysematous change is not evaluated in detail. Quantitative computed tomography (CT) has been widely applied to explore the severity of morphological change and mechanism of disease progression in patients with COPD. Quantitative CT provides information about lung volumes and percent low attenuation volume (LAV%), which is a standard index of emphysematous change, reflects pathological lung destruction and lung hyperinflation. CT assessments can quantify not only the total lung volume but also volumes of lung regions damaged by emphysema-related parenchymal destruction, which cannot be evaluated by physiological assessments. In this seminar, we introduce new image analysis methods, such as nonrigid multimodality image registration following manual correction on results by automated lobe segmentation. As an extension of image registration, "voxel by voxel" analysis of volume changes are available in this technique. Such multiscale image analysis of dynamic lung ventilation may provide us a promising information of various lung diseases such as bronchial asthma and bronchiolitis obliterans which was not available by previous technique.

Luncheon Lecture 2-2

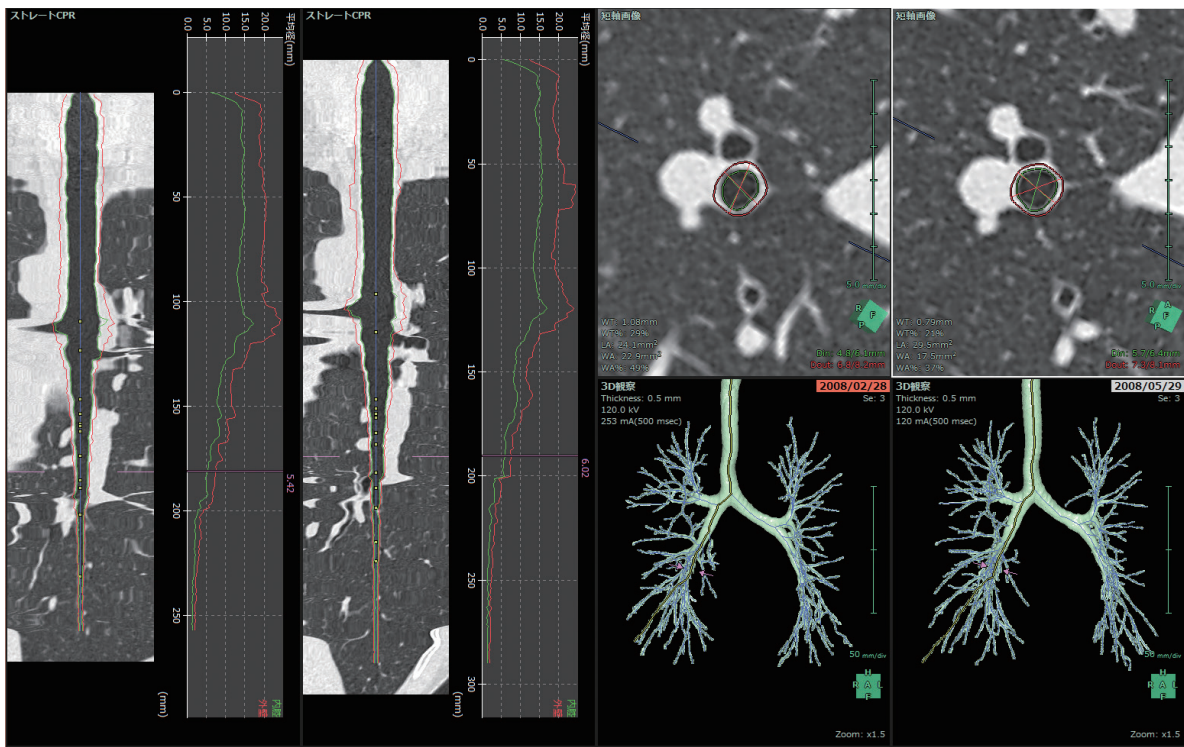
Bronchial dimension analysis of asthmatic patients using automatic route matching technique by SYNAPSE VINCENT[®]

Tsuyoshi Oguma

Kyoto University, Japan

Airway inflammation and remodeling of the airways are fundamental features of asthma, and chest computed tomography (CT) is a useful technique for assessing these structural changes in vivo. CT indices such as the ratio of airway wall area (WA) to total airway wall area (WA%) as well as luminal area (Ai) have been used for the quantitative analysis of airway wall thickening and airway narrowing. Numerous studies have used these indices and recent developments in CT and techniques of image analysis have allowed three-dimensional assessment of airway lesion. These indices calculated automatically at the selected bronchus or point in almost all recent commercial software to lung analysis, but even when comparing indices of same subject at different time, selection of bronchus or slice itself was performed manually in much software. In this seminar, we demonstrate assessment of changes in bronchi dimensions of asthmatic patients before and after treatment using auto route matching technique. Using this technique, the software can automatically select the same bronchus which selected in former CT series (Image 1) and we would take results with less selection bias than manual matching.

(Image 1)



| Luncheon Lecture 3-1

Importance of symptom improvement for COPD treatment

Yasutaka Nakano

Division of Respiratory Medicine, Department of Pulmonology, Shiga University of Medical Science, Japan

Chronic obstructive pulmonary disease (COPD), common preventable and treatable disease, is characterized by persistent airflow limitation that is usually progressive and associated with an enhanced chronic inflammatory response in the airways and the lung to noxious particles or gases (GOLD 2015). The characteristic symptoms of COPD are chronic and progressive dyspnea, cough, and sputum. Chronic and progressive dyspnea causes the COPD patients to reduce daily physical activity. Keeping physical activity is very important for COPD patients because the reduction of physical activity leads the patients with COPD to poor prognosis. To keep the daily physical activity, pharmacologic treatment as well as pulmonary rehabilitation is very important. The symptom improvement, especially the improvement of dyspnea, brought by the pharmacologic treatment could have the COPD patients keep their daily physical activity. In order to get the maximal symptom improvement for the patients with COPD, the combination of long-acting anticholinergic drug (LAMA) and Long-acting beta2 -agonist (LABA) may play an important role. Because of its excellent effect and simplicity, dual bronchodilator (LAMA/LABA) may play a key role in the treatment of COPD.

| Luncheon Lecture 3-2

Importance of inhalational device for COPD treatment

Yuko Komase

St.Marianna University School of Medicine, Yokohama-City Seibu Hospital, Japan

Chronic obstructive pulmonary disease (COPD) is primarily treated with inhaled drugs. Many inhalational devices have become available in recent years. Compound formulations comprising a long-acting muscarinic antagonist (LAMA), long acting β_2 -agonist (LABA), and/or inhaled corticosteroid (ICS) are scheduled to be launched in the near future. The currently available delivery devices are metered dose inhalers (MDIs), dry powder inhalers (DPIs), and soft mist inhalers (SMIs) .

Most COPD patients are elderly people, so inhalation devices should be chosen carefully. The recognition ability decreases in elderly patients, and senior citizens have clumsy hands. It is necessary to choose devices that patients can operate easily and use for inhalation on a daily bases without difficulty.

SMIs can deliver soft and fine particles for more efficient inhalation. Furthermore, elderly patients can use SMI in only by 3 steps. Operation and inhalation should not be done timely. As a result, a greater effect can be obtained.

The inhalation status of elderly patients should be always monitored. It is important that all medical professionals caring for patients cooperate medically and support the treatment of patients. Determining treatment policy with patients is a practice now referred to as "concordance".

| Luncheon Lecture 4-1

Balloon pulmonary angioplasty for chronic thromboembolic pulmonary hypertension: Assessment of CT angiography, MRI, and perfusion scintigraphy

Michinobu Nagao

Department of Molecular Imaging & Diagnosis, Graduate School of Medical Sciences, Kyushu University Hospital, Japan

Chronic thromboembolic pulmonary hypertension (CTEPH) has two distinct features of pulmonary vasculature; macro-vascular thrombotic obstruction and high shear stress induced small-vessel arteriopathy in the patent vessels.

Pulmonary endarterectomy has been a definitive option for central type of CTEPH; however, 40 % of patients are inoperable because of surgically inaccessible lesion type or intolerable condition. Balloon pulmonary angioplasty (BPA) has emerged as a promising therapy for patients with inoperable CTEPH. BPA recanalizes the macro-obstructive vessels and increases its blood flow. Meanwhile BPA is expected to decrease shear stress at the non-BPA vasculature. BPA improved pulmonary hypertension, exercise tolerance and eventually mid-term survival in patients with inoperable CTEPH; however, the mechanism is not understood. CT angiography for pulmonary artery can demonstrate not only thrombosis in the great-vessels but also hypo-enhancement areas in the obstructive vessels territories. Phase-contrast MRI can measure pulmonary blood flow and stroke volume for the proximal portion of pulmonary artery, whereas ^{99m}Tc-MAA-perfusion scintigraphy shows the distribution and the volume of pulmonary vascular bed. This seminar reports the effect of BPA on pulmonary circulation in patients with CTEPH by the comprehensive assessment of CT angiography, cardiac MRI, and perfusion scintigraphy.

| Luncheon Lecture 4-2

MR Application for Cardiopulmonary Diseases

Ichizo Tsujino

Hokkaido University, Japan

Recent progress in the imaging of cardiovascular and respiratory systems has enabled better understanding, early diagnosis and better clinical outcomes of cardiovascular/respiratory diseases. The present luncheon lecture introduces the practical use of magnetic resonance imaging (MRI) in the assessment and management of patients with “cardiopulmonary” disease. In particular, the lecture will focus on two representative diseases: pulmonary hypertension and sarcoidosis that could affect both cardiovascular and respiratory systems.

Luncheon Lecture 5-1

Gemstone Spectral Imaging Technology

Kousuke Sasaki

GE Healthcare Japan Corporation, Japan

Luncheon Lecture 5-2

Update of Thoracic Imaging: new iterative reconstruction and gemstone spectral imaging

Masahiro Yanagawa

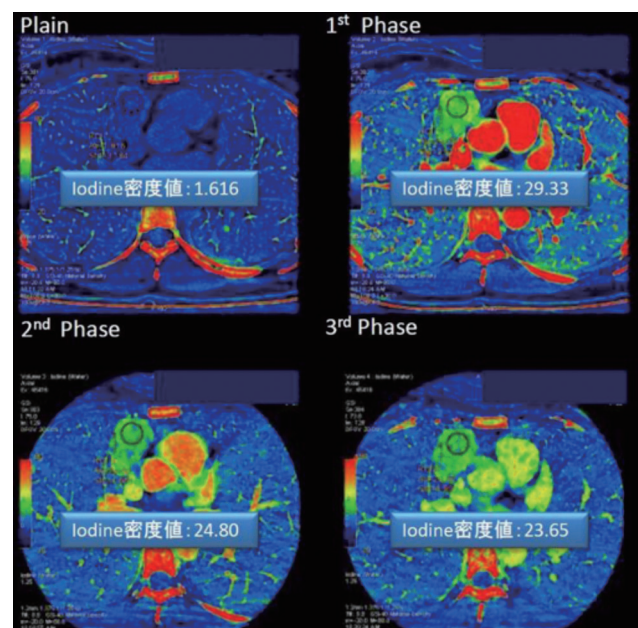
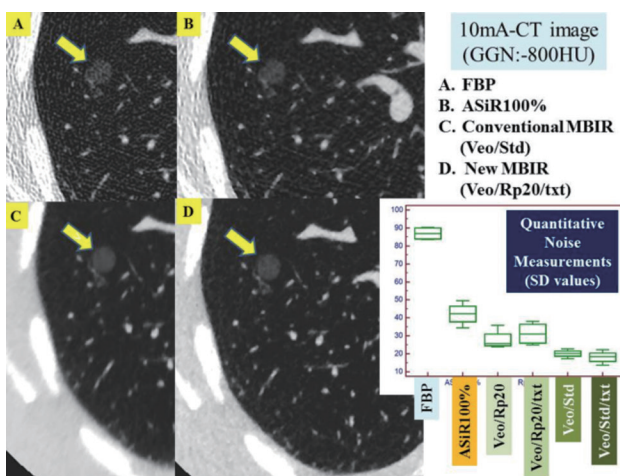
Department of Radiology, Osaka University Graduate School of Medicine, Japan

Recent developments in MDCT technology have made it possible to acquire images of the whole lung with high image quality by vastly improving spatial and temporal resolution. Moreover, high image quality can be obtained even on lower radiation dose by using iterative reconstruction algorithms such as adaptive statistical reconstruction (ASiR) and model based iterative reconstruction (MBiR) available on clinical settings.

Recently, new MBiR has been developed. New MBiR has some selectable parameters for reconstruction, such as RP05, RP20, NR05, and NR40. In addition, we can use Texture Enhancement setting, which rebalances the noise distribution throughout the MBiR image volume and achieves a more isotropic noise behavior. Although conventional MBiR was more advantageous in noise reduction than new MBiR, new MBiR can provide more appropriate image quality for lung even on low dose CT by improving clarity of vessels and nodules than conventional MBiR: it can reduce so-called blotchy findings.

On the other hand, recent MDCT (Discovery CT750HD; GE Healthcare) can provide with various quantitative analyses. As one of techniques, we can use dual energy CT with the fast kilovoltage (kVp) switching technique. The gemstone spectral imaging (GSI) produced by this GE's dual energy CT system can yield monochromatic image sets, which can improve image, differentiate material, reduce artifact, and so on.

In this session, we would like to introduce some papers including our own experiments about recent iterative reconstruction technique 'new MBiR(Veo3)' and quantitative analyses using GSI in thoracic area. It is much appreciated if our information would be useful in your clinical and research setting.



CyberKnife: Real Time Image Guided Radiation Therapy for Lung Cancer

Hideki Nishimura

Department of Radiation Oncology, Kobe Minimally Invasive Cancer Center, Japan
Visiting Associate professor, Kobe University, Japan

Stereotactic ablative radiotherapy has emerged as a promising treatment for early stage non-small cell lung cancer. The CyberKnife image-guided robotic radiosurgery system has unique technical characteristics that make it well suited for stereotactic radiotherapy of tumors that move with breathing, including lung tumors. The CyberKnife is a frameless image-guided robotic radiotherapy system involving a 6-MV linear accelerator mounted on a robotic arm. The imaging system consists of two diagnostic x-ray sources mounted to the ceiling paired with amorphous silicon detectors to acquire live digital radiographic images of the tumor or implanted fiducial markers. The respiratory tracking system enables 4D real-time tracking of tumors that move with respiration. Owing to this system, moving tumors can be treated with an excellent accuracy while patients breathe normally. Image-guided robotic stereotactic radiosurgery of lung tumors with CyberKnife achieves excellent rates of local disease control with limited toxicity to surrounding tissues.

Abstracts

Evening Lecture

| Evening Lecture 1-1

CT-Based Imaging Biomarkers

David A. Lynch

National Jewish Health, USA

Because of its excellent spatial and contrast resolution. Pulmonary CT is in many ways an ideal imaging biomarker for assessing the extent of diffuse lung diseases. Lung attenuation can be used as a direct surrogate of the proportion of lung tissue and air in every voxel. Quantitative CT (QCT) has been used to determine the extent of emphysema for over 25 years, and has led to substantial advances in our understanding of the clinical associations, genetics and natural history of emphysema, as documented in several large multi-center studies. QCT has been used as a biomarker of panlobular emphysema related to alpha-1 antitrypsin deficiency. Gas trapping, measured by quantitative volumetric expiratory CT, is recognized as a useful biomarker of obstructive lung diseases including asthma and COPD, and inspiratory-expiratory registration is a promising technique to distinguish emphysema from non-emphysematous gas trapping. In fibrotic lung diseases, the focus has evolved from simple histogram analysis to measures that use local histogram and textural analysis.

Despite these advances, several important challenges remain before QCT can be accepted as an imaging biomarker. Most important of these is variation in inspiratory and expiratory lung volumes, which has a major influence on lung attenuation values. Other sources of variation include variation in measured CT attenuation across scanner manufacturers and models, differing reconstruction kernels, and varying methods of automatic exposure control. The Quantitative Imaging Biomarkers Alliance (QIBA) is actively addressing all of these issues.

| Evening Lecture 1-2

MR Based Imaging Biomarkers

David L. Levin

Department of Radiology Mayo Clinic, USA

Voluntary Associate Clinical Professor of Radiology University of California, USA

Across imaging modalities, there is an increasing focus on providing quantitative data that can be used to better evaluate patients. These imaging biological markers, or biomarkers, can provide data beyond the qualitative assessment of anatomy and pathology present on an image. Magnetic Resonance (MR) imaging is able to provide a wealth of quantitative data that may be used to predict clinical endpoints, such as mortality, or may act as surrogates for the presence or progression of a given disease. In this presentation, the use of MR measurements as biomarkers will be discussed with respect to lung cancer, pulmonary blood flow and vascular disease, and interstitial lung disease.

| Evening Lecture 2-1

CT assessment of pulmonary hypertension

Sang Min Lee

Asan Medical Center, Korea

1. CT assessment of pulmonary hypertension
 - A. CT provides detailed views of pulmonary vessels and lung parenchyma and becomes a powerful method to determine cause of PH
 - i. To rule out chronic thromboembolic pulmonary hypertension (CTEPH), coronary heart disease (CHD), pulmonary veno-occlusive disease (PVOD), pulmonary capillary hemangiomatosis (PCH)
 - B. CT findings
 - i. Heart
 1. Rt.-side cardiac enlargement and hypertrophy
 2. Wall thickness $\geq 4\text{mm}$
 3. Rt. and Lt. ventricle diameter ratio > 1
 4. Reduction in RV contractility / paradoxical systolic motion of interventricular septum (ECG gated CT)
 5. Flattening or bowing of interventricular septum toward LV
 6. Pericardial effusion
 7. Underlying heart disease: ASD, PDA, VSD, PAPVR or TAPVR
 - ii. Pulmonary vessel
 1. Diameter of main PA measured at bifurcation level: $> 29\text{mm}$ (sensitivity 87%, specificity 89%)
 2. Ratio of diameter of main PA to aorta > 1
 3. Segmental artery-to-bronchus ratio > 1
 4. Peripheral vascular pruning: Vasoconstriction predominantly on subsegmental level
 5. Pulmonary vein: variable
 - A. Small diameter in PH d/t arterial disease
 - B. Enlarged in PH d/t Lt.-sided heart disease
 - iii. Lung
 1. No visually assessable parenchymal changes in primary PAH
 2. Mosaic perfusion: commonly in CTEPH, infrequently in parenchymal disease, primary PAH
 3. Pleural effusion and/or hemorrhagic infarctions
 4. Thickened septal lines, poorly defined nodular lesions and lymphadenopathy in PVOD or CH

Pulmonary Hypertension: Clinical presentation and Functional Assessment Using Imaging

Mark L. Schiebler

University of Wisconsin, School of Medicine and Public Health, Department of Radiology, USA

Abstract

The diagnosis of pulmonary arterial hypertension (PAH) and the many other causes of pulmonary hypertension (PH) is often late in the disease course when damage to the microvasculature of the lung has already occurred. Much like systemic arterial hypertension, PAH is a silent disease that has no simple test for its presence.

The current clinical classification system (Dana Point 2008) is now based on treatment paradigms rather than the underlying physiology and whether or not the cause was pre or post capillary.

The purpose of advanced imaging methods is to determine the causative etiology and determine right ventricular function. Pharmacologic reduction of pulmonary artery pressure improves right ventricular performance and helps to prolong life in these unfortunate patients.

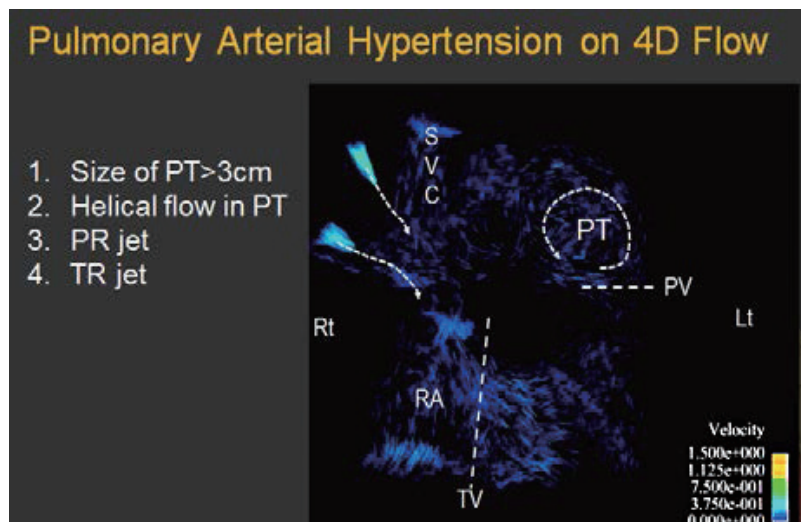


Figure 1: 4D flow in the setting of pulmonary arterial hypertension from partial anomalous pulmonary venous return showing helical flow in the main pulmonary artery and jets of pulmonary valve insufficiency (PR) and tricuspid valve insufficiency (TR).

References

1. Galie N, Hoeper MM, Humbert M, et al. Guidelines for the diagnosis and treatment of pulmonary hypertension: the Task Force for the Diagnosis and Treatment of Pulmonary Hypertension of the European Society of Cardiology (ESC) and the European Respiratory Society (ERS), endorsed by the International Society of Heart and Lung Transplantation (ISHLT). *Eur Heart J.* 2009;30(20):2493-537.
2. Schiebler ML, Bhalla S, Runo J, et al. Magnetic resonance and computed tomography imaging of the structural and functional changes of pulmonary arterial hypertension. *J Thorac Imaging.* 2013;28(3):178-93.

Abstracts

Core Session

Core Session 1 - Invited Speaker 1 -

Distal lesions of chronic thromboembolic pulmonary hypertension and balloon pulmonary angioplasty

Takeshi Ogo

National Cerebral and Cardiovascular Center, Japan

Chronic thromboembolic pulmonary hypertension (CTEPH) is high pulmonary pressure condition caused by obstruction of chronic organized pulmonary thromboembolism, leading to right heart failure and death if left untreated. Surgical procedure, pulmonary endarterectomy, is the gold standard treatment for CTEPH. However, one third of the CTEPH patients are judged as inoperable because of several reasons even in international CTEPH centre. Recently, balloon pulmonary angioplasty (BPA) has been developed as a new alternative treatment for inoperable CTEPH patients. One of the favorable candidates for BPA is high surgery risk due to comorbidity and distal lesions. This new catheter based treatment opens up new world for the treatment of CTEPH. However, distal lesions of CTEPH have not been visualized clearly by conventional imaging modality, which makes angioplasty difficult. Recently we developed a detailed computed tomography imaging to unveil distal CTEPH lesions. This CT imaging opens up a new world of diagnosis of CTEPH and enables us to make a better strategy for BPA in terms of target lesion selection. We presume this distal lesions unveiled by detailed CT is the key elements of CTEPH pathophysiology.

Core Session 1 - Invited Speaker 2 -

Update for Treatment for Pulmonary Thromboembolic Disease

Nobuhiro Tanabe

Department of Advanced Medicine in Pulmonary Hypertension, Graduate School of Medicine, Chiba University, Japan

Pulmonary thromboembolism (PTE) becomes prevalent in Japan, and the annual number of patients has increased from 3492 in 1996 to 16096 in 2011. The increased recognition of PTE and prevalence in CT based diagnosis contribute to the increased PTE patients.

Although the treatment using heparin followed by warfarin is still prevalent, especially in high or intermediate risk acute PTE, recently the novel oral anticoagulants become available in venous thromboembolism, and outpatient based treatment for low risk acute PTE has just started. According to the JAVA study, inferior vena cava (IVC) filter was more frequently used in Japan, but RCT study showed that, compared with anticoagulants alone, a retrievable IVC filter for 3 months in addition to anticoagulants provided no benefit in terms of recurrence or mortality in acute symptomatic PTE. Additional filters should be used in high or intermediate-high risk PTE with extensive deep vein thrombosis, which needs thrombolytic therapy or embolectomy.

Several reports suggest 0.1-9.1% of patients with acute PTE develop chronic thromboembolic pulmonary hypertension (CTEPH), but more than half of CTEPH patients do not have history of PTE. The prognosis of CTEPH was poor in the 1980's (5-year survival ~40%). The mortality of pulmonary endarterectomy has decreased to <5% at expert centers. Advances in balloon angioplasty techniques have resulted in marked improvement in pulmonary hemodynamics and survival for inoperable patients in Japan. A soluble guanylate cyclase activator (riociguat) has become available for patients with inoperable or persistent pulmonary hypertension after surgery. This disease may be cured, once if physicians suspect CTEPH in patients with unexplained exertional dyspnea.

Assessment of pulmonary thromboembolic disease in nuclear medicine

Norinari Honda

Department of Radiology and Radiology Service, Saitama Medical Center, Saitama Medical University, Japan

Diagnosis of acute pulmonary embolism (PE) is now shifted from ventilation/perfusion (V/P) scan to CT pulmonary angiography (CTA) and CT venography (CTV) in conjunction with clinical probability assessed by standardized scoring system such as Wells score. Nuclear medicine physicians changed the long-lasting PIOPED criteria, which categorized V/P scan results into five classes ranging from normal to high probability scans. The new diagnostic schema categorizes V/P scan into PE absent, PE present, and non-diagnostic in conjunction with the scoring system. Recent reports consisting large number of patients show that diagnostic ability of V/P scan with SPECT is comparable to that of CTA/CTV. Also ventilation scan can be safely omitted based on the analysis of PIOPED data base. Recent advance in nuclear medicine technology is utilization of integrated SPECT/CT system for V/P scan, and is shown to have very high diagnostic sensitivity and specificity. The advantage of VP scan over CTA/CTV is smaller radiation dose, availability for patients with past history of severe adverse reaction to iodinated contrast media or renal dysfunction. Also follow up of PE patients with perfusion scan is safer than CTA/CTV. In the diagnosis of chronic thromboembolic pulmonary hypertension, which is rare but unique because of cure by surgery and life-long anticoagulation thereafter, V/P scan plays an important role in differentiation from idiopathic pulmonary arterial hypertension by its very high diagnostic sensitivity and specificity compared with very high specificity but very low sensitivity of CTA/CTV. Nuclear medicine is still valid and should be used in practice.

CT Assessment for Pulmonary Thromboembolism

Jin Hur

Department of Radiology, Severance Hospital, Yonsei University College of Medicine, Korea

Abstract

In the daily clinical routine, CT pulmonary angiography (CTPA) has practically become the first-line modality for imaging of pulmonary circulation in patients suspected of having pulmonary thromboembolism (PTE). However, limitations regarding accurate diagnosis of small peripheral emboli have so far prevented unanimous acceptance of CT as the reference standard for imaging of PTE. Despite the recent encouraging use of CTPA in PTE patients, early meta-analyses on single-slice spiral CTPA have detected strongly varying diagnostic accuracies, with sensitivities ranging from 53% to 100%, and specificities between 83% and 100%. The development of multi-detector row CT (MDCT) has led to improved visualization of peripheral pulmonary arteries and detection of small emboli. With the introduction of the MDCT, diagnostic accuracy has improved consistently over the recent years. The PLOPED II trial used 4-detector, 8-detector, and 16-detector-row CT scanners in a multicenter setting and reached a combined sensitivity and specificity of CTPA and CT venography of 90% and 95%, respectively, establishing the important role of CT angiography as the main diagnostic test in PTE. While the introduction of MDCT technology has improved CT diagnosis of PTE, it has also challenged its users to develop strategies for optimized contrast material delivery, reduction of radiation dose, and management of large-volume data sets created during these examinations.

Risk stratification is important in patients with PTE, because optimal management, monitoring, and therapeutic strategies depend on the prognosis. Acute right-sided heart failure is known to be responsible for circulatory collapse and death in patients with severe PTE. If untreated, PTE is fatal in up to 30% of patients, but the death rate can be reduced to 2% to 10% if PTE is diagnosed and treated promptly.

The typical CT-based cardiovascular parameter measurements that can be derived from a standard CTPA data set include RV and LV short-axis measurements; RV short-axis to LV short-axis (RV/LV) ratios; main pulmonary artery (PA), ascending aorta, azygos vein, and superior vena cava diameters;

and main PA diameter to aorta diameter ratios. A recent study has demonstrated that RV/LV diameter ratio, the diameters of azygos vein, superior vena cava, and aorta, and contrast medium reflux into the inferior vena cava were significantly different between survivors and nonsurvivors after an acute PE event. However, many other CT findings that may allow refinement of the risk stratification are still under evaluation. Although more complex morphologic and functional findings may be useful for the assessment of treatment effectiveness, their effect on prognosis in patients with severe PTE is currently still being debated in the literature.

The introduction of dual-energy CT (DECT) has allowed radiologists to generate functional imaging as well as traditional anatomic imaging. DECT enables the selective visualization of the iodine component in tissues. An example of this selective visualization being utilized is in lung parenchyma imaging which has been enhanced with iodine contrast material, thus providing vital information about lung perfusion. Using this concept, DECT has recently been put to active use in patients with PTE because it can simultaneously demonstrate pulmonary emboli occluding the PA and the resultant perfusion defects in lung parenchyma.

Several studies have shown the feasibility of dual-energy CT (DECT) in the evaluation of acute PTE. The perfusion defect that was found in the corresponding area of the occluded vessel, and visualization of the perfusion defect with DECT showed good agreement with the findings at perfusion scintigraphy. DECT can provide both anatomical and iodine mapping information of whole lungs. This technology has the capacity to improve the diagnostic accuracy of PTE through comprehensive analysis of perfusion of lung parenchyma and CTPA obtained during a single contrast-enhanced chest CT scan in a dual-energy mode. Therefore, DECT may yield more information about the burden of PTE because both perfusion and angiographic images are obtained without an additional radiation dose.

In conclusion, CT will remain the most powerful and clinically most important tool in the evaluation of PTE patients. Routine CTPA offers an accurate and quick depiction of the pulmonary clots, and this method is available nearly everywhere. In addition, CT can provide crucial information on the hemodynamic stability and prognosis of a patient suffering from acute PTE. New acquisition strategies, such as dual-energy techniques (perfusion imaging, ventilation imaging) and very fast and low-dose acquisition protocols using the second-generation dual-source CT (DSCT) will further strengthen this position.

References

1. Goldhaber SZ. Pulmonary embolism. *N Engl J Med* 1998;339:93-104.
2. Miniati M, Marini C, Allesscia G, et al. Non-invasive diagnosis of pulmonary embolism. *Inter J Cardiol* 1998;65 Suppl 1:83-6.
3. Stein PD, Fowler SE, Goodman LR, et al. Multidetector computed tomography for acute pulmonary embolism. *N Engl J Med* 2006;354:2317-2327.
4. Wittram C, Maher MM, Yoo AJ, et al. CT angiography of pulmonary embolism: diagnostic criteria and causes of misdiagnosis. *Radiographics* 2004;24:1219-1238.
5. Ghaye B, Ghuysen A, Willems V, et al. Severe pulmonary embolism: pulmonary artery clot load scores and cardiovascular parameters as predictors of mortality. *Radiology*. 2006;239:884-891.
6. Schoepf UJ, Costello P. CT angiography for diagnosis of pulmonary embolism: state of the art. *Radiology* 2004;230:329-337.
7. Engelke C, Schmidt S, Bakai A, Auer F, Marten K. Computer-assisted detection of pulmonary embolism: performance evaluation in consensus with experienced and inexperienced chest radiologists. *Eur Radiol* 2008;18:298-307.
8. Fink C, Johnson TR, Michaely HJ, et al. Dual-energy CT angiography of the lung in patients with suspected pulmonary embolism: initial results. *Rofo* 2008;180:879-883.
9. Hoey ET, Gopalan D, Ganesh V, et al. Dual-energy CT pulmonary angiography: a novel technique for assessing acute and chronic pulmonary thromboembolism. *Clin Radiol* 2009; 64:414-419.

MR Assessment for Pulmonary Thromboembolic Disease

David L. Levin

Department of Radiology Mayo Clinic, USA
Voluntary Associate Clinical Professor of Radiology University of California, USA

Pulmonary thromboembolic disease is relatively common within the general population and occurs with substantial frequency in select sub-groups of patients. Although variably reported, untreated mortality is significant and is reduced with timely diagnosis and therapy. Currently, computed tomography (CT) is the test of choice for most individuals with suspected pulmonary thromboembolic disease. However, magnetic resonance (MR) imaging may be indicated for selected individuals. Several imaging approaches are available for the MR evaluation of suspected pulmonary thromboembolic disease, including MR angiography, perfusion imaging, and ventilation imaging. Results from older multi-centered trials suggested that the sensitivity of MR angiography was less than that of CT, while the rate of technically inadequate studies was higher. However, results from more recent studies performed at experienced institutions suggest similar overall test performance between CT and MR.

Core Session 1 - Scientific Presentation 1 -

Assessment of Cross-Sectional Lung Ventilation-Perfusion Imbalance in Primary and Passive Pulmonary Hypertension with Automated V/Q Quotient SPECT

Kazuyoshi Suga¹, Munemasa Okada², Naofumi Matsunaga²

1. Department of Radiology, St. Hill Hospital, Japan

2. Department of Radiology, Yamaguchi University, Japan

Purpose: Cross-sectional lung ventilation (V)-perfusion (Q) imbalance in primary pulmonary arterial hypertension (PAH) and passive pulmonary hypertension (PH) was characterized by automated V/Q quotient SPECT.

Materials and Methods: Technegas/MAA SPECT-derived V/Q quotient SPECT and V/Q profile were automatically built to characterize cross-sectional lung V-Q imbalance in 12 patients with primary (idiopathic or familial) PAH and 15 patients with passive PH associated with left ventricular dysfunction or failure. The abnormality of V/Q distribution in these patients was correlated with PaO₂ and pulmonary arterial pressure and with lung morphologic changes on CT.

Results: Markedly low V/Q ratios (reverse V-Q mismatch) in the background lungs with heterogeneous V/Q distribution was seen in 12/12 (100%) patients with primary PAH and in 10/15 (66%) patients with passive PH, which were predominantly seen in upper lung zone. Including these regions with reverse V-Q mismatch, V/Q profile frequently showed flattened peaks with asymmetric and broadened V/Q distribution in all patients, with significant correlation between the standard deviation (SD) of V/Q ratios in the entire lungs and PaO₂ and mean pulmonary arterial pressure (both; P < 0.01). At the lung regions with reverse V-Q mismatch, bronchial lumens compressed by dilated pulmonary arteries and heterogeneous lung attenuations were frequently seen on CT.

Conclusions: Patients with primary PAH and passive PH appear to characteristically have a high prevalence of reverse V-Q mismatch indicative of an inadequate hypoxic vasoconstriction reflex on V/Q quotient SPECT, frequently accompanied with heterogeneous lung attenuations and compressed airways on CT.

Core Session 1 - Scientific Presentation 2 -

Utility of computed tomography-derived measurements of the pulmonary vasculature in the diagnosis and hemodynamic assessment of pulmonary arterial hypertension

Kaoruko Shimizu, Ichizo Tsujino, Hiroshi Ohira, Taku Watanabe, Toshitaka Nakaya, Masaharu Nishimura

First Department of Medicine, Hokkaido University School of Medicine, Japan

We examined the clinical relevance of three computed tomography (CT)-derived indices of the pulmonary vasculature in pulmonary arterial hypertension (PAH) (N=61 Idiopathic ;N=14, Heritable ;N=4, Drugs induced ;N=1, Associated with connective tissue disease; N=34, Associated with portal hypertension; N=8): 1. Ratio of diameter of the pulmonary artery to that of the Aorta (PA/Ao); 2. Diameter of the right lower pulmonary vein (PVD, N=60); and 3. Percent (%) cross sectional area of the small pulmonary vessels for the lung area (%CSA<5). CT data of 28 patients with PAH (Idiopathic;N=10, Associated with connective tissue disease;N=18) was available for the assessment of %CSA<5, which is performed with non-enhanced CT (Matsuoka, et.al AJRCCM 2010) PA/Ao and %CSA<5 were significantly higher in PAH subjects (PA/Ao; 1.19±0.25, %CSA<5; 0.39±0.14 (mean±SD)) as compared with controls without any respiratory or cardiovascular diseases (N=59) (PA/Ao; 0.78±0.10 %CSA<5; 0.31±0.16). PA/Ao positively correlated with pulmonary arterial mean, systolic and diastolic pressure, and pulmonary vascular resistance (PVR). The %CSA<5 negatively correlated with PVR and positively with cardiac index (CI). PVD of PAH subjects (N=60) (9.36±2.26) was similar to that of the controls (9.90±1.90), but had a stronger positive correlation with CI than %CSA<5. ROC analysis for the diagnosis of PAH showed the highest AUC for PA/Ao (0.96) followed by %CSA<5 (0.71) and PVD (0.59). CT-derived indices of the pulmonary vasculature are useful for the diagnosis and hemodynamic assessment of PAH.

Diagnostic Performance of the Combined Pulmonary Arterial MRI and Indirect Magnetic Resonance Venography Using Unenhanced and Contrast-Enhanced Techniques in the Diagnosis of Venous Thromboembolism

Nevzat Karabulut, Furkan Kaya, İsmail Yılmaz

Pamukkale University Medical Center, Turkey

Our aim was to determine the diagnostic performance of the combined pulmonary arterial MRI and indirect magnetic resonance venography (MRV) technique in the diagnosis of venous thromboembolism (VTE).

Forty-four patients (33 male, 11 female) who underwent CTA for suspected pulmonary embolism (PE) constituted the study population. Patients underwent combined pulmonary and lower extremity MRI, and Doppler sonography within 72 hours after CTA. Combined MRI (pulmonary arterial MRI and MRV) included two techniques: unenhanced balanced SSFP and contrast-enhanced 3D-GRE.

CTA showed a total of 244 emboli in 33(75%) of 44 patients whereas deep vein thrombosis (DVT) was observed in 34(77%) subjects. 27(61%) patients had both PE and DVT whereas 6(14%) subjects had only PE, and 4(14%) patients had only DVT. Of 11 patients without PE on CTA, 7(15.9%) had DVT. Sensitivities for SSFP vs 3D-GRE MR respectively in PE detection were 87.9% vs 100% on a per-patient basis, and 53.7% vs 73% on a per-embolus basis. Twenty-eight (90.3%) of 34 patients who had diagnosis of DVT by Doppler ultrasound, were also detected by SSFP sequence ($\kappa=0.879$ on per patient basis; $\kappa=0.857$ on per thrombus basis). 3D-GRE detected thrombus in 31 patients shown by Doppler ultrasound, whereas DVT in three patients was detected only by 3D-GRE imaging ($\kappa=0.821$ on per patient basis; $\kappa=0.896$ on per thrombus basis).

Contrast-enhanced 3D-GRE is the most sensitive sequence in PE and DVT detection. SSFP can be a good alternative if CTA or Doppler ultrasound cannot be performed and there is a contraindication to contrast agents.

| Core Session 2 - Invited Speaker 1 -

An Update on the Management of Lung Nodules

Jin Mo Goo

Department of Radiology, Seoul National University Hospital, Korea

With the widespread utilization of chest CT and success of the National Lung Screening Trial (NLST), the importance of the proper evaluation of lung nodule has increased and many guidelines for lung nodule management have been suggested. However, it is essential to understand the approaches for incidentally found nodules and screen detected nodules are different as the risk of subject is different and the annual repeat CT is usually recommended in a screening setting. Basic determinants of nodule management guidelines such as Fleischner Society recommendations and LungRADS are the size and attenuation of a nodule. A large false positive rate which potentially requires further examinations was an issue in NLST, but recent studies suggested that considerable number of false positive results can be reduced with minimal increase of delayed diagnosis of lung cancer by increasing the size threshold from 4 mm to 6 mm. Although the classification of a nodule according to its attenuation (solid, part-solid GGN, pure GGN) seems simple, there is considerable interobserver variability. In the measurement of solid component in subsolid nodules, lung window settings can provide better results than mediastinal window settings when compared with pathology measurement of invasive component. Despite its high likelihood of malignancy of subsolid nodule, recent studies revealed that more conservative management can be recommended for pure GGNs.

| Core Session 2 - Invited Speaker 2 -

Update of Medical Therapy for Advanced Lung Cancer

Koichi Takayama

Department of Pulmonary Medicine, Kyoto Prefectural University of Medicine, Japan

The prognosis of advanced lung cancer patient has been improved with the progress of medical therapy. 30 years ago, there was no effective anti-cancer drugs for lung cancer, and the median overall survival time of advanced lung cancer patient was shorter than 6 months. Cisplatin prolonged the survival time to one year and longer, and clarified the clinical significance of systemic chemotherapy for advanced lung cancer. Discovery of driver oncogene, EGFR mutation and the development of EGFR tyrosine-kinase inhibitor made a paradigm shift in the field of lung cancer treatment. Currently, the lung cancer patients with EGFR mutation live longer than 4 years. Biomarker-based medicine accelerate the personalized cancer treatment strongly. Immune-checkpoint inhibitor gather attention as an effective drug for lung cancer as well as melanoma recently. The results of clinical trials showed the drug has the possibility to cure this fatal disease. In this paragraph, I look back into the history of lung cancer treatment strategy, and have a view of near-future medical therapy.

Lung cancer treatment assessment in the era of precision medicine: RECIST and beyond

Mizuki Nishino

Department of Radiology, Harvard Medical School, USA

ABSTRACT:

Recent advances in understanding of genomic mechanisms specific to lung cancer and successful clinical application of the knowledge have transformed the oncologist's approach to patients with lung cancer. Imaging plays a key role in objectively characterizing tumor response and progression during therapy and defines trial endpoints, and thus should evolve in parallel with the advancement of cancer treatment. The lecture will 1) provide an overview of the recent advances in precision medicine approaches for lung cancer, 2) define the role of imaging-based tumor response evaluations as a "common language" to describe cancer treatment results, and 3) discuss the state-of-the-art approaches for lung cancer using volumetric and functional imaging.

The conventional tumor response criteria based on RECIST guidelines will be reviewed as a generalized standard method that has been widely adapted in oncology trials and practice. Pitfalls and limitations of RECIST, as well as the efforts to complement the limitations will be introduced, with a focus on novel approaches to capture unconventional responses during cancer immunotherapy including immune-related response criteria (irRC). The lecture will also presents tumor volume analysis as a prognostic marker among lung cancer patients treated with targeted therapy, and as a method to objectively define slow progression during tumor regrowth due to acquired resistance. Lung cancer studies using MRI and PET/CT will also be reviewed, with an emphasis of the concept of imaging as a "common language". Future directions will be discussed for radiologist to be key contributors in the era of the precision medicine for lung cancer.

Reference:

1. **Nishino M**, Hatabu H, Johnson BE, McLoud TC. State of the art: response assessment in lung cancer in the era of genomic medicine. *Radiology*. 2014 Apr;271(1):6-27
2. **Nishino M**, Tirumani SH, Ramaiya NH, Hodi FS. Cancer immunotherapy and immune-related response assessment: the role of radiologists in the new arena of cancer treatment. *Eur J Radiol*. 2015 Jul;84(7):1259-68.
3. **Nishino M**, Jagannathan JP, Krajewski KM, O'Regan KN, Hatabu H, Shapiro G, Ramaiya N. Personalized Tumor Response Assessment in the Era of Molecular Medicine: Cancer-specific and Therapy-specific Response Criteria to Complement Pitfalls of RECIST. *AJR Am J Roentgenol*. 2012 Apr;198(4):737-45.
4. **Nishino M**, Jagannathan JP, Ramaiya N, Van den Abbeele AD. Pictorial review of the new Response Evaluation Criteria in Solid Tumors: revised RECIST guideline version 1.1 – What oncologists want to know and what radiologists need to know. *AJR Am J Roentgenol*. 2010; 195:281-9.

PET Imaging for Prognosis and Treatment Response Assessment in Lung Cancer

Tae Jung Kim

Department of Radiology, Samsung Medical Center, Korea

Computed tomography (CT) and positron emission tomography (PET) using F-18 fluorodeoxyglucose (FDG) play an important role in the diagnosis and management of non-small cell lung cancer (NSCLC). Standardized uptake value (SUV) and maximum SUV are the most commonly used quantitative parameters derived from PET studies. PET/CT proves tumor aggressiveness and metabolic activity and predicts patient outcome and survival independent of the TNM staging. Recent many studies evaluating the association between PET response to conventional cytotoxic therapy and survival in NSCLC patients demonstrated that a reduction in tumor FDG retention is more likely to be associated with both pathologic response and improved survival. PET response Criteria in Solid Tumor (PERCIST) may be used in clinical trials and in structured quantitative reporting. Because of the increased use of molecular targeting therapy in NSCLC patients, recent investigations have attempted to address the utility of FDG PET in quantifying metabolic response of tumors to targeted therapy such as epidermal growth factor receptor (EGFR) tyrosine kinase inhibitor or anaplastic lymphoma kinase (ALK) inhibitor. Advances in image acquisition and processing with PET/CT technology have provided another potential marker for monitoring therapy response. Total body tumor burden, which reflects the volume of tumor tissue demonstrating increased FDG uptake at PET, or metabolic tumor volume (MTV), is now being evaluated as a novel potential prognostic factor. In addition, emerging novel PET tracers for functional and molecular imaging may help to further study the biologic behaviors of lung cancer during therapy.

CAD for Prognosis and Treatment Response Assessment in Lung Cancer

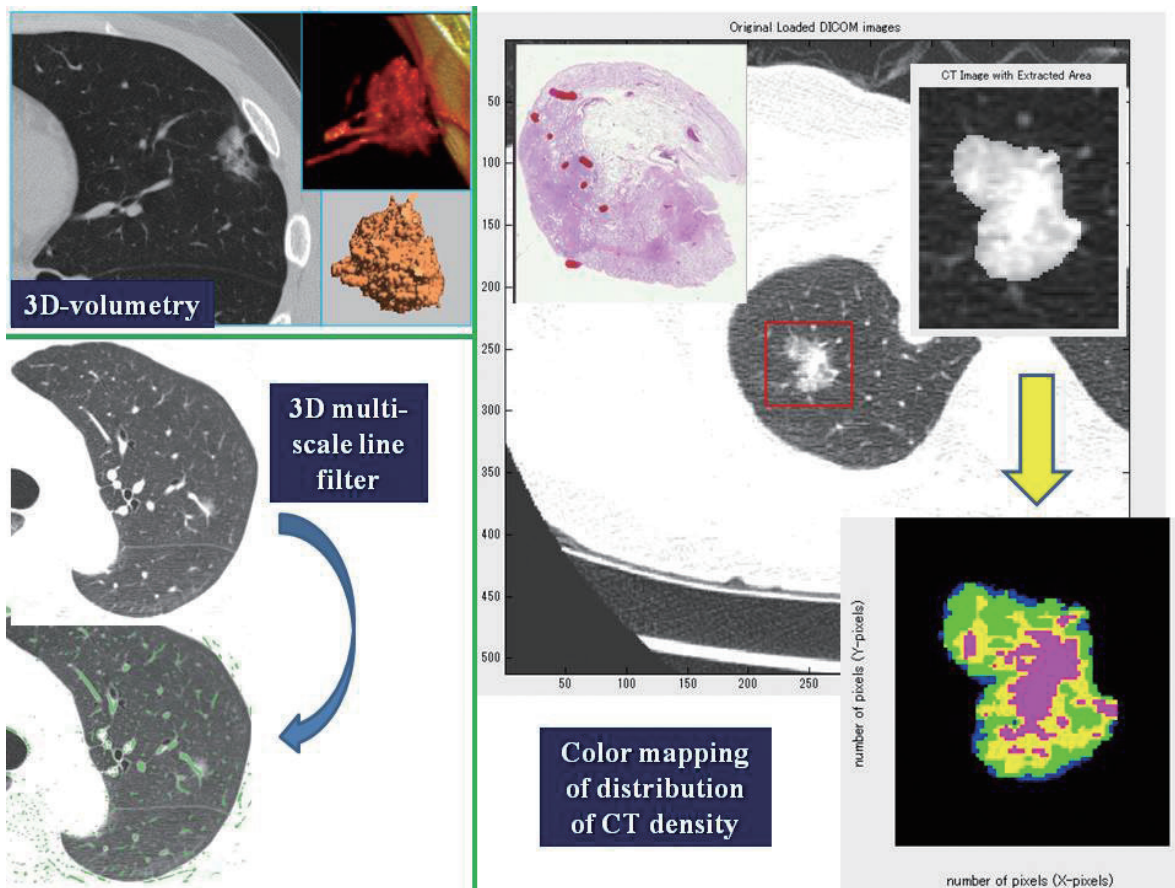
Masahiro Yanagawa

Department of Radiology, Osaka University Graduate School of Medicine, Japan

CT has been considered a promising tool for the detection, characterization and follow-up of lung cancer since back in the day. It goes without saying that morphological evaluation and/or simple manual measurement by radiologists are essential for the diagnosis of lung cancer. However, these subjective evaluations are disadvantageous in the precision of diagnosis and the reproducibility measurements. The recent advances in CT technology have enabled to provide volume data with high image quality. Moreover, many CAD systems have been developing, resulting in the quantitative analyses such as the automatic nodule detection, the assessment of nodule malignancy, and the treatment response assessment in lung cancer.

Although volumetric measurement of nodules is a promising technique that enables both accurate and precise for the quantification of lung nodules, it is more challenging in subsolid nodules because of difficulties in segmentation and accurate delineation between a tumor's ground-glass margins and the adjacent normal parenchyma.

In this session, we would like to introduce some papers about quantitative analyses for lung cancer using CAD systems including our custom-developed CAD system. We summarized the current status of CAD by focusing on the prediction of nodule malignancy and volumetry in assessing the response to treatment. It is much appreciated if our information on CAD would be useful in your clinical and research setting.



Core Session 2 - Invited Speaker 6 -

New MR Techniques for Prognosis and Treatment Response Assessment

Hidetake Yabuuchi

Department of Health Sciences, Graduate School of Medical Sciences, Kyushu University, Japan

Response Evaluation Criteria in Solid Tumors (RECIST) 1.1 is widely used for monitoring malignant solid tumors. However, there are some limitations in the evaluation based on size alone. Inter-observer or intra-observer variance could exist in the evaluation, and long axis diameter of cavitory lesions might not accurately reflect the tumor response. Changes other than tumor size include necrosis, apoptosis, hemorrhage, and hemodynamic change. Especially, molecular-targeted agents are designed to inhibit the cell signal pathway; therefore imaging biomarkers other than size might be able to predict tumor response or prognosis.

There have been many functional imaging studies including perfusion CT, dynamic contrast-enhanced magnetic resonance imaging (DCE-MRI), Diffusion-weighted MRI (DWI), and FDG-PET on the prediction of early response and prognosis after chemotherapy of advanced NSCLC. Among them, DWI is a specific modality that produces in vivo images of biological tissues weighted with the local microstructural characteristics of water diffusion. Apparent diffusion coefficient (ADC) derived from DWI, which reflects the mobility of water molecules in the tissue, has been reported to be a useful marker for prediction and early detection of response to chemotherapy or chemotherapy and radiation therapy in various malignant tumors. Patients could switch anticancer drugs after the first cycle of chemotherapy and avoid unnecessary systemic toxicity if the first-line agents were determined to be ineffective on the basis of the early ADC change.

In this presentation, I will review the recent MR studies on prediction of early response and prognosis after chemotherapy of advanced NSCLC.

Core Session 2 - Invited Speaker 7 -

Radiomics and Radiogenomics in Lung Cancer: Clinical Perspectives

Ho Yun Lee

Samsung Medical Center, Sungkyunkwan University School of Medicine, Korea

Cancers are heterogeneous across a wide range of temporal and spatial scales. In other words, tumors of the same organ and cell type can have remarkably diverse appearances in different patients. Furthermore, even within a single tumor, marked variations in imaging features, such as necrosis or contrast enhancement, are common. Similar spatial variations recently have been reported in genetic profiles. This genetic heterogeneity is a clear barrier to therapy based on molecular targets, since the identified targets do not always represent the entire population of tumor cells in a patient.

Heterogeneity in genetic properties of different cells in the same tumor reflects ongoing intratumoral evolution, which is subject to Darwinian principles, and it is governed by predictable and reproducible interactions between environmental selection forces and cell phenotype (not genotype). This link between regional variations in environmental properties and cellular adaptive strategies may permit clinical imaging to be used to assess and monitor intratumoral evolution in individual patients. In the past several years, radiology research has increasingly focused on quantifying these imaging variations in an effort to understand their clinical and biologic implications. This approach is enabled by new methods that extract, report, and analyze quantitative, reproducible, and mineable clinical imaging data.

Radiomics refers to the extraction and analysis of large amounts of advanced quantitative imaging features with high throughput from medical images obtained with computed tomography, positron emission tomography or magnetic resonance imaging. Radiomics data are in a mineable form that can be used to build descriptive and predictive models relating image features to phenotypes or gene-protein signatures. The core hypothesis of radiomics is that these models, which can include biological or medical data, can provide valuable diagnostic, prognostic or predictive information. In other words, tumor characteristics observable at clinical imaging reflect molecular-, cellular-, and tissue-level dynamics; thus, they may be useful in understanding the underlying evolving biology in individual patients. Ultimately, advances in image analysis will place clinical imaging in an increasingly central role in the development of evolution-based patient-specific cancer therapy.

Core Session 2 - Scientific Presentation 1 -

Prediction of therapeutic effect of chemotherapy for non-small-cell lung cancer using perfusion CT: comparison between regimens with and without anti-angiogenic agent

Hidetake Yabuuchi¹, Satoshi Kawanami², Takeshi Kamitani², Yuzo Yamasaki²,
Torahiko Yamanouchi², Koji Sagiyama², Michinobu Nagao², Hiroshi Honda²

1. Department of Health Sciences, Kyushu University Graduate School of Medical Sciences, Japan

2. Department of Clinical Radiology, Kyushu University Graduate School of Medical Sciences, Japan

Purpose

To elucidate whether the parameters derived from pre-treatment perfusion CT could predict the therapeutic response in patients who underwent chemotherapy for non-small-cell lung cancer.

Materials and Methods

This prospective study was approved by the institutional review board, and informed consent was obtained. Sixty-six patients (42 men, 24 women; age range 29-82 years, mean 63.4) with stage III or IV non-small-cell lung cancer who underwent chemotherapy were enrolled. The chemotherapy regimens were with anti-angiogenic drug (bevacizumab) in 20 and without bevacizumab in 46 patients. All patients underwent perfusion CT within a week before the initiation of chemotherapy. Analyzed parameters were pre-treatment pulmonary artery flow (PAF) and bronchial artery flow (BAF) of the tumors. We calculated the tumor reduction rate two courses after the chemotherapy. Pearson correlation coefficients were used to examine the relationship between the PAF or BAF and the tumor reduction rate after two courses of chemotherapy. We separately evaluated in both regimens with and without bevacizumab.

Results

Significant correlation was found between pre-treatment BAF in regimen with bevacizumab and tumor size reduction rate after two courses of chemotherapy ($r^2 = 0.43$, $P < .01$). Pre-treatment BAF in regimen without bevacizumab, pre-treatment PAF in regimens with and without bevacizumab showed no significant correlation with tumor size reduction rate after two courses of chemotherapy.

Conclusion

Pre-treatment BAF derived from perfusion CT seems to be a promising tool to help predicting the response to chemotherapy with bevacizumab in patients with non-small cell and non-squamous cell lung cancer.

Core Session 2 - Scientific Presentation 2 -

MR evaluation of the treatment response of HCC827 to erlotinib alone or combination with bevacizumab in mice model

Yi-Fang Chen¹, Yeun-Chung Chang², An Yuan³, Jyh-Horng Chen⁴, Chong-Jen Yu³

1. National Taiwan University, Taiwan

2. Departments of Medical Imaging and Internal Medicine, National Taiwan University Hospital, Taiwan

3. National Taiwan University Hospital, Taiwan

4. Department of Electrical Engineering, National Taiwan University Taiwan

This study was to investigate the therapeutic response of non-small cell lung cancer mice model to EGFR-tyrosine kinase inhibitor (TKI) erlotinib and anti-angiogenesis agent bevacizumab using dynamic contrast enhanced (DCE) and diffusion-weighted (DW) MRI. Lung cancer mice model with adenocarcinoma HCC827 (TKI sensitive) and HCC827R (TKI resistant) was used. All animal studies from baseline to follow-up periods were performed using a 7T dedicated animal MR scanner (BioSpec, Bruker, Germany). The results found that the temporal changes in DCE-MRI derived parameters (Ktrans, kep, iAUC90) and apparent diffusion coefficient (ADC) were significantly correlated with corresponding tumor sizes compared to the baseline. Compared to the control group (HCC827), tumor growth was both inhibited in erlotinib only and erlotinib+bevacizumab groups without significant difference. The temporal changes of the Ktrans and kep of erlotinib group and erlotinib+bevacizumab groups significantly decreased at week3 and week4. The temporal change of iAUC90 showed significant decrease only at week4 (68.65% reduction) in erlotinib group and erlotinib+bevacizumab group. Compared to the control group, there was 64.1% reduction in vessel density in erlotinib group and 61.8% reduction in erlotinib+bevacizumab group. Significantly increased tumor apoptosis was found in erlotinib group and in erlotinib+bevacizumab. Increased ADC values of the erlotinib group (75.9% increment) and erlotinib+bevacizumab group (26.4% increment) at week3 were noted. Enlarging areas of central tumor necrosis were also associated with higher ADC values. In contrast to HCC827, progressive enlargement of tumor and no significant differences were found for Ktrans, kep, iAUC90 and ADC in HCC827R.

Dynamic Contrast-Enhanced Integrated PET/MR of Non-Small Cell Lung Cancer: Assessment of Response to Stereotactic Body Radiation Therapy

Yu-Sen Huang^{1,2}, Jenny Ling-Yu Chen^{1,3}, Yao-Hui Tseng^{2,4}, Wei-Chun Ko², Fu-Shan Jaw¹, Yeun-Chung Chang²

1. Institute of Biomedical Engineering, College of Medicine and College of Engineering, National Taiwan University, Taiwan
2. Department of Medical Imaging, National Taiwan University Hospital and National Taiwan University College of Medicine, Taiwan
3. Department of Oncology, National Taiwan University Hospital and National Taiwan University College of Medicine, Taiwan
4. Department of Medical Imaging, National Taiwan University Hospital Yun-Lin Branch, Taiwan

Purpose:

Stereotactic body radiation therapy (SBRT) has shown efficacy as upfront local treatment for non-small cell lung cancer (NSCLC). Several data have suggested that the biological mechanism of SBRT is based on severe vascular damage resulting in reduced blood perfusion and indirect tumor cell death. In this study, we aimed to explore the clinical application of dynamic contrast-enhanced (DCE) integrated PET/MR in patients receiving SBRT, with respect to treatment outcome and prognosis prediction.

Methods and Materials:

Three patients with NSCLC receiving SBRT as primary or salvage treatment underwent DCE integrated PET/MR (Simultaneous hybrid 3T-MR-PET machine, Biograph mMR, Siemens Healthcare) before and two months after SBRT. Image parameters including tumor size, apparent diffusion coefficient (ADC), standardized uptake value (SUV), K_{trans} , k_{ep} , v_e , v_p , and $iAUC_{60}$ were analyzed.

Results:

Tumor size before and after SBRT was 28.3 ± 27.5 mm and 23.3 ± 23.2 mm, respectively, with 18% decrements. The SUV_{max} before and after SBRT was 7.3 ± 5.4 and 3.0 ± 0.7 , respectively, with 44% decrements. Decreased values of all MR-derived parameters were found. Among these parameters, there was a significant decrease of the k_{ep} mean values (before treatment, 1667.0 ± 432.0 ; after treatment, 931.6 ± 345.7 ; 45% reduction; $P = 0.03$).

Conclusions:

MR-PET with functional parameters has the potential to predict early treatment response of patients with NSCLC receiving SBRT.

Core Session 3 - Invited Speaker 1 -

COPD Phenotype and Treatment

Shigeo Muro

Department of Respiratory medicine, Graduate School of Medicine, Kyoto University, Japan

COPD is a heterogeneous disease and the definition of COPD in Global Strategy for Diagnosis, Management and Prevention of COPD (GOLD) includes several concepts. COPD is “a common preventable and treatable disease” and characterized by “persistent airflow limitation that is usually progressive” and associated with “an enhanced chronic inflammatory response in the airways and the lung to noxious particles or gases.” Moreover, exacerbations and comorbidities are important factors to consider the overall severity in individual patients. The pathology of COPD includes two major components such as small airway disease and parenchymal destruction, and the alteration of pulmonary blood vessel pathology may contribute to the COPD pathophysiology. Based on these background several phenotyping are proposed to date. Bronchodilator medications are central to the symptomatic management of COPD and can usually reduce COPD symptoms, reduce the frequency and severity of exacerbations, and improve health status and exercise tolerance. However, it is well known that some patients are “rapid decliners” in pulmonary function and “frequent exacerbators” in spite of the usual treatment. In terms of inflammation, “eosinophilic COPD” may be good responder to inhaled corticosteroid therapy that is, however, is known to be associated with an increased risk of pneumonia. “Emphysema” and “Chronic bronchitis” are classical phenotype and PDE4 inhibitors are beneficial for “Bronchitic COPD”. The concept of “parenchymal destruction” and “airway disease” can be measured and quantified computer assisted images as “low attenuation area” and “airway remodeling”, the former being shown to associate with the severity of comorbidities such as osteoporosis and sarcopenia. The significance of these morphological indices in the selection of medication remains to be elucidated.

Core Session 3 - Invited Speaker 2 -

VENTILATION/PERFUSION TOGRAPHY (V/P SPECT) – THE FUNCTIONAL IMAGING FOR COPD PHENOTYPING

Marika Bajc

Department of Clinical Science, Skåne University Hospital, Sweden

V/P SPECT is imaging technique primarily used in clinical practice for diagnosis of acute pulmonary embolism (PE). However, V/P SPECT has also shown to be a sensitive method in diagnosis of COPD severity and other lung co-morbidity such as PE, pneumonia and left heart failure (LHF).

We are grading severity of COPD based on ventilation distribution after inhalation of Technegas and perfusion distribution after i.v.injection of Tc-MAA. Obstructive bronchitis phenotype is assessed on V defects grading 0-3, based on penetration and deposition of Technegas™ in small airways. Emphysema phenotype is assessed as a matched and reversed mismatch defects of V and P typical pattern. Moreover, recognition of pattern typical for PE, LHF, pneumonia and suspicion of tumor (matched, mismatched or reverse mismatched V/P defects) are always described. All areas with absent/reduced V and or P are then calculated and the reduction of lung function is expressed as a % of the total lung volume.

The distribution of pathological findings in COPD and different pulmonary co_morbidity will be presented as well as calculation of preserved lung function.

Co-existence of obstructive bronchitis and emphysema phenotypes is almost always present in patients with severe COPD. Furthermore, V/P SPECT identified frequently pulmonary co-morbidity in this group of patients. Therefore, conventional diagnostic methods and patient reported outcomes may not be accurate in the assessment of COPD severity.

Core Session 3 - Invited Speaker 3 -

Quantitative CT for COPD phenotyping

Yasutaka Nakano

Division of Respiratory Medicine, Department of Pulmonology, Shiga University of Medical Science, Japan

Chronic obstructive pulmonary disease (COPD) is a disease which is characterized by airflow limitation caused by loss of elastic recoil and/or airway narrowing. The loss of elastic recoil is mainly due to the emphysematous changes, while the airway narrowing is mainly caused by the thickening and narrowing of the membranous bronchioles. These two pathological changes can be quantified using CT. The percentage of low attenuation volume (%LAV) reflects emphysematous lesions and the square root of airway wall area of a hypothetical airway with an internal perimeter of 10 mm (Pi10) shows airway thickening and remodeling. We have recently used these two parameters and reported two separate papers; (I) We previously showed that these two parameters of emphysematous lesions and airway remodeling are independently and complementarily predicted pulmonary function tests. However, the relative contribution of emphysema and airway remodeling to airflow limitation was unclear. We investigated the relative contribution using two separate COPD cohorts. The results showed that both %LAV and Pi10 predicted FEV1/FVC, but the absolute value of the standardized coefficients were 2-3 times higher for %LAV than for Pi10. (II) We also showed that the quantitative CT analysis using these two parameters could divide the COPD patients into four phenotypes: emphysema-dominant, airway-dominant, mixed, and normal-CT phenotype. However, little is known about the characteristics of CT based phenotypes. Quantitative CT analysis found that COPD patients with the mixed phenotype are associated with more severe dyspnea and more frequent hospitalization than the remaining CT based phenotypes.

Core Session 3 - Invited Speaker 4 -

New Quantitative CT Techniques for COPD Phenotyping

Joon Beom Seo

Department of Radiology, University of Ulsan College of Medicine, Asan Medical Center, Korea

In recent studies on COPD, CT has been accepted as one of important research tools in evaluating disease severity and characteristics. The extent of low attenuation area and bronchial wall thickening at segmental and distal level on volumetric CT scan acquired at suspended inspiration state are commonly used as useful markers for evaluating the severity of emphysema and airway wall inflammation, respectively. The clinical values of these two imaging biomarkers are as follows: 1) Many recently studies have proved that the extent of emphysema and bronchial wall thickening are independently related with the degree of airflow limitation, 2) The extent of emphysema is correlated with other clinical parameters such as osteoporosis, exercise capacity, respiratory symptoms and most importantly with BODE index, which is known to be one of best predictors of mortality, 3) Both parameters may be useful in subgrouping/phenotyping of patients, prediction of treatment response, and prediction of disease progression 4) Both parameters are related with frequency of exacerbation. However, volumetric CT, with its superior spatial resolution and superior contrast, has many additional evaluation potentials in assessment and phenotyping of COPD. They include; (1) assessment of air trapping by direct anatomical matching of inspiration and expiration CT, (2) assessment of peripheral vascular changes in COPD, (3) assessment of size of emphysema holes, and (4) direct visualization of ventilation and perfusion function with dual energy CT technique. In this talk, those new CT analysis methods will be introduced with their preliminary clinical research results.

| Core Session 3 - Invited Speaker 5 -

Magnetic Resonance Imaging for Chronic obstructive lung disease phenotyping

Tae Iwasawa

Kanagawa Cardiovascular and Respiratory Center, Japan

The morphological phenotyping of chronic obstructive lung disease (COPD; emphysema or non-emphysema type) has gained considerable attention, because of its relation to genomics. Hyperpolarized helium-3 gas magnetic resonance imaging (MRI) can be used to evaluate airspace enlargement corresponding to emphysema [1]. With clinical proton-MRI, however, it is difficult to visualize both emphysema and bronchial wall thickening because of technical difficulties. The recently developed ultrashort echo time (UTE) pulse sequence can be used to improve pulmonary MR signal; emphysema can be identified without the use of contrast materials [2]. Ohno et al. reported that mean T2* values of the lung measured on UTE correlated with pulmonary function tests and functional lung volume measured on CT [3]. Regarding the assessment of the bronchial wall, Doumes et al. reported that a respiratory-gated, point-wise encoding time reduction with radial acquisition (PERTA) sequence could be used to visualize bronchial wall thickening in patients with cystic fibrosis [4]. In my opinion, morphological COPD phenotyping using clinical MR units will be possible in the near future through such technical developments.

MR can provide a variety of functional information. MR can also be used to assess the comorbidity of COPD, for example, the right ventricular dysfunction [5].

I believe that MR has a great potential for the severity-evaluation and phenotyping of COPD.

1 Kirby M, et al. (2015) *Radiology*:150037

2 Takahashi M, et al. (2010) *J Magn Reson Imaging* 32:326-333

3 Ohno Y, et al. (2014) *J Magn Reson Imaging* 39:988-997

4 Dournes G, et al. (2015) *Radiology* 276:258-265

5 Wells JM, et al. (2015) *Circulation Cardiovascular imaging* 8:e002546

| Core Session 3 - Invited Speaker 6 -

Phenotyping lung disease using optical coherence tomography (OCT)

Harvey O Coxson

Department of Radiology, University of British Columbia, Department of Radiology
Centre for Heart, Lung Innovation, St Paul's Hospital, Canada

Airway diseases are a growing burden around the world. However, the pace of new drug and biomarker discovery has lagged behind those of other common disorders such as cardiovascular diseases and diabetes. One major barrier in airways research has been the inability to accurately visualize large and small airway remodeling using non or minimally invasive instruments. Optical coherence tomography is a new bronchoscopic imaging technique that has generated considerable interest because the spatial resolution approaches that of histology. While relatively more invasive than computed tomography, it has the advantage of not exposing the patient to ionizing radiation. Thus, with the aid of OCT, we may be able to accurately determine and quantify the extent of airway remodeling in asthma and chronic obstructive pulmonary disease. Therefore, these new imaging techniques are very likely to play a front-line role in the study of airways disease and will, hopefully, allow clinicians to phenotype individuals, thereby personalizing their treatment.

Core Session 3 - Scientific Presentation 1 -

Transfer Factor and Blood Gases in the V/P SPECT Emphysema Phenotype of COPD

Marika Bajc¹, Ari Lindqvist², Y Chen³, J Wang⁴, X Y Li⁵, W.M. Shen⁵, C Z Wang⁴, H Huang³, X Y He⁶

1. Skåne University Hospital, Sweden
2. Helsinki University Hospital, Finland
3. Changzheng Hospital, China
4. Xin qiao Hospital, China
5. Hua Dong Hospital, China
6. Suzhou University Affiliated Tumor Hospital, China

In emphysema phenotype (EF) of chronic obstructive pulmonary disease (COPD) lung tissue and blood capillaries disappear locally. Alveolar hypoventilation may cause hypercapnia (partial pressure of CO₂ in blood, PaCO₂ > 45 mmHg) and acidemia (pH < 7.35) and further chronic respiratory acidosis (serum bicarbonate HCO₃⁻ > 30 mmol/L, base excess > 3 mmol/L).

We hypothesized that matched V/P SPECT defects correlate to transfer factor (DLCO), blood gases and acid base status and characterize the pathophysiological consequences of EF in stable COPD.

Sixty six consecutive patients with a confirmed diagnosis of stable COPD (GOLD criteria) and escaping severe cardiac disease, were enrolled in 3 hospitals in Shanghai and Chongqing in an international multicentre trial. Age ranged 44-84 years and smoking pack years from 20-104. Ventilation and perfusion single photon emission tomography (V/P SPECT)1, measurements of DLCO and blood gas status were performed. Matching ventilation and perfusion defects (EP of COPD) were quantitated by measuring percentages of total lung function that was missing (E%). Concomitant pathological ventilation and perfusion defects in V/P SPECT were excluded from the analysis.

A high correlation was found between E% and DLCO (r²=0,60). E% was significantly related to elevation of PaCO₂ (r²=0,30) and bicarbonate and base excess (r²>0,20). E% was not significantly correlated to PaO₂ or blood pH, but hypercapnia and acidemia and chronic respiratory acidosis were found only in patients with E% > 60-70%.

The results suggested that matched ventilation and perfusion defect in V/P SPECT constitutes a pathophysiological meaningful and clinically significant measure of EP in COPD.

Core Session 3 - Scientific Presentation 2 -

Continuous quantitative measurements of proximal airway dimensions and lung density on dynamic-ventilation CT in smokers: a novel imaging approach using a 320-row detector CT scanner

Tsuneo Yamashiro¹, Hiroshi Moriya², Maho Tsubakimoto¹, Kotaro Sakuma², Sadayuki Murayama¹

1. University of the Ryukyus, Japan
2. Ohara General Hospital, Japan

Rationale: The dynamic-ventilation CT imaging demonstrates continuous movements of the airways and lungs, which cannot be depicted with conventional CT. We aimed to investigate continuous changes in airway dimensions and in lung density, and assessed their correlations with spirometric values in smokers.

Methods: Our retrospective study was approved by our Institutional Review Board and informed consent was waived. Twenty-one smokers including six COPD patients underwent dynamic-ventilation CT during free breathing (16 cm in length). At least one cycle from inspiratory to expiratory phases was scanned. Mean lung density (MLD) of scanned lungs and luminal areas (Ai) of fixed points on the trachea and right proximal bronchi (main bronchus, upper bronchus, bronchus intermedius, and lower bronchus) were continuously measured. Concordance between the time curve for MLD and that of airway Ai values was expressed by cross-correlation coefficients. Associations between these quantitative measurements and FEV_{1.0}/FVC values were assessed by Spearman rank correlation analysis.

Results: On the time curve for MLD, delta-MLD1.05 values between the peak inspiratory frame to the later third frame (1.05 sec later) were strongly correlated with FEV_{1.0}/FVC (r=0.76, P<0.0001). Cross-correlation coefficients between airway Ai and MLD values were significantly correlated with FEV_{1.0}/FVC (r=-0.56 to -0.66, P<0.01), except for the right upper bronchus. This suggested that synchrony between airway movement and lung movement was lost in patients with severe airflow limitation.

Conclusion: Respiratory changes in MLD and synchrony between airway Ai and MLD measured with dynamic-ventilation CT were correlated with patient spirometric values.

Morpho-functional 1H-MRI of the lung in COPD: Short-term test-retest reliability

Mark O Wielpuetz, Bertram J Jobst, Simon MF Tripan, Angela Anjorin, Julia Ley-Zaporozhan, Sebastian Ley, Jurgen Biederer, Oliver Sedlacek, Hans-Ulrich Kauczor

University of Heidelberg, Germany

Purpose:

Magnetic resonance imaging (1H-MRI) allows for a radiation-free non-invasive assessment of regional lung structure and function as a putative end-point for interventional trials and tailored treatment regimes in chronic obstructive pulmonary disease (COPD). The aim of this study was to evaluate the short-term reproducibility of a comprehensive morpho-functional MRI protocol in COPD.

Methods:

20 COPD patients (GOLD I-IV) underwent 1H-MRI at 1.5T on two consecutive days, including sequences for morphology, contrast-enhanced perfusion, and respiratory mechanics. Image quality and COPD-related morphological and functional changes were evaluated in consensus by three chest radiologists using a previously evaluated visual scoring system. Test-retest reliability was calculated per lung lobe for the extent of large and small airway abnormalities, parenchymal defects, and perfusion defects. Tracheal narrowing, dystelectasis, pleural effusion, and motion patterns of diaphragm/chest wall were assessed per lung. Image quality was assessed per sequence.

Results:

Median global scores [10(Q1:8.00;Q3:16.00) vs.11(Q1:6.00;Q3:15.00)] as well as category subscores were similar between MRI1 and MRI2, and showed "almost perfect" agreement ($\kappa=0.86$, 95%CI=0.81-0.91). Most subscores showed at least "substantial" agreement ($\kappa=0.64-1.00$), whereas the agreement for dystelectasis/effusion was "moderate" ($\kappa=0.42$, 95%CI=0.00-0.93), and of tracheal abnormality "fair" ($\kappa=0.21$, 95%CI=0.00-0.75). Most sequences showed diagnostic quality at MRI1 (276/278) and MRI2 (259/264).

Conclusion:

Lung 1H-MRI provides stable image quality and high reproducibility of COPD-related morphological and functional abnormalities. This underlines its potential value for the monitoring of regional lung characteristics in COPD trials.

Basics of Computational Analysis for Pulmonary Imaging

Namkug Kim

Department of Convergence Medicine/Radiology, University of Ulsan College of Medicine, Asan Medical Center, Korea

Due to recent development of medical imaging modality, most of medical images can be digitalized and used for various clinical purposes. Therefore, spatial and temporal resolution is becoming more and more precise. Besides these technical aspects, various kinds of clinical applications including new drug development, imaging biomarker, quantitative imaging lead to clinical paradigm shifts and megatrends. However, the usability of archived images is far from satisfaction. In the clinical field, the images are qualitatively referred only once by a radiologist and a clinician for diagnosis and treatment, and then discarded into the repository.

In this talk, basics of computational analysis for pulmonary imaging which consists of image pre-processing, image segmentation, registration, quantitative imaging, and imaging biomarker will be presented. Since 2004, medical imaging and robotics laboratory established to develop imaging software for the center of chronic obstructive pulmonary disease, AMC in 2004. The motto of this lab was “developing clinically applicable software. The structural and functional analysis of pulmonary imaging including airway segmentation, airway wall measurement, lobe segmentation, size based emphysema analysis, parenchyma textual analysis, registration, air trapping analysis, pulmonary perfusion and ventilation on MRI or/and dual energy CT will be covered in this talk. Especially, the DECT based world first V/Q mismatch analysis was developed and published in our group. Based on these MIRC works, various other technical groups including IOWA, Utrecht, Chicago, Mevis and commercials will be referred and discussed.

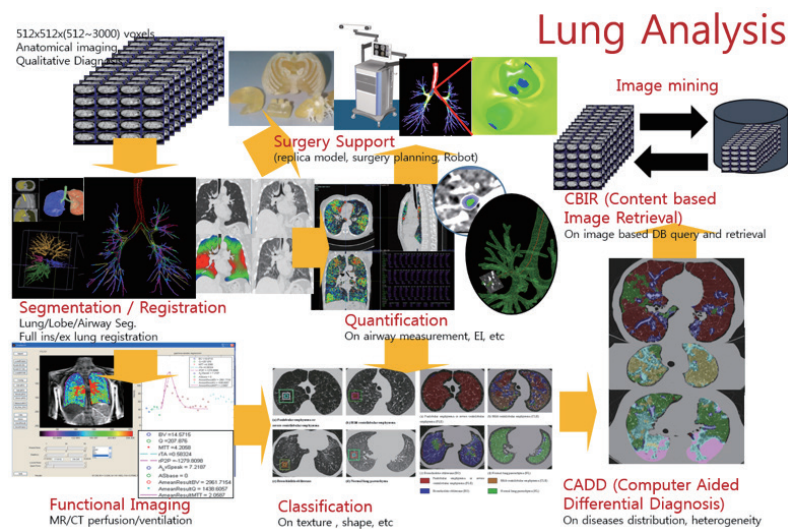


Fig 1. Overview of computational analysis for pulmonary imaging in medical imaging and robotics lab., Asan Medical Center

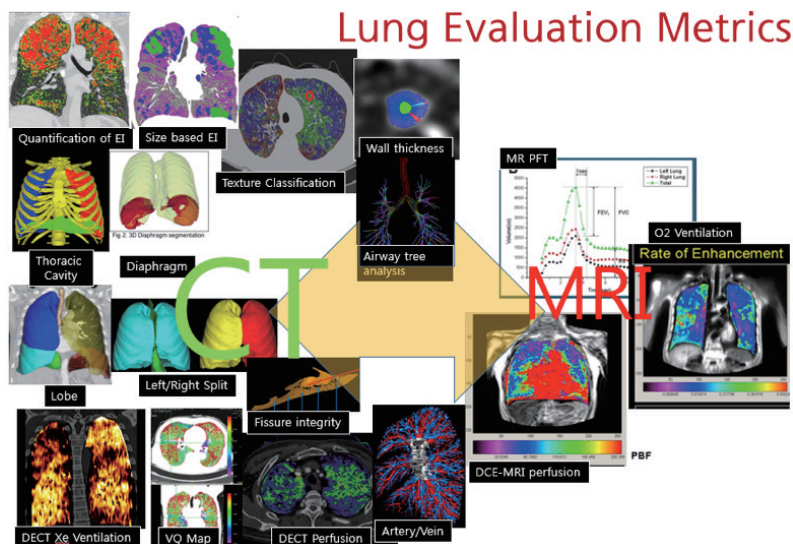


Fig 2. Quantitative lung evaluation metrics of pulmonary imaging in MIRC@AMC

| Core Session 4 - Invited Speaker 2 -

Basics of Computational Assessment for Diffuse Lung Diseases (DLDs)

Shoji Kido

Applied Medical Engineering Science, Graduate School of Medicine, Yamaguchi University, Japan

The diagnostic accuracy for diffuse lung diseases (DLDs) has increased greatly because of the improvement of CT apparatus. Especially, high-resolution CT (HRCT) can enable us to obtain high-resolution images which are equal to pathological images. The radiologists can diagnose DLDs based on minute anatomical structures of the lungs. Moreover, radiologists can analyze three-dimensional (3D) structures by use of multi-detector row CT images. However, the diagnosis of DLDs is basically based on subjective recognition of radiologists. So, the quantification of DLDs are required for improvement of the diagnostic accuracy. In computational assessment for DLDs, quantification and classification of DLDs are useful. For example, in COPD assessment, the low attenuation areas and the diameters of bronchi are measured for assessment for the disease severity. Classification of opacity patterns using textures are also performed for evaluation of DLDs. These approaches are very useful, but do not exactly cover the needs of radiologists. We have developed the CAD algorithm of similar image retrieval. This algorithm can retrieve and display the similar images which radiologists have to diagnose from the huge database which storage many diagnosed cases. This is also useful for daily clinical diagnosis. Recently, many major IT companies such as Google, Apple and IBM have been researching techniques of artificial intelligence (AI). Now, AI is popular in our daily life because machine learning (ML) techniques progress. One of core techniques of ML is "Deep Learning." It may change CAD approach revolutionarily. In this lecture, I introduce the survey of computational assessment of DLDs.

| Core Session 4 - Invited Speaker 3 -

Lung CAD

Noboru Niki

Tokushima University, Japan

Medical imaging is one of the major tools that have enriched medical sciences, and disease detection and treatment. Computed tomography (CT) is the most widely used imaging modality in clinical practice for cancer detection, oncologic diagnosis, and treatment guidance. CT modality allows clinicians to assess the characteristics of human tissue noninvasively. Recent advances in CT imaging technologies allow the high-throughput extraction of informative imaging features to quantify the differences that oncologic tissues exhibit. A key challenge is to transform a myriad of spatially and temporally quantified features into medical knowledge: the process of integrating diverse information (demographic, clinicopathological, and quantitative imaging) to provide personalized clinical predictions that can accurately estimate cancer probability and predict patients outcomes for risk-adaptive treatment. A main goal of our research is to develop cancer computer-aided detection/diagnosis (CADE/CADx) systems based on the multidisciplinary computational anatomy models which support clinicians to detect early-stage cancers and to determine risk-adaptive treatments. In this presentation, we describe the overview of our project and the potential benefits of implementing our CAD systems clinically.

Computer aided detection system for lung cancer, COPD, and osteoporosis in low-dose CT screening

Hidenobu Suzuki¹, Mikio Matsuhira¹, Yoshiki Kawata¹, Noboru Niki¹, Hironobu Ohmatsu², Yasutaka Nakano³, Masahiko Kusumoto², Takaaki Tsuchida⁴, Kenji Eguchi⁵, Masahiro Kaneko⁶

1. Tokushima University, Japan
2. National Cancer Center Hospital East, Japan
3. Shiga University of Medical Science, Japan
4. National Cancer Center Hospital, Japan
5. Teikyo University, Japan
6. Tokyo Health Service Association, Japan

Lung cancer is the leading cause of cancer death in Japan (2013). The National Lung Screening Trial Research Team found approximately 15 percent to 20 percent fewer lung cancer deaths among trial participants screened with low-dose helical CT relative to chest X-ray (NEJM, 2011). Centers for Medicare and Medicaid Services (Medicare) issued its final decision about coverage of low-dose CT lung cancer screening (CAG-00439N, 2015). CT scan takes a lot of images of a participant. Computer aided detection (CADe) system is an intelligent technology that assists physicians by improving efficiency. We have developed a CADe system for lung cancer CT screening. After a physician inputted thin-section low-dose CT dataset of one scan, CADe system provides suspicious regions of lung cancer, low attenuation volume, and osteoporosis automatically. This system has graphical user interface and four modules, (1) DICOM Query/Retrieve function, (2) thoracic organ analysis (body, rib, spine, lungs, trachea, bronchi, pulmonary blood vessel, and aorta), (3) detection (lung nodule, low attenuation volume, and osteoporosis), and (4) comparative reading assistance. Training and testing CT dataset for CADe were obtained with 120 kV, 15mAs, 1mm slice thickness, 512x512 matrix, pixel size of 0.625mm, and 1mm reconstruction interval. CADe system has been evaluated clinically in four medical institutions since March, 2014. This presentation demonstrates effectiveness of our CADe system for lung cancer CT screening.

Update for Diagnosis of Interstitial Lung disease

Gong Yong Jin

Chonbuk National University Medical School and Hospital, Korea

In 2002, the American Thoracic Society (ATS) and the European Respiratory Society (ERS) published a classification of idiopathic interstitial pneumonias. This classification included usual interstitial pneumonia (UIP), non-specific interstitial pneumonia (NSIP), desquamative interstitial pneumonia (DIP), respiratory bronchiolitis-associated interstitial lung disease (RB-ILD), cryptogenic organising pneumonia (COP), acute interstitial pneumonia (AIP) and lymphoid interstitial pneumonia (LIP) [1]. According to the revised 2013 ATS/ERS classification system, these entities were divided into major idiopathic interstitial pneumonias (IIPs) [idiopathic pulmonary fibrosis (IPF), idiopathic NSIP, RB-ILD, DIP, COP, and AIP], rare IIPs (idiopathic lymphoid interstitial pneumonia, idiopathic pleuroparenchymal fibroelastosis), and unclassifiable idiopathic interstitial pneumonias [2]. The major entities grouped into (a) “chronic fibrosing IIPs” (IPF and idiopathic NSIP), (b) “smoking-related IIPs” (RB-ILD and DIP), (c) “acute or subacute IIPs” (COP and AIP), and (d) “rare IIPs” (LIP and idiopathic pleuroparenchymal fibroelastosis) [3]. Idiopathic pleuroparenchymal fibroelastosis (IPPF) has been newly included and CT appearances of IPPF are distinctive, with irregular pleural thickening and “tags” in the upper zones that merge with fibrotic changes in the subjacent lung, associated with evidence of substantial upper lobe volume loss (architectural distortion, traction bronchiectasis, and hilar elevation) [3]. In addition, in the updated classification, a final diagnosis cannot always be achieved despite extensive multidisciplinary discussion, and such cases are considered “unclassifiable” [2].

The revision of the IIP classification has provided incremental but important advances in the understanding of IIPs. To important, the knowledge of IIP features on HRCT images help radiologists in diagnosis.

Reference

1. American Thoracic Society; European Respiratory Society (2002) American Thoracic Society/ European Respiratory Society International Multidisciplinary Consensus Classification of the Idiopathic Interstitial Pneumonias. This joint statement of the American Thoracic Society (ATS) and the European Respiratory Society (ERS) was adopted by the ATS board of directors, June 2001, and by the ERS Executive Committee, June 2001. *Am J Respir Crit Care Med* 165(2):277–304
2. Travis WD, Costabel U, Hansell DM, King TE Jr, Lynch DA, Nicholson AG, Ryerson CJ, Ryu JH, Selman M, Wells AU, Behr J, Bours D, Brown KK, Colby TV, Collard HR, Cordeiro CR, Cottin V, Crestani B, Drent M, Dudden RF, Egan J, Flaherty K, Hogaboam C, Inoue Y, Johkoh T, Kim DS, Kitaichi M, Loyd J, Martinez FJ, Myers J, Protzko S, Raghu G, Richeldi L, Sverzellati N, Swigris J, Valeyre D (2013) ATS/ERS committee on idiopathic interstitial pneumonias. *Am J Respir Crit Care Med* 188(6):733–748
3. American Thoracic Society-European Respiratory Society Classification of the Idiopathic Interstitial Pneumonias: Advances in Knowledge since 2002. Sverzellati N, Lynch DA, Hansell DM, Johkoh T, King TE Jr, Travis WD. *Radiographics*. 2015 Oct 9:140334. [Epub ahead of print]

Core Session 5 - Invited Speaker 2 -

Recent advances in the treatment of idiopathic pulmonary fibrosis

Noboru Hattori

Department of Molecular and Internal Medicine, Institute of Biomedical & Health Sciences, Hiroshima University, Japan

Idiopathic pulmonary fibrosis (IPF) is the most common and lethal type of the idiopathic interstitial pneumonias. It carries a median survival of two to three years, but clinical course is markedly varies from patient to patient. Not a small portion of patients are also known to suffer from acute exacerbation of this disease. Empirically, a combination of corticosteroids, immunosuppressants, and/or N-acetylsysteine has been used for the treatment; however, we have now learned that this therapy had been failing to add any benefits for IPF patients. Just recently, through a number of disappointing results from clinical trials evaluating novel potential therapies, pirfenidone and nintedanib, two compounds with pleiotropic mechanisms of action, have proven effective in slowing functional decline and disease progression in IPF patients. In October 2014, these two drugs became the first agents to be approved by the US Food and Drug Administration for the treatment of IPF. Most notably in Japan, pirfenidone has been licensed to use for the treatment of IPF since October 2008 on the basis of its effect to slow functional decline proved by a clinical trial in Japan. In August 2015, the use of nintedanib for IPF is also approved in Japan. Although there must be differences in potential benefits and risks between pirfenidone and nintedanib, the landscape for management of IPF has markedly changed with the advent of these drugs. This presentation provides an overview of the most recent clinical trials in IPF and discusses how these results will change the clinical management of IPF patients.

Core Session 5 - Invited Speaker 3 -

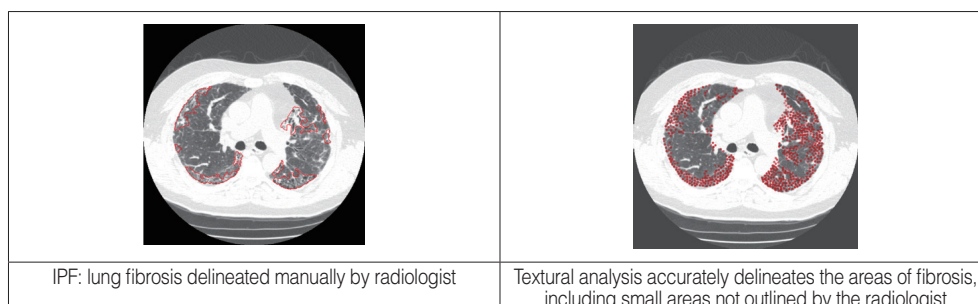
Quantitative CT Assessment for ILD

David A. Lynch

National Jewish Health, USA

Despite limitations, physiologically measured lung volumes (forced vital capacity (FVC) and lung diffusing capacity (DLco)) remain the most widely used measures for assessing severity of interstitial lung abnormality. Visual, semi-quantitative CT assessment, though subjective, clearly adds important information regarding disease severity and prognosis. However, visual assessment of disease progression remains challenging. Global measures derived from the CT histogram can be effective in documenting progression. Several groups have developed more sophisticated quantitative measures based on local histogram measures and/or textural analysis. These measures correlate quite well with physiologic measurements and can be used to document progression over time. In one recent study of a local histogram based technique, evidence of progression on serial CT was correlated with survival. Textural analysis requires training of an algorithm using radiologist-defined regions of interest demonstrating specific imaging features (reticular, honeycombing, normal, etc.). The algorithm is then tested in a separate population. Measurement of disease progression using such techniques has been shown to correlate better with physiologic progression than histogram based methods. However, several important issues remain to be resolved, particularly those of repeatability, and sources of variation (lung volume, reconstruction algorithm, etc.). While the algorithms appear to be effective in discriminating between normal and fibrotic lung, discrimination of disease pattern (honeycombing, reticular) is more difficult, perhaps because of the difficulty in acquiring training samples with pure examples of these findings.

Figure



Quantitative MRI Assessment for ILD

Yoshiharu Ohno

Division of Functional and Diagnostic Imaging Research, Department of Radiology, Kobe University School of Medicine, Japan
Advanced Biomedical Imaging Research Center, Kobe University Graduate School of Medicine, Japan

Pulmonary magnetic resonance imaging (MRI) has been studied as a new research and diagnostic tool as well as CT and nuclear medicine study in various pulmonary diseases. However, pulmonary MRI has been difficult to use because of inherently low proton density, a multitude of air-tissue interfaces, which create significant magnetic field distortions and are commonly referred to as susceptibility artifacts, diminishing signal in the lung, and respiratory and/or cardiac motion artifacts. To overcome these drawbacks, various technical advances made during the last decade have been reported as useful for functional and morphological assessment of pulmonary diseases.

Recently, pulmonary MRI is suggested as having the potential to provide not only morphology related, but also pulmonary function related information. In addition, several MR techniques evaluating ventilation and perfusion as well as oxygen diffusion and T2 star (T2*) have been proposed for quantitative and/or qualitative assessment of disease severity in interstitial lung disease (ILD) subjects. It has the potential to replace nuclear medicine and CT studies for the identification of regional pulmonary function and may perform a complementary role in ILD assessments and patient managements instead of these studies.

This lecture covers 1) how to perform quantitative evaluation of pulmonary MR techniques for morphological and functional assessments, 2) its clinical applications in ILD and 3) future direction of pulmonary functional MR imaging.

I hope that this lecture will enhance your knowledge, and encourage you to apply quantitatively assessed pulmonary MR imaging to ILD for academic and clinical purposes in your institutions.

Core Session 5 - Scientific Presentation 1 -

Evaluation of Drug efficacy of Ethyl Pyruvate on the Pulmonary Fibrosis in mice with Hyperpolarized ^{129}Xe MRI Pulmonary Function Diagnosis

Shota Hodono¹, Akihiro Shimokawa¹, Hideaki Fujiwara², Hirohiko Imai³, Atsuomi Kimura¹

1. Department of Medical Physics and Engineering, Division of Health Sciences, Graduate School of Medicine, Osaka University, Japan
2. Office for University-Industry Collaboration, Osaka University, Japan
3. Department of Systems Science, Graduate School of Informatics, Kyoto University, Japan

The efficacy of ethyl pyruvate (EP) on pulmonary disease in small rodents has been investigated by applying hyperpolarized ^{129}Xe (HPXe) MRI for the evaluation of pulmonary function. Three mice groups were prepared: (i) a fibrosis group (N=4), to which bleomycin was administered intratracheally to induce pulmonary fibrosis; (ii) an EP group (N=5), to which EP was administered five days per week for three weeks after administration of bleomycin; (iii) a control group (N=4), to which saline was administered in the same manner as EP. For assessing pulmonary function, parameters of fractional ventilation (r_a) and gas-exchange (f_D) were obtained using HPXe MRI. Each mouse was measured at four time-points; two weeks after administration of bleomycin or saline (week 0) and one, two and three weeks later. Both r_a and f_D of fibrosis mice decreased continuously over 3 weeks, whilst the f_D of EP mice increased and the pulmonary function of control mice was approximately constant. At week 3, functional parameters of the EP group ($r_a=0.24\pm0.02$, $f_D=6.5\pm0.9$) were significantly higher ($P<0.05$) than those of the fibrosis group ($r_a=0.16\pm0.03$, $f_D=4.1\pm0.7$). Moreover, the pulmonary function of the EP group agreed well with that of the control group. These results indicate that continuing to administer EP would further inhibit disease progression and may fully recover pulmonary function. This study is the first assessment of EP efficacy on pulmonary fibrosis with HPXe MRI and the longitudinal design can be easily applied to other diseases to assess new drug efficacy.

Core Session 5 - Scientific Presentation 2 -

The association between pulmonary hemodynamics measured by phase-contrast MRI and acute exacerbations of interstitial lung diseases

Nanae Tsuchiya¹, Tae Iwasawa², Tsuneo Yamashiro¹, Takashi Ogura³, Sadayuki Murayama¹

1. Department of Radiology, Graduate School of Medical Science, University of the Ryukyus, Japan
2. Department of Radiology, Kanagawa Cardiovascular and Respiratory Center, Japan
3. Department of Respiratory Medicine, Kanagawa Cardiovascular and Respiratory Center, Japan

Purpose:

Exacerbations of interstitial lung diseases (ILDs) are associated with an accelerated decline in lung function and death. Pulmonary hypertension is an important complication of ILDs and a risk factor for acute exacerbations. Phase-contrast MRI (PC-MRI) can estimate pulmonary hemodynamics noninvasively. This study aimed to determine the association between pulmonary hemodynamics measured by PC-MRI and a history of acute exacerbations in patients with ILDs.

Method:

The institutional review board approved this study and waived informed consent. Pulmonary hemodynamics, measured by PC-MRI in 43 patients with ILDs, were reviewed retrospectively. Patients were divided into the exacerbation group (Ex: n=8) and the non-exacerbation group (NEx: n=35). The exacerbation group had acute exacerbations requiring hospitalization after PC-MRI was performed. Evaluation criteria were heart rate (HR), average flow (AveFlow), average velocity (AveVel), acceleration time (AT) and ratio calculated from a time-intensity curve in a pulmonary trunk. Ratio was defined as the maximal change in flow rate during ejection divided by the acceleration volume. Statistical comparisons were by t-tests.

Result:

AveFlow (Ex: 74.4 ± 24.1 vs. NEx: 61.8 ± 9.7 ml/s; $P=0.01$) and AveVel (Ex: 12.8 ± 4.6 vs. NEx: 10.3 ± 1.8 cm/s; $P=0.01$) were significantly reduced in the exacerbation group. HR (Ex: 74 ± 11 vs. NEx: 77 ± 10 bpm; $P=0.4$), AT (Ex: 109 ± 19 vs. NEx: 103 ± 19 msec; $P=0.4$), and ratio (Ex: 255 ± 90 vs. NEx: 327 ± 175 /secsuperscript²; $P=0.3$) were not statistically significant.

Conclusions:

Pulmonary blood flow reduction, as detected by PC-MRI, was associated with acute exacerbations in patients with ILDs.

Abstracts

Poster Session

Poster Session P1-1

Potential role of CT metrics in chronic obstructive pulmonary disease with pulmonary hypertension

Katsutoshi Ando¹, Hiroshi Kuraishi², Tetsutaro Nagaoka¹, Takeo Tsutsumi¹, Yoshito Hoshika³, Toru Kimura⁴, Hiroki Ienaga³, Yoshiteru Morio¹, Kazuhisa Takahashi¹

1. Department of Internal Medicine, Division of Respiratory Medicine, Juntendo University Graduate School of Medicine, Japan
2. Department of Pulmonology, Nagano Red Cross Hospital, Japan
3. Department of Pulmonology, Koshigaya Municipal Hospital, Japan
4. Department of Cardiovascular Medicine, Koshigaya Municipal Hospital, Japan

Purpose: Recent imaging studies demonstrated the usefulness of quantitative computed tomographic (CT) analysis assessing pulmonary hypertension in patients with chronic obstructive lung disease (COPD-PH). The aim of this study was to investigate whether it would be also valuable for predicting and evaluating the effect of pulmonary vasodilators in patients with COPD-PH.

Methods: We analyzed a correlation between the extent of cystic destruction (LAA%) and total cross-sectional areas of small pulmonary vessels less than 5 mm² (%CSA<5) in many CT slices from each of four COPD-PH patients before and after the initiation of pulmonary vasodilator. To evaluate those generalized data from patients with COPD, we evaluated multiple slices from 42 patients whose PH was not clinically suspicious. We also selected five PH patients with idiopathic interstitial pneumonia (IIP-PH) and analyzed serial changes of pulmonary artery enlargement (PA:A ratio).

Results: In 42 COPD patients without PH, LAA% had a statistically significant negative correlation with %CSA<5. However, three of four COPD-PH patients manifested no such correlation. In two patients, clinical findings were dramatically improved after the initiation of pulmonary vasodilator. Notably, LAA% and %CSA<5 in those patients correlated significantly after its treatment. In COPD-PH, the PA:A ratio was significantly decreased after the initiation of pulmonary vasodilator therapy (1.25 ± 0.13 vs. 1.13 ± 0.11 , $p = 0.019$), but not in IIP-PH.

Conclusions: Our study demonstrates that the use of quantitative CT analysis is a plausible and beneficial tool for predicting and evaluating the effect of pulmonary vasodilators in patients with COPD-PH.

Poster Session P1-2

Ratio of pulmonary arterial to aortic diameter and right to left ventricular diameter associate with poor outcome in medically-treated chronic thromboembolic pulmonary hypertension

Ryogo Ema, Toshihiko Sugiura, Naoko Kawata, Rintaro Nishimura, Takayuki Jujo, Ayako Shigeta, Seiichiro Sakao, Nobuhiro Tanabe, Koichiro Tatsumi

Graduate School of Medicine Chiba University, Japan

Background: The dilatation of pulmonary artery (PA) and right ventricle (RV) on chest computed tomography (CT) are often observed in clinical practice of pulmonary hypertension. The clinical meanings of these signs have not been clearly explained in patients with chronic thromboembolic pulmonary hypertension (CTEPH). So, we investigate whether these signs at the diagnosis correlate the poor outcome.

Methods: This study was a retrospective cohort investigation of 60 subjects with inoperable CTEPH diagnosed consecutively between 1997 and 2010 at Chiba University Hospital. Digital scout CT images of the chest were obtained with a multi-detector CT scanner. At the mediastinal window setting of the axial images, the main PA/AA ratio was calculated as the ratio of main pulmonary arterial to ascending aortic diameter, and RV/LV ratio as the ratio of right to left ventricular diameter. Outcome was obtained from hospital chart reviews, and telephone interviews with the referring physician.

Results: Main PA/AA ratio ranged from 0.85 to 1.84 (mean, 1.15 ± 0.23), and RV/LV ratio ranged from 0.71 to 2.88 (mean, 1.34 ± 0.53). During a median follow-up of 1284.5 days (range, 21 to 4550 days), 14 patients got worse and hospitalized. Among them, 6 patients died. Kaplan-Meier analysis showed definite differences in hospitalization between patients with main PA/AA ratio ≥ 1.1 and those with main PA/AA ratio < 1.1 (Log-rank test, $P = 0.014$), and between RV/LV ratio ≥ 1.2 and those with RV/LV ratio < 1.2 (Log-rank test, $P = 0.013$).

Conclusions: Main PA/AA ratio and RV/LV ratio by contrast CT were associated with poor outcome in medically-treated CTEPH.

Poster Session P1-3

Mean Pulmonary Artery Pressure by echocardiography in chronic thromboembolic pulmonary hypertension

Hajime Kasai¹, Akane Matsumura¹, Toshihiko Sugiura¹, Ayako Shigeta¹, Nobuhiro Tanabe^{1,2}, Keiko Yamamoto¹, Hideki Miwa¹, Ryogo Ema¹, Takayuki Jyujō^{1,2}, Seiichiro Sakao¹, Koichiro Tatsumi¹

1. Department of Respiriology, Graduate School of Medicine, Chiba University, Japan
2. Department of Advanced Medicine in Pulmonary Hypertension, Graduate School of Medicine, Chiba University, Japan

Background: Mean pulmonary arterial pressure (MPAP) is important pulmonary hemodynamic parameter in the management of patients with chronic thromboembolic pulmonary hypertension (CTEPH). We compared a variety of echocardiography-derived prediction indices with direct right heart catheterization (RHC) to identify the most reliable noninvasive prediction of MPAP in patients with CTEPH.

Patients and methods: Echocardiography and RHC were performed sequentially in 56 patients (mean age: 60.5±12.0 years; 44 females) with PH. We measured the tricuspid regurgitation pressure gradient (TRPG) using echocardiography. Mean systolic right ventricular (RV)-right atrial (RA) gradient calculated by tracing the TR time velocity integral. Systolic and mean pulmonary artery pressure predicted from a peak flow velocity of TR (SPAPTR, MPAPTR, respectively) was calculated adding right atrial pressure based on the combination of diameter and respiratory variation of the inferior vena cava. MPAPChemla was calculated using a following formula : $0.61 \times \text{SPAPTR} + 1.95 \text{ mmHg}$. Finally, correlations between these echocardiographic predictors of MPAP and the MPAPRHC obtained from RHC were assessed.

Results: The mean pulmonary arterial pressure (MPAPRHC) and PVR derived from RHC were 35.9±11.3 mmHg and 6.6±3.6 Wood units, respectively. The mean± SD of the differences between MPAPRHC and MPAPTR, MPAPChemla were -1.5± 18.1 mm, -4.6± 19.9 mm Hg, respectively. Accuracy (MPAPTR, MPAPChemla within 10 mmHg and 5 mmHg of MPAPRHC) was 80.4% and 46.4%, 71.4% and 48.2%, respectively.

Conclusions: MPAPTR and MPAPChemla are reliable predictors of MPAPRHC in patients with CTEPH.

Poster Session P1-4

Quantitative analysis of thrombosis using CT images

Kaori Fujisawa¹, Mikio Matsuhira², Hidenobu Suzuki², Yoshiki Kawata², Noboru Niki², Toshihiko Sugiura³, Nobuhiro Tanabe³, Yuichi Takiguchi³, Koichiro Tatsumi³

1. Graduate School of Advanced Technology and Science, Tokushima University, Japan
2. Institute of Technology and Science, Tokushima University, Japan
3. Department of Respiriology, Graduate School of Medicine, Chiba University, Japan

In the diagnosis of thrombosis with no specific clinic symptoms, diagnostic imaging plays an important role. Particularly, contrast enhanced CT image is low invasive diagnostics. Thrombus in the pulmonary artery can be detected using a low density without the contrast effect. Moreover, because describing the change of concentration in lung field and the decline in lung blood vessel shadow is also possible, it is indispensable to diagnose thrombosis. Using image diagnosis, it is necessary to classify the pulmonary artery and vein that related to the thrombosis, and to analyze the lung blood vessel quantitatively. In this study, we analyzed the pulmonary artery by automatic extraction, measuring volume of the pulmonary trunk and analyzing shape of this artery surface. We have analyzed the shape using the diameter and three-dimensional curvature of the pulmonary artery the high part of the contrast effect as a region of interest with the exception of thrombus site. Moreover, by analyzing the shape of the pulmonary blood vessels distal portion, we confirm the presence or absence of thrombus. We examined the method of thrombosis detection by comparing the normal and chronic cases.

Poster Session P1-5

Energy efficiency after balloon pulmonary angioplasty in chronic thromboembolic pulmonary hypertension: Assessment by phase-contrast MRI

Michinobu Nagao¹, Yuzo Yamasaki², Satoshi Kawanami¹, Takeshi Kamitani², Torahiko Yamanouchi², Kohtarō Abe³, Kazuya Hosokawa³, Hidetake Yabuuchi⁴, Yuji Watanabe¹, Hiroshi Honda²

1. Molecular Imaging and Diagnosis, Kyushu University, Japan
2. Clinical Radiology, Kyushu University, Japan
3. Cardiovascular Medicine, Kyushu University, Japan
4. Medical Science, Kyushu University, Japan

Introduction

Balloon pulmonary angioplasty (BPA) improves exercise tolerance and symptoms in patients with chronic thromboembolic pulmonary hypertension (CTEPH); however, the mechanism is not understood. The purpose is to analyze changes in pulmonary artery (PA) flow after BPA using phase-contrast MRI (PC-MRI).

Methods

Data from PC-MRI using 3-Tesla and flow sensitive gradient echo at pre- and post-condition of 44 BPA procedures for 25 CTEPH patients were analyzed. Output (ml/min) and mean velocity (mm/sec) for main PA were calculated from time-flow curve derived from PC-MRI. Based on Bernoulli principle, the energy for main PA flow was identified as one-half of the square of mean velocity ($\mu\text{J}/\text{kg}$). Accordingly, energy efficiency was defined as dividing the output by the energy (ml/ $\mu\text{J}/\text{kg}$). In addition, right and left PA outputs were calculated by PC-MRI. Comparison of parameters between pre- and post-BPA was analyzed by paired t-test.

Results

Energy efficiency was significantly greater at post-BPA than at pre-BPA (2.00 ± 1.00 vs. 1.61 ± 0.76 ml/ $\mu\text{J}/\text{kg}$, $p=0.01$). There was no difference in output between pre- and post-BPA (4142 ± 1151 vs. 4077 ± 1052 ml/min). The unilateral output for BPA side was significantly greater at post-BPA than at pre-BPA (1860 ± 685 vs. 1606 ± 551 ml/min, $p<0.01$) whereas that for non-BPA side was smaller at post-BPA than at pre-BPA (1847 ± 414 vs. 2074 ± 670 ml/min). The ratios of right to left PA output were 0.84 ± 0.39 and 1.02 ± 0.44 at pre- and post-BPA.

Conclusion

BPA improves energy efficiency in pulmonary hemodynamics in CTEPH while a right to left PA flow becomes homogeneous with remaining unchanged total output.

Poster Session P1-6

Relationship between Improved Pulmonary Arterial Pressure and Changes in the Wall Thickness of Right Ventricle Myocardium by 320-slice CT in Patients Under Pulmonary Endarterectomy

Toshihiko Sugiura¹, Akane Sasaki¹, Nobuhiro Tanabe², Hajime Kasai¹, Naoko Kawata¹, Yukiko Matsuura¹, Ryogo Ema¹, Seiichiro Sakao¹, Koichiro Tatsumi¹

1. Department of Respirology, Graduate School of Medicine, Chiba University, Japan
2. Department of Advanced Medicine in Pulmonary Hypertension, Chiba University, Japan

Objective: We retrospectively determined whether changes of the wall thickness of right ventricle (RV) myocardium measured by ECG-gated 320-slice CT were influenced by improved pulmonary artery (PA) pressure in patients with chronic thromboembolic pulmonary hypertension (CTEPH) undergoing pulmonary endarterectomy (PEA).

Methods: Twenty-three patients (6 male, 60 ± 11 yrs) with proven CTEPH underwent right heart catheterization (RHC) and double-volume retrospective ECG-gated enhanced volume scanning using 320-slice CT before PEA and one year after PEA. CT images were reconstructed every 5% from 0 to 95% of the R-R interval, and a series of short-axis images of the heart at the level of the left ventricle papillary muscle was acquired using double-oblique multiplanar reformation. We quantified wall thickness of RV myocardium in end diastole. The relationships between wall thickness of RV myocardium and hemodynamics measured by RHC before and one year after PEA were evaluated by linear regression analysis.

Results: The correlation coefficients of wall thickness of RV myocardium with mean PA pressure (mPAP) before and one year after PEA were -0.12 ($P=0.59$) and -0.09 ($P=0.67$), respectively. The change in wall thickness of RV myocardium before and one year after PEA was correlated with the change in mPAP ($r=-0.50$, $P=0.01$) and the change in PVR ($r=-0.34$, $P=0.08$).

Conclusions: The wall thickness of RV myocardium based on ECG-gated 320-slice CT can be used to estimate improved hemodynamics in patients undergoing PEA.

Poster Session P2-1-1

Correlation of early PET findings with tumor response to sensitive molecular targeted agents in patients with advanced non-small cell lung cancer

Tomonobu Koizumi, Toshirou Fukushima, Daisuke Gomi, Takashi Kobayashi, Nodoka Sekiguchi, Akiyuki Sakamoto, Shigeru Sasaki, Keiko Mamiya, Kazunari Tateish, Akane Katou, Kazuhiko Oguchi

Shinshu University School of Medicine, Japan

Recent advances in positron emission tomography (PET) with fluorine-18-fluorodeoxyglucose (18F-FDG) have facilitated not only the diagnosis and staging of lung cancer but also the prediction of treatment outcome. Molecular targeted agents, such as gefitinib, an epidermal growth factor receptor (EGFR) tyrosine kinase inhibitor (TKI), and crizotinib, an anaplastic lymphoma kinase (ALK) inhibitor, showed a high response rate and prolonged progression-free survival compared with first line chemotherapy in patients with advanced non-small cell lung cancer (NSCLC) harboring the specific genes mutations and rearrangement. We conducted a study to assess the usefulness of early FDG-PET examination for a subsequent response in tumor size reduction to gefitinib (n=7) or crizotinib (n=3), in advanced NSCLC with the sensitive gene anomalies, respectively. In 23 targeted lesions of 10 NSCLC patients, changes in FDG uptakes before and day 7 after the initiation of molecular targeted therapy were compared with radiographic tumor reduction by RECIST. FDG uptake was evaluated as the maximum standardized uptake value (SUVmax) of each target lesion. SUVmax decreased in all lesions after gefitinib or crizotinib therapy (mean SUVmax 8.3±3.4 before to 3.7±1.8 after therapy, p<0.05). The % decrease in SUVmax of each lesion was significantly correlated with the % tumor size reduction. (r=0.44). The present study indicated that early reduction in FDG-PET uptake after an initiation of molecular targeted agents was able to predict subsequent tumor reduction in patients harboring EGFR-mutated or ALK-positive NSCLC.

Poster Session P2-1-2

Stereotactic radiotherapy with Cyberknife for stage I non-small-cell lung cancer at our institute: Radiation pneumonitis

Masaki Nakamura¹, Hideki Nishimura¹, Yoshiro Matsuo², Shinji Tsudo¹, Hiroshi Mayahara¹, Haruka Uezono¹, Aya Harada¹, Naoki Hashimoto¹, Toshiyuki Ogata¹, Ryohei Sasaki²

1. Kobe Minimally Invasive Cancer Center, Japan

2. Kobe University, Japan

(Purpose)

Cyberknife Robotic Radiosurgery System can deliver the prescribed dose by using many different angles converging on the target, with real-time motion tracking system. The purpose of this study is to investigate if Cyberknife using ablative radiation doses for stage I non-small-cell lung cancers achieves acceptable local control and toxicity.

(Materials and Methods)

A review of treatment details for 40 patients with histologically proven or clinical cancers treated by image-guided robotic stereotactic radiotherapy at our institute between May 2013 and November 2014 and were followed for a minimum of 6 months was analysed.

(Results)

Total doses ranged from 48Gy to 66Gy delivered in 4-10 equal fractions.

Of the 40 patients treated, over Grade 2 pneumonitis observed in 2 patients.

Local failure was observed in 4 patients. There have been no regional lymph node recurrences. At a median follow-up of 10.5 months, the crude survival rate is 97.5%, with 1 death due to bacterial pneumonitis.

(Conclusion)

Image-guided robotic stereotactic radiosurgery of lung tumors with Cyberknife achieves acceptable toxicity to surrounding tissues. Longer follow-up is needed to investigate exact local control rates and survival rates.

Poster Session P2-1-3

A case of acute arterial thrombosis in patient with postoperative adjuvant cisplatin-based chemotherapy for completely resected lung adenocarcinoma

Kenichi Okuda¹, Hiroyuki Tamiya¹, Chihiro Sato², Satoshi Noguchi¹, Yosuke Amano¹, Hirokazu Urushiyama¹, Kosuke Watanabe¹, Osamu Narumoto¹, Akihisa Mitani¹, Hidenori Kage¹, Yasuhiro Yamauchi¹, Go Tanaka¹, Takahide Nagase¹

1. Department of Respiratory Medicine, Graduate School of Medicine, The University of Tokyo, Japan

2. General Education Center, The University of Tokyo Hospital, Japan

Malignant tumor can cause a hypercoagulable state and often coexists thrombosis. Cisplatin-based chemotherapy has also been reported to cause vascular side effects including aortic thrombosis. We report a case of acute arterial thrombosis in patient with postoperative adjuvant cisplatin-based chemotherapy for completely resected lung cancer. A 68-year-old man with a history of right upper lobectomy for lung adenocarcinoma (pT2aN1M0; stage IIA) complained of an acute onset of pain in the right leg and intermittent claudication after 13 days of the first cycle of postoperative chemotherapy with cisplatin and vinorelbine. Palpation of the right lower extremities revealed coldness in the peripheral part from the lower leg and absence of pulsation in the femoral, popliteal and dorsalis pedis arteries. The right leg had severely decreased ankle brachial pressure index. Computed tomography (CT) angiography showed an extensive thrombi involving the descending aorta and common iliac artery with an abrupt interruption in the right popliteal artery. We made a diagnosis of acute arterial thrombosis and immediately began an administration of unfractionated heparin, followed by warfarin. Two weeks later, the symptoms of patient had mostly improved and a follow-up CT scan revealed decreased thrombi. Thereafter, chemotherapy was discontinued and the patient has remained free of any symptoms and recurrence of the cancer for four months. It is important for clinicians to carefully observe patients with cisplatin-based chemotherapy because of a possible risk of arterial thrombosis, even in the absence of primary malignant tumor.

Poster Session P2-1-4

Characterization of F-18-FDG Uptake in Irradiated Lung on Dual-Time-Point PET/CT Scan

Kazuyoshi Suga, Yasuhiko Kawakami, Ayame Shimizu

Department of Radiology, St. Hill Hospital, Japan

Purpose: The aim of this study is to characterize F-18-FDG uptake in irradiated lung on dual-time-point PET/CT scan.

Methods: The subjects were 29 patients who underwent FDG PET/CT scan 2-14 months after radiation therapy (RT) with 30-62 Gy to thoracic region for malignant neoplasms, where 12 patients underwent the scan two or three times during the same period. PET/CT scan was performed at 60 min and 120 min after intravenous injection of FDG. SUV on early and delayed scans and retention index (RI) were measured at irradiated and non-irradiated lungs.

Results: All 29 patients showed increased FDG uptakes in irradiated lungs both on early and delayed scans, with or without in irradiated lungs even without abnormal opacities. The mean values of early and delayed SUV, and RI were 2.4 ± 0.6 , 2.3 ± 0.6 and $-1.7\% \pm 13.7$ in the irradiated lungs with abnormal opacities, and 0.8 ± 0.2 , 0.7 ± 0.2 and $-7.0\% \pm 24.9$ in those without abnormal opacities, respectively. All these values were significantly higher than those of the contralateral non-irradiated lungs ($P < 0.0005$). 11 (91.6%) of 12 repeatedly-studied patients showed a significant decreasing of SUV in the irradiated lungs on the subsequent scans ($P < 0.01$).

Conclusions: Irradiated lungs around 3 months after RT show increased FDG uptake and retention compared with normal lungs, with or without morphologic abnormality, and that pleural/subpleural curvilinear FDG uptake can be a characteristic sign of radiation-induced lung injury.

Poster Session P2-1-5

Initial Experience of Trans Pulmonary Arterial Marker Placement for Respiratory Gated Lung Stereotactic Radiotherapy

Yumiko Onishi¹, Jun Ishida¹, Naoki Kanata¹, Hideki Nishimura², Masahiko Fujii¹

1. Department of Radiology, Kobe Minimally Invasive Cancer Center, Japan

2. Department of Radiotherapy, Kobe Minimally Invasive Cancer Center, Japan

Purpose:

Stereotactic radiotherapy in the lung is a non-surgical radiation therapy used to treat lung cancer or lung metastasis. Respiratory gate system using lung marker can reduce field sizes and risk of toxicity to normal lung. Gold markers have been placed trans bronchially, but we started the trial of trans arterial placement.

The purpose of this study is to describe our initial experience with trans pulmonary artery marker placement.

Material and Method:

Platinum coils were placed around lung tumors trans pulmonary arterially for total of 56 tumors in 50 patients. Prior to the placement, the relative artery was evaluated on the multiplanar reformatted CT images. After the placement, the linkage between tumor and marker was evaluated. We also evaluated the technical and clinical success rate of the procedure and the frequency of the complication.

Results:

The technical success was perfect (56/56), and clinical success was 82% (46/56). The reason of clinical failure were as follows: No respiratory displacement of tumor were 9%(5/56), No linkage between tumor and markers were 5%(3/56), Failure of respiratory-gating were 4%(2/56). Only one case had hemorrhage of the puncture as complication.

Conclusion:

Our new technique of marker placement appears to be useful for stereotactic body radiotherapy due to its good safety and certainty.

Poster Session P2-2-1

Radiology's Role in Lung Cancer Screening Programs

Fuldem Mutlu, Yasemin Gunduz

Sakarya University Education and Research Hospital, Turkey

Lung cancer is the most common cause of cancer death worldwide, and there is accumulating higher level evidence that a mortality benefit exists with screening of carefully selected patients. While it's going to be "absolutely critical" to have a strong multidisciplinary team in place and assembled, radiology must take the initiative in monitoring the day-to-day operations of the program.

Lung association recommendations, advantages and disadvantages of screening are all discussed in our report.

There is increasing evidence that low dose lung cancer screening benefits outweigh the risks at this time for selected patient groups. There is continued debate over the cost effectiveness of screening, but it may be cost effective if limited to the study population or selected subgroups of the study population.

Refining lung cancer screening strategy, including a possible volume-based nodule assessment rather than single longest dimension assessment.

Administrators are going to start looking at their radiology departments and ask, 'What's the status of our lung screening program?'

Poster Session P2-2-2

Ground Glass Nodule (GGN) Detection by Chest Digital Tomosynthesis (CDT) with Iterative Reconstruction (IR): a phantom study using simulated nodules and clinical evaluation in 79 cases

Yukihiro Nagatani¹, Masashi Takahashi², Mitsuru Ikeda³, Norihisa Nitta¹, Satoru Matsuo⁴, Yasutaka Nakano¹, Jun Hanaoka¹, Katsunori Miyata¹, Yuto Hamada¹, Noritoshi Ushio¹, Akinaga Sonoda¹, Hideji Otani¹, Kiyoshi Murata¹

1. Shiga University of Medical Science, Japan
2. Yujin Yamazaki Hospital, Japan
3. Nagoya University Graduate School of Medicine, Japan
4. Kyoto College of Medical Science, Japan

The purpose of this study is to evaluate the influence of radiation dose level and IR algorithm on detectability of simulated GGNs in CDT and compare detection performance of GGNs in clinical cases between CDT and chest radiography (CR) at ultra-low dose (ULD). Detectability of 74 simulated GGNs placed in an anthropomorphic phantom in CDT by 10 observers was compared among 6 different radiation levels with and without IR. Detectability of 105 GGNs in 79 clinical cases by 7 observers was compared among CDT at 120kV-10mA with and without IR, and CR (effective dose: 0.081 and 0.117 mSv). As results, CDT demonstrated sufficient detection sensitivity (DS) for more attenuated simulated GGNs with the diameter of 8mm or more (73.5±6.0 %) even in the lowest radiation level (0.08mSv) and improved DS for less attenuated simulated GGNs with the diameter of 10mm (56.3±11.9 %) at submilli-Sv with IR. For GGNs in clinical cases, detectability at ULD-CDT with IR was higher than either that at ULD-CDT without IR or CR, as area under ROC curve was 0.66 ± 0.02, 0.59 ± 0.01 and 0.52 ± 0.01, respectively (p < 0.05), with increased DS for larger GGNs with the longest diameter of 9mm or more (44.6 ± 7.7%) or more attenuated GGNs with the CT attenuation value of -600 HU or more (47.5 ± 8.1%). In conclusion, ULD-CDT with IR has a potential to be used for detection of larger and more attenuated GGN.

Poster Session P2-2-3

Atypical Adenomatous Hyperplasia of Lung Presenting as Pure Ground Glass Nodules or Part Solid Nodules: A Retrospective Study

Yung Liang Wan¹, Tiing Yee Siow¹, Chih Wei Wang², Yi Chen Wu³

1. Department of Medical Imaging and Intervention, Chang Gung Memorial Hospital at Linkou, Taiwan / Institute for Radiological Research, College of Medicine, Chang Gung University, Taiwan
2. Department of Anatomic Pathology, Chang Gung Memorial Hospital at Linkou, College of Medicine, Chang Gung University, Taiwan
3. Division of Thoracic & Cardiovascular Surgery, Chang Gung Memorial Hospital at Linkou, College of Medicine, Chang Gung University, Taiwan

Objective: To evaluate the computed tomography (CT) appearances of atypical adenomatous hyperplasia (AAH) of lung.

Methods: The medical records and CT images of histologically proven AAH in 15 patients encountered in the past 6 years were retrospectively reviewed.

Results: Among all AAH lesions, thirteen lesions were located in right lung, including 6 in lower lobe, 6 in upper lobe and 1 in middle lobe. Two lesions occurred in left lung, both in lower lobe. No multiplicity of AAH was found. All AAH nodules appeared as round (n = 9), oval (n = 5) or irregular (n = 1), with the largest dimensions ranged from 0.55 to 1.70 cm (mean: 0.84 cm). Of 15 lesions, 13 featured pure ground glass nodules (GGNs), and 2 presented as part solid nodules due to thickened alveolar septa and dense collagenous stroma shown by histology. The average internal attenuation of the GGNs ranged from -729 to -284 HU (mean ± standard deviation: -538±106 HU).

Conclusion: An AAH features a lung nodule ranging from 0.55 to 1.70 (mean: 0.84) cm in diameter. It mainly presents as GGN, but may sometimes appears part-solid due to thickening of alveolar septa.

Incidental nodular lesion in anterior mediastinum on chest CT screening: incidence and characteristics

Soon Ho Yoon¹, Chang Hyun Kang², Jin Mo Goo¹, Chang Min Park¹, Chang Hyun Lee¹, Hyun Ju Lee¹

1. Department of Radiology, Seoul National University College of Medicine, Korea

2. Department of Thoracic Surgery, Seoul National University College of Medicine, Korea

Purpose: To assess the incidence and characteristics of anterior mediastinal nodular lesion incidentally found on chest CT screening for healthy people.

Methods: We retrospectively extracted cases with incidentally found anterior mediastinal lesion by reviewing the formal radiology report of screening chest CT taken in healthy people from 2006 through 2013 at the center for health promotion of a tertiary hospital. Most CT scans were performed using low-dose CT protocol with a section thickness of 3mm or less. Incidence and characteristics of incidental nodular lesion (≥ 5 mm in short-axis diameter) were evaluated with the exclusion of cases suggestive of typical thymic remnant, thymic hyperplasia, intrathoracic goiter, and pericardial cyst.

Results: Of 56358 healthy people undergoing chest CT screening, four hundred forty one nodular lesions were identified (median age, 57; incidence, 0.78%; 95% CI, 0.71-0.86%). Median attenuation of nodular lesions was 43 HU with bi-modal distribution. Final diagnosis was obtained in 50 of 441 lesions (11.3%) by surgical resection and CT angiography. Among them, 38 of 50 (76%; size, 1.7 ± 0.8 cm) were benign and the most prevalent pathology was thymic cyst. Follow-up CT scans were taken at least 2 year after baseline CT scan in 202 of 442 lesions (45.7%; median follow-up, 50 months). 181 of 204 those lesions (88.4%) had been stable or decreased in size.

Conclusion: Anterior mediastinal nodular lesion is incidentally found in 0.8 % of healthy people on screening chest CT scan and can be conservatively managed especially when the lesion size is less than 2cm.

Comparison of Thin-section CT Features of T1 Invasive Adenocarcinomas of Lungs According to the sub-classification Diagnosed by using New WHO Classification

Daisuke Takenaka¹, Saori Hirabayashi¹, Toshiko Sakuma², Mika Nakabayashi¹, Tomohisa Hashimoto¹, Munenobu Nogami¹, Yoshitaka Abe¹, Masahiro Yoshimura³, Shuji Adachi¹

1. Department of Diagnostic Radiology, Hyogo Cancer Center, Japan

2. Department of Diagnostic Histology, Hyogo Cancer Center, Japan

3. Department of Thoracic Surgery, Hyogo Cancer Center, Japan

Purpose: The purpose of this study was to compare the CT features of T1 invasive lung adenocarcinoma between the histological sub-classifications histologically diagnosed by using new WHO classification.

Materials and Methods: One hundred eighty two patients were enrolled for this study who were diagnosed with pT1 invasive adenocarcinomas of lung by post-surgical histological examination. Three patients had two synchronous primary adenocarcinomas, so 185 five invasive adenocarcinomas were diagnosed. All patients underwent CT examination before surgery. All CT examinations were performed with 16 or 80-detector row CT scanner; collimation 1 mm x 16 or 80, reconstruction 1mm/1mm. The CT images were reviewed with lung window setting and mediastinal window setting. The age, sex, Brinkman index of all patient were obtained from clinical record, All lung cancers were measured its longitudinal diameter and visually interpreted presence or absence of the following morphologic features; pure ground glass nodule (pure GGN), part-solid GGN, solid nodule, smooth margin, lobulated margin, speculated margin, air-bronchogram, cavity, pleural indentation/tag, satellite lesion, atelectasis, necrosis, necrosis, CT angiogram sign, calcification, hilar lymphadenopathy, pleural effusion, on CT images. The statistical analysis were performed by using Student's t-test and/or Fisher's exact test.

Results: There were 46 lepidic predominant adenocarcinoma, 15 acinar predominant adenocarcinomas, 103 papillary predominant adenocarcinomas, 11 solid predominant adenocarcinomas, and 10 invasive mucinous adenocarcinomas. Brinkman index and the rate of solid nodule of acinar and solid predominant invasive adenocarcinoma were significantly higher than those of others ($p < 0.05$). The rate of necrosis of solid predominant invasive adenocarcinoma was significantly higher. The rate of part-solid GGN and lobulated margin of lepidic predominant invasive adenocarcinoma were significantly higher. The rate of pleural indentation/tag of papillary predominant invasive adenocarcinoma was significantly higher.

Conclusion: This study revealed association between CT features and sub-classification of lung invasive adenocarcinoma according to the new WHO classification at pT1-stage; lepidic predominant invasive adenocarcinoma with part-solid GGN, acinar predominant invasive adenocarcinoma with smoking and solid nodule, solid predominant invasive adenocarcinoma with smoking, solid nodule and necrosis, and lepidic predominant invasive adenocarcinoma with part-solid GGN and lobulated margin.

Poster Session P2-3-1

Diffusion-Weighted MRI vs. FDG-PET/CT: Utility for the Management of Thymic Epithelial Tumors

Hisanobu Koyama, Yoshiharu Ohno, Shinichiro Seki, Yuji Kishida, Kazuro Sugimura

Kobe University Graduate School of Medicine, Japan

Purpose: To directly compare the capabilities for managing thymic epithelial tumors between FDG-PET/CT and diffusion-weighted MR imaging (DWI).

Material and Methods: The study had institutional review board approval; written informed consents were obtained from all subjects. Twenty-seven consecutive patients (mean age 53.6 years) with thymic epithelial tumors were enrolled. Based on pathological examination and/or more than 2-year follow-up examinations, all tumors were divided into two groups from the point of view of WHO classification (Group A: hyperplasia and thymoma type A, AB, and B1 [n=13] vs. Group B: thymoma type B2, B3, and thymic cancer [n=14]) and clinical staging except hyperplasia (early [n=14] vs. advanced [n=10]). In each tumor, maximum standardized uptake value (SUVmax) on PET/CT and apparent diffusion coefficient (ADC) and lesion-to-spinal cord ratio (LSR) in DWI were assessed by ROI measurements. Each index was statistically compared between Groups A and B, and between early and advanced stage. The differentiation capabilities of SUVmax were also statistically compared with those of ADC and LSR.

Results: The ADC and LSR of Group A were significantly different from those of Group B ($p<0.05$). The SUVmax of early stage was significantly lower than that of advanced ($p<0.05$). While the differentiation capabilities of PET/CT between Groups A and B had no significant difference from those of DWI ($p>0.05$), they were significantly higher than the clinical staging evaluation ($p<0.05$).

Conclusion: PET/CT and DWI may be considered for managing thymic epithelial tumors from the points of view of clinical stage and WHO classification, respectively.

Poster Session P2-3-2

Appropriate b Value Selection at Chest Computed Diffusion-Weighted Imaging for Improving Pulmonary Nodule/Mass Differentiation

Hisanobu Koyama¹, Yoshiharu Ohno¹, Shinichiro Seki¹, Yuji Kishida¹, Takeshi Yoshikawa¹, Masao Yui², Katsusuke Kyotani³, Kazuro Sugimura¹

1. Kobe University Graduate School of Medicine, Japan

2. Toshiba Medical Systems Corporation, Japan

3. Kobe University Hospital, Japan

PURPOSE: Computed diffusion-weighted imaging (cDWI) is the newly proposed method and to generate DWI with arbitrary b values. Therefore, the choice of b value is clinically important, and may have an influence to diagnostic performance of cDWI. The purpose of this study is to determine an appropriate b value selection for improving pulmonary nodule/mass differentiation.

METHOD AND MATERIALS: One hundred seventy-six patients (mean age; 69.5 years) with 208 pulmonary nodules/masses underwent DWI with b values at 0, 500 and 1000s/mm² by 1.5T MRI. According to pathological and/or follow up examinations, these pulmonary lesions were divided into malignancy (n=166) and benign (n=42). By our propriety software, cDWIs with six different b values from 600 (cDWI600) to 1600 (cDWI1600) s/mm² were computationally generated from actually acquired DWIs (aDWI) with b values at 0 and 500 s/mm². Lesion to spinal cord ratio (LSR) on each DWI was calculated for quantitative diagnosis of pulmonary lesion, and differentiation capabilities of each cDWI and aDWI1000 were compared.

RESULTS: Differentiation capability of cDWI800 was highest (sensitivity [SE], 77.7%; specificity, 73.8%; and accuracy [AC], 76.9%), and SE of cDWI800 was significantly higher than those of cDWI600 (SE; 74.1%, $p<0.05$), cDWI1400 (SE; 71.1%, $p<0.05$), and cDWI1600 (SE; 68.7%, $p<0.05$). Meanwhile, there were no significant difference of differentiation capability among cDWI800, cDWI1000, cDWI1200 and aDWI1000 ($p>0.05$).

CONCLUSION: On diagnosis of pulmonary nodules/masses, cDWI would be better to be generated from aDWI with 500s/mm² as b value at 800-1200s/mm², and considered at least as valuable as aDWI with 1000s/mm².

Poster Session P2-3-3

Evaluation of the detectability of pulmonary micrometastases of 5 mm and smaller in dual time point TOF FDG PET/CT

Tsuyoshi Komori, Akira Higashiyama, Hiroshi Jyuri, Yoshikazu Tanaka, Mitsuhiro Koyama, Takamitsu Hamada, Yoshifumi Narumi

Osaka Medical College, Japan

Purpose: To evaluate the diagnostic efficacy of TOF PET/CT for detecting pulmonary micrometastases of 5 mm and smaller in patients with cancer.

Subjects and Methods: The subjects were patients with cancer who underwent TOF PET/CT between October 2014 and March 2015, showed at least one nodule of 5 mm or smaller in at least one lung field in CT, and later had the nodule malignancy determined. This study included 11 patients and 82 nodules. The diagnostic efficacy of TOF PET/CT for determination of malignancy from early images and delayed images was evaluated retrospectively. Free-breathing images were obtained with a PET/CT scanner (Discovery PET/CT 710 Q, Suite Vision, GE). Early images were obtained 1 hour after FDG injection and delayed images were obtained 2 hours after FDG injection.

Results: The overall results were as follows: with early images, detectability was 15.9% (13/82). With delayed images, detectability was 34.1% (28/82). The detectability of delayed images was higher than that of early images ($p = 0.12$). Diagnostic efficacy with delayed images was also calculated separately by location in the lung field. For the upper lung field, detectability was 51.4% (19/37), while for the lower lung field, detectability was 20.0% (9/45).

Conclusions: The efficacy of free-breathing TOF FDG-PET for detecting pulmonary micrometastases of 5 mm and smaller was superior with delayed images than with early images and was highest with delayed images of the upper lung field.

Poster Session P2-3-4

FDG-PET/CT findings of primary lung cancer arising from the cyst wall or cavity

Maki Otomo¹, Hayato Nose², Hideki Otsuka³, Yoichi Otomi¹, Kaori Terazawa¹, Takayoshi Shinya¹, Masafumi Harada¹

1. Department of Radiology, Tokushima University Hospital, Japan

2. Department of Radiology, Tokushima Prefectural Central Hospital, Japan

3. Department of Medical Imaging / Nuclear Medicine, Tokushima University Graduate School, Japan

Bullous emphysema and interstitial pneumonia are important risk factors for lung cancer. It can be difficult, however, to differentiate lung cancer with a cavity from cavitating benign pulmonary lesions such as aspergilloma or other pneumonia. We present five cases of primary lung cancer arising from the cyst wall or cavity. All cases were men and all were heavy smokers.

Case 1: A 63-year-old patient presented with a nodular lesion arose from a solitary cyst. The lesion was diagnosed as lung adenocarcinoma. Fluorodeoxyglucose (FDG)-positron emission tomography (PET)/computed tomography (CT) detected it in the early stage. Case 2: A 67-year-old patient presented with interstitial pneumonia. An FDG-positive nodule arose from the interstitial change. The pathological organization was squamous cell carcinoma (SCC) and was diagnosed as a primary lesion of brain metastasis. Case 3: A 73-year-old patient presented with interstitial pneumonia and nontuberculous mycobacterial infection. An FDG-positive nodule arose from a giant bulla wall. Histologically, SCC was identified in the inner wall around the cavity. Case 4: A 65-year-old patient was diagnosed with pulmonary bullae. During follow-up of pancreatic carcinoma, we found a new FDG-positive nodule close to the bulla wall and FDG-PET/CT detected early-stage lung adenocarcinoma. Case 5: A 78-year-old patient was diagnosed with a pulmonary bulla, showing high FDG uptake in the increasing mass. FDG-PET/CT detected early-stage SCC. In conclusion, regular chest CT and FDG-PET/CT is recommended for patients with emphysematous bulla or interstitial pneumonia to detect lung cancer in early stage.

Poster Session P2-3-5

Value of 4 dimensional PET/CT in the diagnosis for primary lung cancer to compare with 3D PET/CT

Jun Sato¹, Satoru Miwa¹, Fumiya Nihashi¹, Yuya Aono¹, Yusuke Amano¹, Masanori Harada¹, Tomohiro Uto¹, Shiro Imokawa¹, Mitsuru Taniguchi², Takafumi Suda³

1. Department of Respiratory Medicine, Iwata City Hospital, Japan

2. Department of Radiology, Juzen Memorial Hospital, Japan

3. Second Division, Department of Internal Medicine, Hamamatsu University School of Medicine, Japan

Aim; Our aim was to evaluate the effect for 4D PET/CT in the diagnosis for primary lung cancer in comparison with 3D PET/CT. **Methods;** Thirty-two pulmonary lesions were evaluated in 26 patients diagnosed with primary lung cancer (18 male and 8 female; 17 adenocarcinoma, 5 squamous cell carcinoma, and 1 small cell carcinoma) with a median age of 73 year-old. All patients were underwent 3D whole-body static PET/CT (3D PET/CT) and 4D PET/CT with Discovery PET/CT 710 (GE healthcare) in Juzen Memorial hospital. The Real-Time Position Management Respiratory Gating System (Variant Medical Systems) was used for the gating tool. We divided the respiratory cycle into 5 periods, and examined PET/CT images in the expiratory phase. In both studies, maximum SUV (SUVmax) was determined for each lesion. Data are expressed as mean \pm SD. **Results;** Thirty of 32 lesions showed an increase of SUVmax in 4D PET/CT studies to compare with 3D PET/CT studies. 4D PET/CT studies showed a statistically significant increase in SUVmax as compared to 3D PET/CT studies ($p < 0.01$; 13.80 ± 10.58 , and 11.31 ± 8.97 , respectively). The percentage difference in SUVmax between 3D and 4D PET/CT studies was $22.49 \pm 17.93\%$. However, no statistical differences dependent on the location and the size of the lesions were observed. **Conclusions;** In comparison to 3D PET/CT, 4D PET/CT may improve the diagnosis for primary lung cancer. We need future studies on the benefits of 4D PET/CT depend on the location and size of lesions.

Poster Session P2-4-1

Clinical features of lung cancer and effect of its resection on pulmonary function in patients with combined pulmonary fibrosis and emphysema

Katsutoshi Ando¹, Mariko Fukui², Kazuhiro Suzuki³, Shiaki Oh², Kazuhisa Takahashi¹, Kenji Suzuki², Kazuya Takamochi²

1. Department of Respiratory Medicine, Juntendo University School of Medicine, Japan

2. Department of General Thoracic Surgery, Juntendo University School of Medicine, Japan

3. Departments of Radiology, Juntendo University School of Medicine, Japan

Introduction: Patients with combined pulmonary fibrosis and emphysema (CPFE) have a high risk of developing lung cancer. Recent studies report that pulmonary fibrotic change contributes more to the development of lung cancer than emphysema. However, clinical features of lung cancer remain unclear because parenchymal findings and the extent of emphysema vary in each patient.

Methods: We classified 83 patients with CPFE and 110 patients with interstitial pneumonia (IP) who had undergone surgical resection for primary lung cancer into three groups: (1) "usual interstitial pneumonia (UIP) pattern," (2) "possible UIP pattern," and (3) "inconsistent with UIP pattern", and evaluated their clinical features.

Results: In patients with "possible UIP" and "inconsistent with UIP patterns," clinical features were similar between CPFE and IP. Meanwhile, in patients with UIP pattern, lung cancer was associated with emphysema if it produced severe changes in the upper lobes. After resection, smaller amounts of vital capacity decline were observed in patients with lung cancer in emphysema than in those with IP lesions. After reviewing previous chest CT data at CPFE follow-up, we found varying sizes of lung cancer lesions with having grown to over 10 mm in approximately 1 year.

Conclusions: Clinical features of lung cancer in CPFE were different in each IP pattern; however, its predilection site could be predicted by the IP pattern and extent of emphysema. Our results suggest that annual screening for lung cancer would be useful.

Poster Session P2-4-2

Evaluation of lung cancer by enhanced dual-energy CT: Association between three-dimensional iodine concentration and tumor differentiation

Shingo Iwano, Kazuhiro Shimamoto, Hiroyasu Umakoshi, Rintaro Ito, Shinji Ito, Shinji Naganawa
Department of Radiology, Nagoya University Graduate School of Medicine, Japan

Objectives: To investigate the correlation between iodine attenuation of dual-energy CT (DECT) and histopathology of surgically resected primary lung cancers.

Methods: We reviewed the medical records, post-operative pathological records, and preoperative DECT images of patients who underwent surgical lung resection for primary lung cancer. After injection of iodinated contrast media, arterial and delayed phases were scanned using 140-kV and 80-kV tube voltages. Three-dimensional iodine attenuation (iodine volume) of primary tumors was calculated using lung nodule application software.

Results: A total of 60 patients (37 males, 23 females; age range, 39-84 years; mean age, 69 years) with 62 lung cancers were analyzed. The resected tumors were histopathologically classified into well-differentiated (G1; n=20), moderately-differentiated (G2; n=29), poorly-differentiated (G3; n=9), and undifferentiated (G4; n=4) groups by degree of tumor differentiation (DTD). The mean±standard deviation of iodine volume at the delayed phase was 59.6±18.6 HU in G1 tumors, 46.5±11.3 HU in G2 tumors, 34.3±15.0 HU in G3 tumors, and 28.8±6.4 HU in G4 tumors; significant differences were observed between groups ($p < 0.001$). Univariate logistic analysis showed that iodine volumes both at the early and delayed phases were significantly correlated with DTD ($p = 0.006$ and $p = 0.001$, respectively), while gender, body weight, and tumor size were not ($p = 0.084$, $p = 0.062$, and $p = 0.391$, respectively).

Conclusions: The iodine volume of lung cancers was significantly associated with their DTD. High-grade tumors tended to have lower iodine volumes than low-grade tumors.

Poster Session P2-4-3

Classifications and Measurements in Subsolid Nodules: Which Window Setting is Better?

Roh-Eul Yoo, Jin Mo Goo, Eui Jin Hwang, Soon Ho Yoon, Chang Hyun Lee, Chang Min Park
Seoul National University Hospital, Korea

Purpose: To compare interobserver agreements among multiple readers and accuracy for the assessment of solid components in subsolid nodules between the lung and mediastinal window settings.

Materials and Methods: Seventy-seven nodules with solid components smaller than 8 mm, which were surgically resected, were included in this study. In both lung and mediastinal window settings, five readers independently assessed the presence and the size of solid component on the representative section of each nodule. The overall sizes of the nodules were measured on lung windows. Bootstrapping was used to compare the interobserver agreement (Fleiss' kappa and intraclass correlation coefficients [ICC]) between the two window settings. Imaging-pathology correlation was performed to evaluate the accuracy.

Results: There were no significant differences in the interobserver agreements between the two window settings in both nodule classifications (lung windows, $k = 0.51$; mediastinal windows, $k = 0.57$) and solid component measurements (lung windows, ICC = 0.70; mediastinal windows, ICC = 0.69). The incidence of false negative results (cases in which invasive components were present on pathology although there were no discernible solid components on CT) and the mean absolute difference between the solid component size and the invasive component size were significantly higher on mediastinal windows than on lung windows ($P < .001$ and $P < .001$, respectively).

Conclusion: The lung window setting had a comparable reproducibility but a higher accuracy than the mediastinal window setting for nodule classifications and solid component measurements in subsolid nodules.

Poster Session P2-4-4

Utility of Dual-Energy CT for Differentiation of Pulmonary Nodules: Comparison of Dual-Energy CT and FDG-PET/CT

Sachiko Miura¹, Yoshiharu Ohno², Takeshi Kawaguchi³, Takashi Tojo³, Kimihiko Kichikawa¹

1. Department of Radiology, Nara Medical University, Japan
2. Advanced Biomedical Imaging Research Center, Kobe University Graduate School of Medicine / Division of Functional and Diagnostic Imaging Research, Department of Radiology, Kobe University Graduate School of Medicine, Japan
3. Department of Thoracic and Cardiovascular Surgery, Nara Medical University, Japan

Purpose: To investigate the capability of dual-energy CT (DECT) for differentiation of pulmonary nodules as compared with FDG-PET/CT.

Materials and methods: Fifteen patients who had 19 lung nodules totally underwent dual-point contrast-enhanced (CE-) DECT and FDG-PET/CT, and pathological and/or follow-up examinations. All nodules were divided into malignant (n=15) and benign (n=4) groups. From DECT data, we generated virtual non-contrast (VNC) images and iodine maps at each phase. ROIs were placed over all nodules to measure the values and calculate the difference of them between the two phases on VNC image (Δ VNC). On FDG-PET/CT, SUVmax of each nodule was also assessed. Student's t-test and ROC-based positive test were performed to evaluate all indices and determine feasible threshold values. Finally, sensitivity (SE), specificity (SP) and accuracy (AC) were compared using McNemar's test.

Results: There were significant differences on Δ VNC (malignant vs. benign: 0.67 ± 4.2 HU vs. 10.8 ± 7.6 HU, $p=0.002$) and SUVmax (malignant vs. benign: 6.7 ± 4.6 vs. 1.5 ± 0.58 , $p=0.0007$). When the feasible threshold values were applied, SE: 100 [15/15] %, SP: 50 [2/4] % and AC: 89.5 [17/19] % of Δ VNC were better than those of SUVmax (SE: 86.7 [13/15] %, SP: 50 [2/4] %, AC: 78.9 [15/19] %), not significant though ($p>0.05$).

Conclusion: Dual-energy CT is considered at least as valuable as FDG-PET/CT for differentiation of pulmonary nodules.

Poster Session P3-1-1

Quantitative and qualitative analysis for chest CT with statistical or model-based iterative reconstruction: a chest phantom study

Satoshi Kawanami¹, Takeshi Kamitani², Torahiko Yamanouchi², Koji Sagiyama¹, Hidetake Yabuuchi³, Michinobu Nagao¹, Yuko Tanaka², Yuzo Yamasaki², Masatoshi Kondo⁴, Hiroshi Honda²

1. Department of Molecular Imaging & Diagnosis, Graduate School of Medical Sciences, Kyushu University, Japan
2. Department of Clinical Radiology, Graduate School of Medical Sciences, Kyushu University, Japan
3. Department of Health Sciences, Faculty of Medical Sciences, Kyushu University, Japan
4. Department of Radiological Technology, Kyushu University Hospital, Japan

Objectives: To evaluate the reliability of quantitative and qualitative analysis for chest CT with filtered back projection (FBP), statistical iterative reconstruction (iDose4) or iterative model-based reconstruction (IMR). Methods: A chest phantom data was scanned with a 256-section MDCT system in 12-bit depth: tube voltage, 120kV; slice-thickness, 0.625mm. Four different effective tube current time product (200, 100, 30 and 10mAs) and 4 different reconstruction algorithms [FBP, iDose4, IMR and IMR with ultra-sharp (IMRus)] were selected. Area under -800HU was retrieved as the simulated lung, then total lung capacity (TLC), mean lung density (MLD) and percentage of low-attenuation area (LAA%) were produced and determined by the analysis of variance (ANOVA). Correlation coefficient was calculated by histogram data from -1000 to -800HU. Visual assessments were performed for ground-glass nodules and pneumothorax. Goddard score was also derived. Results: TLC, MLD and LAA% was as follows; FBP [4.93(1), -851(HU), 16.0(%)], iDose4 [4.93, -851, 9.1], IMR [4.92, -852, 4.1], IMRus [4.87, -867, 27.2], 200mAs [4.90, -857, 10.3], 100mAs [4.91, -856, 10.8], 30mAs [4.92, -854, 12.4] and 10mAs [4.92, -851, 14.3]. From 30 to 200mAs, excellent correlation ($\rho>0.996$) was observed in FBP, iDose4 and IMR, and visual assessment score was acceptable except IMRus. Conclusion: TLC and MLD were reliable with FBP (≥ 100 mAs), iDose4 (≥ 30 mAs) or IMR (≥ 10 mAs). Visual assessment, Goddard score and LAA% were variable owing to reconstruction algorithm, especially in 10 and 30mAs. Careful optimization is sufficient to improve the reliability of quantitative and qualitative analysis for chest CT.

The impact of iterative reconstruction onto quantitative evaluation of COPD using fully automated lobar segmentation

Hyun-ju Lim¹, Oliver Weinheimer¹, Mark O. Wielputz¹, Julien Dinkel^{1,2}, Thomas Hielscher³, Daniela Gompelmann^{2,4}, Hans-Ulrich Kauczor^{1,2}, Claus Peter Heussel¹

1. Department of Diagnostic and Interventional Radiology, University Hospital of Heidelberg, Germany

2. Translational Lung Research Center Heidelberg (TLRC), Member of the German Center for Lung Research (DZL), Germany

3. Division of Biostatistics, German Cancer Research Center (dkfz), Germany

4. Department of Pneumology and Respiratory Critical Care Medicine, Thoraxklinik at University, Germany

Objectives

The purpose of this study was to evaluate the influence of iterative reconstruction (IR) on fully automated lobe based emphysema quantification.

Material and methods

63 patients (35 men; age 63 ± 7 years; BMI 26 ± 5 kg/m²) suffering from GOLD stage II-IV COPD underwent MDCT. Reconstructions were performed with both filtered back projection (FBP) and raw-data-based IR. Lobe based emphysema quantification parameters were calculated by the software YACTA (version v.2.4.3.1) and compared for FBP and IR by limits of agreement (LoA) using Bland-Altman approach. Image noise of for FBP and IR were also measured and compared.

Results

Image noise was significantly lower for IR as compared to FBP ($p < 0.001$). By visual interpretation, IR changed lobar segmentation of the middle lobe in 5 patients, subsequently affecting emphysema quantification. The mean difference was 0 ml ($p = 0.98$, no difference that reaches statistical significance could be found) for segmented lobar volume (LoA: ± 213 ml). Difference of mean lung density was less than 1 HU ($p = 0.70$) (LoA: -20 to +18 HU). The mean difference was 3 HU ($p < 0.05$) (LoA: -2, +7 HU) for 15th percentile lung density, which was the only parameter significantly different and was higher with IR. The emphysema index showed a mean difference of 1% ($p = 0.24$) (LoA: -5 to +3%). The mean difference between FBP and IR was 17 ml ($p = 0.36$) (LoA: -84 to +51 ml) for emphysema volume.

Conclusions

This study showed that FBP and IR may deliver different results for lobar segmentation and subsequently for emphysema quantification. This should be considered for longitudinal studies of emphysema progression.

Poster Session P3-1-3

Assessment of regional xenon-ventilation, perfusion and ventilation-perfusion mismatch Using Dual-Energy Computed Tomography in COPD Patients

Hye Jeon Hwang^{1,2}, Joon Beom Seo², Sang Min Lee², Sang Young Oh², Namkug Kim², Taekjin Jang², Jae Seung Lee², Sei Won Lee², Yeon-Mok Oh²

1. Hallym University College of Medicine, Hallym University Sacred Heart Hospital, Korea

2. University of Ulsan College of Medicine, Asan Medical Center, Korea

Rationale: Ventilation-perfusion imbalance is important in COPD patients. Dual-energy CT (DECT) can provide concurrently high-resolution anatomic information and parenchymal perfusion or ventilation.

Objectives: To evaluate the potential of DECT with combined xenon-ventilation (V) and contrast-perfusion (Q) imaging for the comprehensive evaluation of regional V and Q status in COPD patients.

Methods: Combined V-Q DECT was performed in fifty-two COPD patients. Virtual noncontrast (VNC) image, V map, Q map and V/Qratio map were anatomically co-registered using in-house software. V/Qratio pattern was visually determined as matched, mismatched and reversed-mismatched, and compared with regional disease patterns of each segment (emphysema with/without bronchial wall thickening, bronchial wall thickening, and normal) on VNC image. Quantified CT parameters of each patient were compared with PFTs parameters using Pearson correlation test.

Measurements and Main Results: Segments with normal parenchyma demonstrated matched V/Qratio, while segments with bronchial wall thickening commonly showed reversed-mismatched V/Qratio. Matched V/Qratio and reversed mismatched V/Qratio patterns were mixed within emphysema areas. Quantified mean V, Q, VQmin (smaller value between V and Q in each pixel) and V/Qratio values in each patients were positively correlated with PFT ($r = 0.290 \sim 0.815$; $p < 0.05$). V/Qsd (standard deviation of V/Qratio) was negatively correlated with PFT ($r = -0.439 \sim -0.736$; $p < 0.001$). VQmin values demonstrated the best correlation with PFT ($r = 0.483 \sim 0.815$; $p < 0.001$).

Conclusions: Combined V-Q DECT provides reliable information of regional V and Q and V-Q relationship, with significant correlation with PFT in patients with COPD.

Poster Session P3-1-4

Longitudinal Follow-up Study of Smoking-induced Emphysema Progressing using Low-dose CT Screening

Kohji Shimada¹, Mikio Matsuhira¹, Hidenobu Suzuki¹, Yoshiki Kawata¹, Noboru Niki¹, Yasutaka Nakano², Hironobu Ohmatsu³, Masahiko Kusumoto³, Takaaki Tsuchida⁴, Kenji Eguchi⁵, Masahiro Kaneko⁶

1. Tokushima University, Japan

2. Shiga University of Medical Science, Japan

3. National Cancer Center Hospital East, Japan

4. National Cancer Center Hospital, Japan

5. Teikyo University, Japan

6. Tokyo Health Service Association, Japan

Death by lung cancer is the fifth of death by cancer. In recent years, CT screening of lung is applied for early detection of lung cancer. The loss of lung parenchyma associated with emphysema represents low attenuation volume (LAV) in CT images. CT images of lung cancer have shown usability in detection of Chronic Obstructive Pulmonary Disease(COPD). Consequently, early detection of COPD by CT images of lung cancer is expected. Reduction of deaths by smoking cessation is important. In this study, we extracted LAV through CT images of lung cancer. The annual changes of LAV by smoking status were measured in each lung lobe as well. It shows the aging of the lung lobe another emphysema lesions due to smoking history by using a lung cancer CT screening image.

Poster Session P3-1-5

Correlation of clinical characteristics by the grade of pulmonary emphysema in combined pulmonary fibrosis and emphysema

Keishi Sugino¹, Kenta Furuya¹, Yasuhiko Nakamura¹, Kyoko Gocho¹, Go Sano¹, Kazutoshi Isobe¹, Susumu Sakamoto¹, Yujiro Takai¹, Keiko Matsumoto², Nobuyuki Shiraga², Sakae Homma¹

1. Department of Respiratory Medicine, Toho University Omori Medical Center, Japan

2. Department of Diagnostic Radiology, Toho University Omori Medical Center, Japan

Aim: The aim of this study was to clarify the differences of clinical characteristics by the percentage grade of pulmonary emphysema in combined pulmonary fibrosis and emphysema (CPFE), which is defined as pulmonary emphysema associated with idiopathic pulmonary fibrosis (IPF).

Patients and Methods: Of consecutive 131 IPF patients admitted to our hospital between April 2003 and March 2014, 47 patients were diagnosed as CPFE and 84 patients were diagnosed as IPF alone. Patients with CPFE were classified into 2 subtypes: CPFE with > %LAA of 20% or ≤%LAA of 20%. This threshold was chosen by calculating a median value. We retrospectively compared the clinical features, pulmonary function test findings, and prognosis between these CPFE groups and IPF alone.

Results: Baseline values of %FVC, %TLC, and the annual increase in estimated pulmonary artery pressure in each CPFE group were significantly higher than those in IPF alone patients, whereas %fibrosis extent, %FEV1 / FVC, and %DLco/VA were significantly lower in CPFE groups. Survival time was significantly lower in patients with CPFE with ≤%LAA of 20% than in those with CPFE with > %LAA of 20% and IPF alone, respectively (MST: 20 vs. 37 vs. 47.9 months, P = 0.019). Moreover, survival time was significantly shorter in patients with CPFE with ≤%LAA of 20% than in those with IPF alone (P = 0.006). The multivariate Cox regression model showed that the predictive factors were decreased %FEV1, presence of emphysema and acute exacerbation.

Conclusions: This study demonstrated that patients with CPFE have a worse prognosis than those with IPF alone. In particular, CPFE patients with ≤%LAA of 20% have an extremely poor prognosis.

Poster Session P3-2-1

Evaluation of pharmacological volume reduction effect induced by tiotropium via 3D-CT image analysis

Kazuya Tanimura, Susumu Sato, Tsuyoshi Oguma, Atsuyasu Sato, Koichi Hasegawa, Kiyoshi Uemasu, Yoko Hamakawa, Toyohiro Hirai, Michiaki Mishima, Shigeo Muro

Department of Respiratory Medicine, Graduate School of Medicine, Kyoto University, Japan

Background

Since CT volumetry in serial series of chest CT images enables to evaluate lung volume changes, CT volumetry can evaluate an effect of bronchodilator in COPD patients by looking at volume reduction before and after administration. In addition to our previous report (Tanabe, et al. Respir Med 2012), we evaluated the local volume reduction by tiotropium in COPD patients using lobe segmentation methods and nonrigid multimodality image registration techniques.

Patients and Methods

Outpatients with stable COPD who underwent chest CT scan and pulmonary function test before and one year after starting tiotropium treatment (Tio group, n=25) and who underwent these tests twice at a yearly interval without tiotropium (Control group, n=12) were enrolled (age 72.7±7.1 years, %FEV1 46.6±11.7%) and were quantitatively evaluated the therapeutic effect of tiotropium. In CT analysis, we calculated the absolute value and the ratio of change in the whole lung volume or the lobar volume by using SYNAPSE VINCENT (FUJIFILM Medical Co., Ltd., Tokyo, Japan).

Results

The whole lung volume in Tio group showed a trend to decrease (-148mL vs 10mL, p=0.1), but there was no significant difference in patients' characteristics and the ratio of change in the volume between these two groups. The lobar analysis revealed that the volume of the left upper lobe significantly decreased and all the lobes except the right median lobe showed a trend to decrease.

Conclusion

3D-CT analysis of the lobar volume may detect the pharmacological volume reduction effect by tiotropium better than that of whole lung volume.

Poster Session P3-2-2

Morphologic and Functional change after bronchoscopic lung volume reduction in COPD assessed with combined xenon ventilation and iodine perfusion dual energy CT

Joon Beom Seo¹, Sei Won Lee², Sang Min Lee¹, Namkug Kim¹, Sang Hyun Paik³,
Yeon-Mok Oh², Sang-Do Lee²

1. University of Ulsan College of Medicine, Asan Medical Center, Korea

2. Pulmonology and Critical Care Medicine, Asan Medical Center, Korea

3. Radiology, Soon Chun Hyang University Bucheon Hospital, Korea

Purpose: In this study, we analyzed the morphologic and physiologic changes after BLVR by using xenon-enhanced ventilation (V) and iodine-enhanced perfusion (Q) dual-energy computed tomography (DECT) to prove the hypothesis.

Methods: Twenty Patients with advanced emphysema were eligible to this procedure. Pulmonary function tests, 6-minutes walking distance test (6MWD) and combined V-Q DECT were performed at baseline and after BLVR (mean interval = 110 days). Mean V and Q values and sum of V and Q values in the whole lung, each lobe, ipsi- and contralateral lung were measured in both initial and follow up DECT images. After image co-registration, V/Q ratio was measured. Each measured values on initial and follow up CT were compared. The ratios of change in lung volume, V, Q and V/Q ratio in ipsi- and contralateral lung were compared.

Results: After treatment, the mean of V and sum of V values in the whole lung and ipsilateral lung increased significantly despite of decreased lung volume (all $p < 0.05$, paired t-test). The increase in mean V and mean Q values in ipsilateral lung were significantly higher than those of contralateral lung of treatment. FEV1 and 6MWD increased significantly after BLVR. Improvement was pronounced in patient with successful BLVR. Ventilation perfusion (V/Q) mismatch improved after BLVR, mainly attributable to improved ventilation.

Conclusion: Regional ventilation and perfusion change of the lung after BLVR can be visualized and quantified with combine V and Q DECT. Both ventilation and V/Q mismatch measured with DECT improved after BLVR.

Poster Session P3-2-3

Exertional dyspnoea and cortical oxygenation in patients with COPD

Yuji Higashimoto, Toshiyuki Yamagata, Akiko Sano, Osamu Nishiyama, Hiroyuki Sano,
Takashi Iwanaga, Yuji Tohda

Kinki University, Japan

This study was designed to investigate the association of perceived dyspnoea intensity with cortical oxygenation and cortical activation during exercise in patients with chronic obstructive pulmonary disease (COPD) and exertional hypoxaemia.

Low-intensity exercise was performed at a constant work rate by patients with COPD and exertional hypoxaemia (n=11) or no hypoxaemia (n=16), and in control participants (n=11). Cortical oxyhaemoglobin and deoxyhaemoglobin concentrations were measured by multichannel near-infrared spectroscopy. Increased deoxyhaemoglobin is assumed to reflect impaired oxygenation, whereas decreased deoxyhaemoglobin signifies cortical activation.

Exercise decreased cortical deoxyhaemoglobin in control and non-hypoxaemic patients. Deoxyhaemoglobin was increased in hypoxaemic patients, and oxygen supplementation improved cortical oxygenation. Decreased deoxyhaemoglobin in the premotor area (PMA) was significantly correlated with exertional dyspnoea in control participants and patients with COPD without hypoxaemia. In contrast, increased cortical deoxyhaemoglobin concentration was correlated with dyspnoea in patients with COPD and hypoxaemia. With the administration of oxygen supplementation, exertional dyspnoea was correlated with decreased deoxyhaemoglobin in the PMA of COPD patients with hypoxaemia.

During exercise, cortical oxygenation was impaired in patients with COPD and hypoxaemia compared with control and non-hypoxaemic patients; this difference was ameliorated with oxygen supplementation. Exertional dyspnoea was related to activation of the premotor cortex in COPD patients.

Poster Session P3-2-4

Assessment of CT-derived airway wall area in COPD patients with indacaterol therapy

Ruriko Seto¹, Emiko Ogawa¹, Kaoruko Shimizu², Hironi Makita², Kenichi Goto¹, Yuichi Higami¹, Rie Kanda¹, Hiroaki Nakagawa¹, Kentaro Fukunaga¹, Yasuki Uchida¹, Masafumi Yamaguchi¹, Taishi Nagao¹, Masaharu Nishimura², Yasutaka Nakano¹

1. Division of Respiratory Medicine, Shiga University of Medical Science, Japan

2. First Department of Medicine, Hokkaido University School of Medicine, Japan

Background

The square root of airway wall area of hypothetical airway with an internal perimeter of 10 mm (\sqrt{Aaw} at Pi10) has been used as a comparable index of airway dimensions and has been shown to be correlated with pulmonary function measurements. However, it is not clear how to interpret the change of \sqrt{Aaw} at Pi10 before and after treatment. We hypothesized that the change of \sqrt{Aaw} with Pi between 6-20 mm would be a sensitive marker for the effects of bronchodilation.

Methods

Twenty seven COPD patients were enrolled in this study. Chest CT scan and pulmonary function tests were performed before and one month after inhalation of indacaterol (long acting β_2 agonist). \sqrt{Aaw} were plotted against the inner perimeter between 6-20 mm, and \sqrt{Aaw} at Pi5, 10, 15, 20 and 25 of each visit were calculated. The subjects were divided into two groups; responders and non-responders by cutoff value of 120 ml improvement of FEV1 after inhalation of indacaterol.

Result

The patients' clinical characteristics and \sqrt{Aaw} at Pi5, 10, 15, 20 and 25 were similar between the two groups at baseline. The treatment of indacaterol tended to decrease CAT score and \sqrt{Aaw} in both groups. When we focused on the responders, \sqrt{Aaw} at Pi10 and 15 were significantly smaller after inhalation, while there was no significant difference in \sqrt{Aaw} at Pi25 which represents relatively central airway.

Conclusion

The changes of \sqrt{Aaw} at Pi10 and 15 may sensitively reflect the effectiveness of indacaterol.

Poster Session P3-2-5

Computer tomography (CT)-assessed bronchodilation induced by inhaled indacaterol and glycopyrronium /indacaterol combination in COPD

Kaoruko Shimizu¹, Ruriko Seto², Hironi Makita¹, Masaru Suzuki¹, Satoshi Konno¹, Rie Kanda², Emiko Ogawa², Yasutaka Nakano², Masaharu Nishimura¹

1. First Department of Medicine, Hokkaido University School of Medicine, Japan

2. Shiga University of Medical Science, Japan

Background: Site of bronchodilation may be different between β_2 agonists and anticholinergics in COPD.

Aim: To quantitatively assess the bronchodilation by generation of the airways, using 3D CT, when induced by inhaled indacaterol and glycopyrronium/indacaterol combination.

Methods: We conducted CT scans at full inspiration and lung function tests in 26 patients with moderate-severe COPD before and 4 week after daily inhalation of indacaterol and again another 4 week after inhalation of glycopyrronium /indacaterol combination. We analyzed airway luminal area (A_i) at the 3rd (segmental) to 6th generation of 8 selected bronchi, a total of 32 sites, in the right lung on 3 occasions. Our proprietary software enables us to select the same airways and the same measurement sites for comparison, by simultaneously displaying two screens on the computer.

Results: Baseline FEV1 (1.42 ± 0.10 L SD) increased to 1.50 ± 0.10 L with indacaterol and then to 1.60 ± 0.10 L with glycopyrronium/indacaterol combination. The overall increase of A_i ($\Delta A_i\%$) averaged at all 32 measurement sites had a significant correlation with FEV1 improvement ($\Delta FEV1, \%$) ($r=0.755$, $p<.0001$). The $\Delta A_i\%$ with indacaterol alone was 8.9 ± 3.5 , 19.2 ± 3.8 , 21.5 ± 5.6 , and $21.8 \pm 5.9\%$ at the 3rd to 6th generation, and the additional $\Delta A_i\%$ with glycopyrronium/indacaterol combination was 15.8 ± 2.8 , 18.3 ± 3.8 , 28.9 ± 5.2 and $25.9 \pm 5.7\%$, respectively.

Conclusions: Site-specific differences in bronchodilation were not detected between the effect of indacaterol and the additional effect of glycopyrronium.

Poster Session P3-3-1

Quantitative analysis of combined pulmonary fibrosis and emphysema (CPFE): correlation with impairment of lung function

Kum Ju Chae, Gong Yong Jin

Department of Radiology, Chonbuk National University Hospital, Korea

Purpose: To evaluate the characteristic lung density histogram parameters in combined pulmonary fibrosis and emphysema (CPFE) and correlate with pulmonary physiologic abnormality.

Materials and methods: Quantitative CT indexes such as skewness, kurtosis, airway wall thickness (Pi10) and emphysema index (% lung <-950HU) in 41 patients with CPFE were assessed using software (VIDA diagnostics, Coralville, IA), and compared with normal case-controlled subjects (n=41). Other physiologic parameters of lung including FVC, FEV1/FVC, FEV1 and diffusion capacity for carbon monoxide (DLco) were also evaluated, and Quantitative CT indexes and physiologic parameters of lung were correlated using Pearson's correlation analysis.

Results: Mean values of skewness, kurtosis, Pi10, %<-950HU in CPFE patients were 1.93, 2.85, 4.04, 6.99 resp

ectively, and they had lower skewness, kurtosis, decreased airway wall thickness, and higher extent of emphysema than normal subjects (mean values: 2.38, 4.76, 4.31, 1.25, $p < 0.001$). DLco had moderate correlation with histogram features, skewness showed the greatest degree of correlation with DLco ($r = 0.691$, $p = 0.009$).

Conclusion: In patients with CPFE, quantitative CT analysis could be useful for predicting impaired lung function.

Poster Session P3-3-2

Association of Epicardial Adipose Tissue with Airway Lesion of Chronic Obstructive Pulmonary Disease in Vietnamese

Yuichi Higami¹, Emiko Ogawa^{1,2}, Yasushi Ryujin¹, Kenichi Goto¹, Ruriko Seto¹, Hiroshi Wada¹, Nguyen VanTho^{1,3}, Le Thi Tuyet Lan³, Yasutaka Nakano¹

1. Division of Respiratory Medicine, Department of Internal Medicine, Shiga University of Medical Science, Japan

2. Health Administration Center, Shiga University of Medical Science, Japan

3. Respiratory Care Center, University Medical Center, Vietnam

RATIONALE:

Cardiovascular disease (CVD) is one of the major causes of death in chronic obstructive pulmonary disease (COPD) patients. Epicardial adipose tissue (EAT) has been shown as a non-invasive marker to predict the progression of CVD. It has been reported that EAT volume was increased in COPD patients. However, little is known about which phenotypes of COPD are associated with increased EAT. We hypothesized that CT phenotypes were associated with a risk of CVD.

METHODS:

Vietnamese patients with COPD were recruited if they met the following criteria: age older than 40 years, and a former or current cigarette smoker with more than 10 pack-years smoking history. Chest CT was used for the quantification of emphysematous lesions, airway lesions, and EAT. These lesions were assessed by the percentage of low attenuation volume (LAV%), the square root of airway wall area of a hypothetical airway with an internal perimeter of 10 mm (\sqrt{Aaw} at Pi10) and EAT area, respectively.

RESULTS:

Two hundred and twenty five patients were diagnosed as COPD based on a $FEV_1/FVC < 0.70$. EAT area was significantly associated with BMI, LAV%, and \sqrt{Aaw} at Pi10. Multiple regression analyses showed that only BMI, and \sqrt{Aaw} at Pi10 were independently associated with EAT area ($R^2 = 0.29$, $p < 0.0001$).

CONCLUSIONS:

EAT area is independently associated with airway wall thickness. Since EAT is also an independent predictor of CVD risk, these data suggest a mechanistic link between the airway lesion of COPD and CVD.

Poster Session P3-3-3

Robustness of the power law analysis of emphysema hole size distribution to the variation of lung inflation level and correlation with clinical parameters in KOLD cohort

Jeogneun Hwang, Namkug Kim, Joon Beom Seo, Yeon-Mok Oh

University of Ulsan College of Medicine, Asan Medical Center, Korea

In quantifying the severity of pulmonary emphysema with X-ray chest CT, the irregularities in the inflation level have been a major confounding factor. The increase in the emphysematous volume fraction (EI) of CT images in COPD patients have been reported to represent the severity of pulmonary emphysema. However, EI are susceptible to the occasional variations in the inflation level of the lung. On the contrary, the statistical properties of the emphysema hole size distribution may stay largely unaffected.

We examined the statistical properties of the emphysema hole size distribution in 76 COPD patients (71 males and 5 females, age 67 ± 7.6) both in full inspiration and in full expiration state. The diameters of the emphysema holes were quantified with fully automatic algorithm. The estimated diameters of the emphysema holes showed a power-law distribution, where the power-law exponent D may represent the complexity of the emphysematous lesion.

The slopes of inspiratory and expiratory CT of a patient had ICC (Inter-class Correlation Coefficient) >0.8 which means absolute agreement between inspiratory and expiratory CT in measuring the power law exponent, while the EI failed to achieve an agreement between inspiratory and expiratory CT. The power law exponent D also correlated well with clinical lung function parameters: correlation coefficient $r=0.62$, $p<0.05$ for DLCO.

These findings suggest that the power law exponent D of emphysema hole size distribution is both robust to the inflation level variations and sensible for the severity of emphysema.

Poster Session P3-3-4

Automatic evaluation on fissure integrity for target lobe selection of endobronchial valve volume reduction procedure using volumetric chest CT: Validation with radiologic visual evaluation

Minho Lee, Namkug Kim, Sang Min Lee, Joon Beom Seo

University of Ulsan College of Medicine, Asan Medical Center, Korea

To evaluate quantitative fissure integrity ratios (FIR) to select target lobe for endobronchial valve volume reduction procedure (EVVR) and to compare them with radiologic visual evaluation.

Twenty patients with severe COPD patients for EVVR procedure were scanned by a 64-MD dual-energy CT scanner. Lung, airway and pulmonary vessel were extracted using thresholding, 3D region growing with semi-automatic interaction. Lung left and right split and lobe segmentation were performed with 3D free-formed surface fitting on possible fissure voxels which were detected by hessian matrix analysis within lung except dilated airway and pulmonary vessel regions. Based on this fissure segmentation in left lung, we evaluated FIRs based on histogram of z-axis projected image with maximum likelihood threshold method. Two thoracic radiologists (rad1, rad2) evaluated fissure integrity as completeness, incomplete fissure lengths on axial and sagittal planes. In disagreement case, third thoracic radiologist (radc) with more than 10 years' experience finally determined the completeness.

Optimal threshold for differentiation between complete and incomplete fissure was evaluated as -901HU. At that threshold, optimal threshold of FIR to determine completeness (CAD) are 0.982 considering radiologist's decisions. Accuracy between computer and radiologic decision in consensus are 85% and FIR in complete and incomplete are significantly correlated with radiologic visual evaluations (all p-values <0.01) and different ($p=0.011$, t-test). Cohen's kappa values are all substantial (rad1 vs rad2, 0.694; CAD vs rad1, 0.681, CAD vs rad2, 0.588; CAD vs radc, 0.700).

Automatic quantitative evaluation on fissure integrity based on lobe segmentation were developed and evaluated with radiologic decision.

Estimated postoperative pulmonary function calculated with lung volume in 3D-CT for lung cancer patients with and without COPD

Masanori Yokoba^{1,2}, Tsuyoshi Ichikawa³, Akira Takakura¹, Tomoya Fukui¹, Satoshi Igawa¹, Masaru Kubota¹, Shouko Hayashi⁴, Mototsugu Ono⁴, Dai Sonoda⁴, Yoshio Matsui⁴, Kazu Shiomi⁴, Yukitoshi Sato⁴, Noriyuki Masuda¹, Masato Katagiri^{1,2}

1. Kitasato University Hospital Pulmonary Medicine, Japan
2. Kitasato University School of Allied Health Sciences, Japan
3. Tokai University Oiso Hospital, Japan
4. Kitasato University Hospital Thoracic Surgery, Japan

The evaluation of a postoperative pulmonary function is important for estimating the risk of complications and long-term disability after pulmonary resection in patients with COPD. The aim of this study is to reveal the differentiation between 1) actual values examined after lobectomy (PO), estimated postoperative values calculated with 2-a) the proportion of the resected lung (ePOpro), 2-b) number of segments method (ePOseg), 2-c) resected lobular volume by 3D-CT (ePO_{CT}), and 2-d) resected lobular volume including its low attenuation area obtained by 3D-CT (ePO_{CTLAA}) on i) BSA corrected FEV₁, ii) %FEV₁, iii) %DLco/V_A, and iv) %VC. The ePO_{CTLAA} was calculated with following formula: (preoperative value) X [(total lung volume) - {(lobular volume that will be resected) x (1 - LAA volume of the lobe that will be resected/100)} / (total lung volume)].

21 COPD patients (GOLD1/2 : 8/13) and 15 non COPD patients were enrolled.

For BSA corrected FEV₁ and %FEV₁, ePOpro was smaller than PO in non COPD patients, and ePOpro and ePOseg were smaller than PO in GOLD2 patients.

For %DLco/V_A and %VC, ePOseg was smaller than PO in GOLD2 patients.

ePO_{CT} was smaller than ePO_{CTLAA} in non COPD and GOLD2 patients for all four pulmonary function values.

We concluded that 1) the differences between estimated postoperative pulmonary function and actual values examined after lobectomy were different depending on the severity of COPD, 2) estimated postoperative values of pulmonary function that calculated with traditional methods sometimes showed lower than actual values.

Verification of Co-Morbidities: an Additional Value of V/P SPECT in COPD

Marika Bajc¹, X Y He², Y Chen³, J Wang⁴, X Y Li⁵, W.M. Shen⁵, C Z Wang⁴, H Huang³, Ari Lndqvist⁶

1. Skåne University Hospital, Sweden
2. Suzhou University Affiliated Tumor Hospital, China
3. Changzheng Hospital Shanghai, China
4. Xin qiao Hospital Chongqing, China
5. Hua Dong Hospital Shanghai, China
6. Helsinki University Hospital, Finland

Sixty six consecutive patients with a confirmed diagnosis of a stable COPD (GOLD criteria, men 84%) were enrolled in 3 hospitals in Shanghai and Chongqing in an international multicentre trial. Age ranged 44-86 years and smoking pack years from 20-104. The ventilation and perfusion single photon emission tomography (V/P SPECT) was performed and analysed blindly 1. Total preserved lung function (TPLF%) (preserved ventilation and perfusion) was evaluated semi-quantitatively and expressed in percent (%) of the estimated total lung function¹.

Co-morbidities in COPD (n=66)

Co-morbidities	Number of cases	%	TPLF%
Pulmonary embolism (PE)	19 (68% chronic)		29 49 (20-70)
Left heart failure (LHF)	17	26	34 (15-60)
Susp. tumor	10	15	48 (20-80)
Pneumonia	3	5	38 (35-40)
No co-morbidities	29	44	30 (15-60)

The average size (range) of a PE defect was 21 (5-60) % of the total lung function.

Combinations of co-morbidities in COPD

Co-morbidities	Number of cases	%	TPLF%
PE+LHF+susp. tumor	1	1,5	50
PE+LHF	4	6	45 (30-60)
PE+susp. tumor	3	4,5	57 (40-70)
PE only	11	17	48 (20-70)
Pneumonia only	2	3	38 (35-40)
LHF only	10	15	30 (15-60)
LHF+pneumonia+susp. tumor	1	1,5	-
LHF+susp. tumor	1	1,5	20
Susp. tumor only	4	6	48 (25-85)
No co-morbidities	29	44	30 (15-60)
Total	66	100	37 (15-85)

Comorbidities like PE, LHF and pneumonia are common in stable COPD patients and may contribute to prognosis. V/P SPECT image may raise suspicion of lung tumor. V/P SPECT is useful in identifying COPD symptoms and disease heterogeneity.

¹Bajc et al, Ann. Nucl. Med. 2015; 29: 91.

Poster Session P3-4-2

Obstructive Bronchitis and Emphysema Phenotypes by V/P SPECT Co-Exist in Severe COPD

Marika Bajc¹, Y Chen², J Wang³, X Y Li⁴, W.M. Shen⁴, C Z Wang³, H Huang², Ari Lindqvist⁵, X Y He⁶

1. Skåne University Hospital, Sweden
2. Changzheng Hospital Shanghai, China
3. Xin qiao Hospital Chongqing, China
4. Hua Dong Hospital Shanghai, China
5. Helsinki University Hospital, Finland
6. Suzhou University Affiliated Tumor Hospital, China

In sixty six patients (men 84%) enrolled in multicentre trial in 3 hospitals in China, COPD (GOLD criteria) was studied with ventilation (V) and perfusion (P) SPECT and analyzed blindly. Age ranged 44-86 y and smoking pack years 20-104.

Reduction of ventilation (obstructive bronchitis phenotype) was classified by penetration of Technegas™ to the periphery: grade 2=deposition of aerosols in intermediate and large airways and diminished penetration; grade 3=deposition in large airways with severely impaired or abolished ventilation. Matching V/P defects that determined emphysema phenotype were quantified and was expressed as a percentages of the total lung function that was missing (E%). Total preserved lung function (TPLF%) was evaluated semi-quantitatively. Co-morbidities of COPD like pulmonary embolism, left heart failure, pneumonia and suspicion of tumor were detected on V/P SPECT.

In patients with grade 2 to 3 ventilation defects without any co-morbidity (n=29), V/P defects were always matched. E% and (1-TPLF%) increased from grade 2 to grade 3, from 38+/-13% to 63+/-14% and from 55+/-17% to 73+/-8%, respectively (p's<0,05). Adding patients with comorbidity (n=52) to the analysis, E% and (1-TPLF%) increased from 21+/-17% to 59+/-20% and from 51+/-13% to 72+/-8%, (p's<0,05) for grade 2 to 3 ventilation defects, respectively.

In severe COPD, V/P SPECT showed that obstructive and emphysema phenotypes generally co-exist. The severity of emphysema and loss of total estimated lung function increase with the impairment of obstructive bronchitis. The co-morbidities of COPD do not remarkably interfere with this relation.

Poster Session P3-4-3

Relationship between Brain and Pulmonary Function Studied by Hyperpolarized ¹²⁹Xe MRI/MRS

Akihiro Shimokawa¹, Hironobu Matsumoto¹, Yukiko Yamaguchi¹, Shota Hodono¹, Shintaro Okumura¹, Neil J Stewart¹, Hirohiko Imai², Hideaki Fujiwara³, Atsuomi Kimura¹

1. Department of Medical Physics and Engineering, Area of Medical Technology and Science, Division of Health Sciences, Graduate School of Medicine, Osaka University, Japan
2. Department of Systems Science, Graduate School of Informatics, Kyoto University, Japan
3. Office for University-Industry Collaboration, Osaka University, Japan

The comorbidity of chronic obstructive pulmonary disease (COPD) accompanied by brain dysfunction has recently been recognized. By investigating the relationship between brain and pulmonary functions in a mouse model of COPD, it may be possible to identify the mechanism of comorbidity and facilitate earlier treatment. Therefore, in this study, we observed and analyzed this relationship by means of ¹²⁹Xe MRI/MRS.

Cigarette smoke solution and lipopolysaccharide were administered to twelve male ddY mice for six weeks to induce COPD. Nine healthy mice were used as a control group. MRI/MRS measurements were performed on mice spontaneously respiring hyperpolarized ¹²⁹Xe. Xenon polarization transfer contrast images were acquired to quantify the fractional depolarization parameter, fD, which describes the efficiency of gas exchange. The uptake of xenon into the brain was pursued by MRS using saturation recovery sequences. By analyzing the saturation recovery of signal intensity of ¹²⁹Xe in brain tissue, the exponential attenuation constant for xenon uptake, α , was derived. The perfusion rate was measured to calculate the T1 of ¹²⁹Xe in brain tissue (T1i).

α was strongly dependent on fD and both parameters decreased in COPD mice. In contrast, α and fD of control mice remained approximately constant. T1i correlated with fD, suggesting that the oxygen supply to the brain was inhibited by COPD progression. Also, we expect the pulmonary dysfunction accompanied by brain dysfunction is dependent on the perfusion. This method is readily adaptable and can be extended to elucidate the treatment efficacy of new drugs, e.g. ethyl pyruvate.

Poster Session P3-4-4

Analysis of the microstructure of the secondary pulmonary lobulus by a synchrotron radiation CT

Kohichi Minami¹, Kohki Maeda¹, Yoshiki Kawata¹, Noboru Niki¹, Keiji Umetani², Yasutaka Nakano³, Hiroaki Sakai⁴, Hironobu Ohmatsu⁵, Harumi Itoh⁶

1. Tokushima University, Japan
2. Japan Synchrotron Radiation Research Institute, Japan
3. Shiga University of Medical Science, Japan
4. Hyogo Prefectural Amagasaki Hospital, Japan
5. National Cancer Center Hospital East, Japan
6. Fukui University, Japan

Conversion of images at micro level of the normal lung and those with very early stage lung disease, and the quantitative analysis of morphology on the images can contribute to the thoracic image diagnosis of the next generation. The collection of every minute CT images is necessary in using high luminance synchrotron radiation CT for converting the images. The purpose of this study is to analyze the structure of secondary pulmonary lobules. We also show the structure of the secondary pulmonary lobule by means of extending our vision to a wider field through the image reconfiguration from the projection image of the synchrotron radiation CT.

Poster Session P3-4-5

Quantitative study of airway changes in murine asthma models on micro-CT: comparison with pathologic findings

Sanghyun Paik

Soon Chun Hyang University Hospital, Korea

Purpose

To evaluate airway changes in ovalbumin-induced asthmatic mice on postmortem micro-CT images with pathological correlation.

Materials and Methods

Asthma models (n = 6) were created by intraperitoneal injection and nasal instillation of ovalbumin-aluminium-hydroxide into mice. The bronchial luminal area was measured in main bronchial lumen of distal 3rd bronchus branch level (six parts per each mouse) in axial scans of Micro-CT, using Lucion's smart pen (semi-automated) and curve pen (manual). The bronchial wall thickness was obtained in four sections (two levels on both side) after 3rd bronchial branch by measuring the diameter which is perpendicular to the longitudinal axis of main bronchus in curved MPR images. The histologic slides were obtained from the lesions that matched with the CT images, and the bronchial wall thicknesses were determined.

Results

The mean bronchial luminal area of asthmatic mice was 0.196 ± 0.072 mm² and that of controls was 0.243 ± 0.116 mm²; difference was significant. The bronchial wall thickness of asthmatic mice on micro-CT images and in pathological specimens were thicker than those of controls (mean, 0.119 ± 0.01 vs. 0.108 ± 0.013 mm; mean, 0.066 ± 0.011 vs. 0.041 ± 0.009 mm). BWT on micro-CT images correlated well with pathological thickness (asthmatic mice: $r = 0.712$; controls: $r = 0.46$). Thick bronchial wall of asthma models demonstrated submucosal hypertrophy with goblet cell hyperplasia and smooth muscle hyperplasia.

Conclusions

Airways of murine asthma models displayed thicker bronchial walls and narrower luminal areas than those of controls on micro-CT images and were significantly correlated with pathological findings.

Poster Session P4-1-1

Classifying regional texture patterns of diffuse lung disease at HRCT with deep convolutional neural networks : Comparison with support vector machine

Guk Bae Kim, Yeha Lee, Hyun-Jun Kim, Kyu-Hwan Jung, Joon Beom Seo, JuneGoo Lee, Namkug Kim

University of Ulsan College of Medicine, Asan Medical Center, Korea

To introduce deep convolution neural network (CNN) based feature extraction method for the given task to classify six kinds of regional patterns in diffuse lung disease.

HRCT images were selected from images of 106 patients having diffuse lung disease from a Siemens CT scanner (Sensation 16) and 212 patients from a GE CT scanner (Lightspeed 16). Two experienced radiologists marked sets of 600 rectangular regions of interest (ROIs) with 20×20 pixels on HRCT images obtained from GE and Siemens scanners, respectively. These were consisted of a hundred of ROIs for each of six local patterns including normal, consolidation, emphysema, ground-glass opacity, honeycombing, and reticular opacity. Performance of CNN classifier was compared with that of support vector machine (SVM). In the SVM classifier, typical 22 features were extracted. In the CNN classifier, a hundred features in the last layer (FC #1), were extracted automatically.

The accuracies of the SVM classifier were achieved 92.34 ± 2.26 % at 600 ROI images acquired in a single scanner (GE) and 91.18 ± 1.91 % at 1200 ROI images of the integrated data set (GE and Siemens). The accuracies of the CNN classifier showed a higher performance of 93.72 ± 1.95 % and 94.47 ± 1.19 % in a single and the integrated HRCT, respectively.

The CNN performance in the integrated data might be better, due to more robustness to image noise and higher performance in larger data set. In addition, the CNN shows higher performance than the SVM in both of data types.

Poster Session P4-1-2

Comparison of skeleton based- and offset surfaces methods on pulmonary artery and veins: Validation with artificial vessel phantom and normal 3D volumetric CT

Jang Pyo Bae, Namkug Kim, Myungsoo Bae, Sang Min Lee, Joon Beom Seo

University of Ulsan College of Medicine, Asan Medical Center, Korea

The quantification method of small pulmonary artery and vein separately was developed based on skeleton from 3D volumetric chest CT images.

Non-contrast volumetric chest CT scans with sub-millimeter thickness of 10 normal control (NC) were used. Pulmonary vessels were segmented using a thresholding (-700 HU) from CT images. The hilar region was removed from the initial vessel to divide the vessel tree into separated sub-trees. Minimum spanning tree algorithm were used to separate the mixed artery and vein tree based on the skeletons extracted using a 3D thinning method. The accuracy of this method was evaluated with the artificial phantom (512×512×512 volume with a vessel tree with 400 terminal nodes. vessel radius: 4.26 ± 2.68) by a Vascusynth software. The radius error was 1.57 ± 0.51 mm and the direction error was 8.77 ± 17.20 %. In NC CT image, pulmonary arteries and veins were separated and determined manually by an expert thoracic radiologist. With this method, diameter, tapering ratio, branch angle were 0.35 ± 0.03 , 0.85 ± 0.33 , 0.85 ± 0.33 , and 82.56 ± 25.39 o in artery, and 0.39 ± 0.04 , 0.84 ± 0.37 , 0.84 ± 0.37 , 82.11 ± 25.76 o in vein, respectively. With the offset surfaces methods, the diameters of artery are 1.51 ± 0.16 , 1.84 ± 0.11 , 1.93 ± 0.08 , 1.96 ± 0.07 , 1.96 ± 0.09 and 1.96 ± 0.09 mm from distal to proximal surfaces with 5 mm intervals, respectively.

The skeleton method can extract more complex parameters including tapering ratio, branch angle, etc. We developed a voxel based quantitative measurement method based on the artery and vein structure from 3D volumetric chest CT images, which will be used to artery and vein quantification.

Poster Session P4-1-3

Three-dimensional morphological analysis of spiculated pulmonary nodules in thoracic CT images

Yoshiki Kawata¹, Noboru Niki¹, Hironobu Ohmatsu², Keiju Aokage², Masahiko Kusumoto², Takaaki Tsuchida³, Kenji Eguchi⁴, Masahiro Kaneko⁵

1. Tokushima University, Japan
2. National Cancer Center Hospital East, Japan
3. National Cancer Center Hospital, Japan
4. Teikyo University School of Medicine, Japan
5. Tokyo Health Service Association, Japan

Spiculation is considered as one of the indicators of nodule malignancy and an important feature to assess requirements on a patient-tailored follow-up procedure. However, the spiculation is also observed in some benign nodules, particularly in tuberculoma. The elucidation of the spiculation morphology in three-dimensional (3D) thoracic CT images is an important preliminary step towards developing the malignant discrimination strategies from benign nodules. Needle-like structures can often be identified at the spiculated margin of nodule on CT images, but a spatial configuration of spiculation remains elusive. In this study, we present a morphological analysis method to reveal a spatial configuration of spiculation of pulmonary nodules in 3D thoracic CT images. Applying the method to malignant nodules with the spiculated margins, the preliminary analysis result of the spatial configuration reveals the sheet-like structures of spiculation.

Poster Session P4-1-4

Computer-aided diagnosis for osteoporosis using chest 3D CT images

Kazuya Yoneda¹, Mikio Matsui², Hidenobu Suzuki², Yoshiki Kawata², Noboru Niki², Yasutaka Nakano³, Hironobu Ohmatsu⁴, Masahiko Kusumoto⁴, Takaaki Tsuchida⁵, Tsuchida Eguchi⁶, Masahiro Kaneko⁷

1. System Innovation Engineering Graduate School of Advanced Technology and Science The University of Tokushima, Japan
2. Institute of Technology and Science The University of Tokushima, Japan
3. Shiga University of Medical Science, Japan
4. National Cancer Hospital East, Japan
5. National Cancer Center Hospital, Japan
6. Faculty of medicine, Teikyo University, Japan
7. Tokyo Health Service association, Japan

Sufferers of osteoporosis is increasing with the rapid aging. The patients of osteoporosis comprised of about 13 million people in Japan and it is one of the problems the aging society has. In order to prevent the osteoporosis, it is necessary to do early detection and treatment. There is a quantitative computed tomography (QCT) as an auxiliary role dual-energy X-ray absorptiometry (DXA) has been used in the diagnosis of osteoporosis. In recent years, the effectiveness of osteoporosis diagnosis by 3D-QCT is growing. Development of osteoporosis diagnosis support system is required for this. In this paper, we have carried out the extraction of the vertebral body by the code of the vertebral body of the spine of the 3-dimensional CT images. By measuring the bone density of the cancellous bone and the height of the vertebral body, we construct a system that presents the decrease in bone density and fractures for supporting diagnosis of osteoporosis. The result of applying for the training data 416 cases, extraction rate of vertebral body was 99.95%. Extraction rate is 98.76% of the normal dose 500 cases of test data, 98.61% in the low dose 500 cases.

Poster Session P4-2-1

Novel Airway Segmentation Technique in Low-dose CT Images: Global Validation with EXACT09

Sang Joon Park, Doohee Lee, Jin Mo Goo

Seoul National University Hospital, Korea

Airway segmentation in CT images is a challenging tasks because of the limitations in image quality inherent to CT image acquisition, especially low-dose CT for clinical routine environment. Besides, complex anatomy and abnormal lesions in the lung parenchyma makes segmentation difficult because contrast in CT images are determined by the differential absorption of X-rays by neighboring structures, such as tissue, vessel or several pathological conditions. Thus, we attempted to develop an intelligent segmentation technique for Bronchial trees. The images were obtained with low-dose chest CT using soft reconstruction kernel (40 mAs at 120 kVp). Our PC-based in-house software (MISLAB, medical imaging solution for lung and bronchial trees) initially segmented the pulmonary airways with intensity adaptive region-growing (IARG) technique. Then candidates of small airways were detected using by eigenvalues-ratio of the Hessian matrix. To enhance and increase the small airways, our proposed vector stream information (VSI) technique were applied to the images. After finishing above steps, for careful discriminate the faithful airways, false positive (FP) reduction process were performed. The performance of final results from the proposed technique was evaluated with single Hessian-based method and VSI without FP reduction scheme and was compared to that of IARG for the EXACT09 dataset. Thus, results show that FP rate decreased by $0.89\pm 1.64\%$ after applying VSI with FP reduction scheme ($p<0.001$). This study can be a vital role as a preprocessing step for regional analysis of pulmonary airways and their functions in the lung parenchyma for various lung diseases in the clinical environment.

Poster Session P4-2-2

Blood Flow Contribution Analysis for Pulmonary Artery and Aorta using Contrast Enhanced Images

Tomoki Saka¹, Toshiyuki Gotoh¹, Seiichiro Kagei¹, Tae Iwasawa²

1. Graduate School of Environment and Information Sciences, Yokohama National University, Japan

2. Department of Radiology, Kanagawa Cardiovascular and Respiratory Center, Japan

PURPOSE

In pulmonary blood flow analysis, effective methods to discriminate between blood flows through artery and aorta are desired to be established. In this paper, a method to separately identify the effects of the pulmonary artery and aorta flows from a time sequence signal observed in a contrast enhanced image is proposed.

METHOD

Assuming that bloodstream in the lung field consists of the sum of blood flows through artery and aorta, we proposed a model which evaluate the residue amount of the contrast enhanced agent at local area in a lung field from an impulse response of a total blood flow system, and a method of a numerical analysis to evaluate each blood flow contribution accurately.

RESULT

This method enables to analyze the intensity transition of contrast enhanced agent which include perfusions separately with a high degree of accuracy. And it makes aware that it can evaluate quantitatively that inflow through aorta is larger at cancer.

CONCLUSION

The proposed solution managed to separate blood flow through an artery and blood flow through an aorta, and obtain each analysis result.

Poster Session P4-2-3

3D Partial Rigid Registration with ICP for airways using point classification

Leonardo Ishida-Abe¹, Toshiyuki Gotoh¹, Seiichiro Kagei¹, Marcos S. G. Tsuzuki², Tae Iwasawa³

1. Yokohama National University, Japan
2. Escola Politecnica da Universidade de Sao Paulo, Brazil
3. Kanagawa Cardiovascular Respiratory Center, Japan

PURPOSE

To develop a reliable rigid registration method which registers two point cloud models of the lungs airways segmented from 3D CT images. The algorithm should be able to calculate all large amplitude movements between the structures, leaving only the small deformations.

METHOD AND MATERIALS

Our research uses a variation of the Iterative Closest Point (ICP) method, used in rigid registration for point clouds that splits the already segmented lungs airways into "tube like" segments and registers each of them independently. To make sure that ICP works correctly, two data sets are registered simultaneously, the surface point cloud and its medial skeleton[1]. The combination of data gives stability to the algorithm. A voxel based 3D Voronoi Diagram[2] is also used to make the ICP faster.

RESULTS

This approach calculates all large amplitude movements between the branches of the airways without needing an elastic algorithm. The skeletons contains vector information, meaning that valuable parameters such as angle of movement, contraction/dilation of the segment and bifurcations movement can be measured.

CONCLUSION

The proposed solution managed to calculate the large amplitude movements by using a partial rigid registration method, leaving only the small deformations on the surfaces. The results are prepared for elastic registration methods.

REFERENCES

1. J. Cao, A. Tagliasacchi, et.al., Point Cloud Skeletons via Laplacian-Based Contraction, IEEE SMI, 2010.
2. F.Y. Shih, Y.T. Wu, Fast Euclidean distance transformation in two scans using a 3x3 neighborhood, Computer Vision and Image Understanding, 93, 2004.

Poster Session P4-2-4

Extraction algorithm of bronchi and pulmonary artery and vein using anatomical features based on multi-slice CT images

Mikio Matsuhira¹, Hidenobu Suzuki¹, Yoshiki Kawata¹, Noboru Niki¹, Yasutaka Nakano², Hironobu Ohmatsu³, Masahiko Kusumoto³, Takayuki Tsuchida⁴, Kenji Eguchi⁵, Masahiko Kaneko⁶

1. Institute of Technology and Science, Tokushima University, Japan
2. Department of Respiratory Medicine, Shiga University of Medical Science, Japan
3. National Cancer Hospital East, Japan
4. National Cancer Center Hospital, Japan
5. Faculty of medicine, Teikyo University, Japan
6. Tokyo Health Service Association, Japan

With the development of multi-slice CT technology, obtaining accurate 3D images of lung field in a short time becomes possible. To support that, a lot of image processing methods need to be developed. In diagnostic imaging, it is important to study and analyze lung structure. Therefore, localization of thorax structures such as bronchi and pulmonary artery and vein provide useful information for diagnosis of lung diseases. An algorithm for analyzing in details is expected as basic technologies that can diagnose lung structure based on anatomy and detect early-stage lesion. Bronchi and pulmonary artery and vein provide useful information for classification of lung segments. In this report, we describe an algorithm which extract bronchi, artery and vein from multi-slice thoracic CT images.

Our dataset were acquired with Toshiba Aquilion, Slice thickness, 1.0 mm, electric current, 30 mA, voltage, 120 kV, and 300 average number of slices per scan. Each slice is 512x512 pixels, and pixel size is 0.625mm. Extraction algorithm of bronchi, pulmonary artery and vein is as follows.

First, we extract coarse bronchi using region growing method. Lung fields are extracted by threshold processing and morphological operation. Pulmonary blood vessel are extracted by threshold processing within lung field. Classification of pulmonary artery from pulmonary blood vessel and fine extraction of bronchi is achieved using anatomical feature. Details of algorithm and result are described in the presentation.

Poster Session P4-2-5

A Temporal Subtraction Technique from Thoracic MDCT Images Based on Image Registration Technique

Masashi Kondo¹, Hyoungseop Kim¹, Joo Kooi Tan¹, Seiji Ishikawa¹, Seiichi Murakami^{1,2}, Takashi Terasawa², Takatoshi Aoki²

1. Kyushu Institute of Technology, Japan

2. Department of Radiology, University of Occupational & Environment, Japan

Introduction: A temporal subtraction (TS) image which is obtained by subtraction of a previous image from a current one can be enhanced interval changes on two images by removing the normal structures such as blood vessel and airway. In this paper, we propose a TS technique from thoracic MDCT images based on nonlinear image warping technique.

Methods: Our computerized scheme for enhancing the temporal changes included three steps, mainly: preprocessing (tri-linear interpolation and segmentation), global matching (initial registration based on GGVF), and local matching (final registration). Finally, TS images are made by subtraction operation from a warped previous image to current one by non-rigid image warping technique.

Results: We applied our computerized scheme for enhancing the temporal changes on thoracic MDCT image onto 50 image sets which obtained different time series. We evaluate the effect of reducing the subtraction artifacts and satisfaction experimental results are obtained.

Conclusions: In this paper, we have developed two step temporal subtraction technique to reduce subtraction artifacts on TS image. We believe that TS image technique can be used as a useful tool in visual screening.

Acknowledgement: This work is supported from the Ministry of Education, Culture, Sports, Science and Technology of Japan under grant number 26461842.

Poster Session P5-1

Survival analysis with quantified regional disease patterns at thin section CT in patients with idiopathic pulmonary fibrosis

Sang Min Lee, Joon Beom Seo, Sang Min Lee, Sang Young Oh, Namkug Kim, Jin Woo Song, Heejun Park

Asan Medical Center, Korea

Purpose

To know if the extent of quantified regional disease patterns at thin section CT, which is measured with texture-based automated quantification system, shows different prognosis of idiopathic pulmonary fibrosis (IPF).

Method and Materials

Total 194 IPF patients with thin section CT at the time of diagnosis were included. Mean follow-up period was 36 ± 19 months. Using in-house, texture-based automated system, the area percent of five regional disease patterns (ground glass opacity(GGO), reticular opacity(RO), honeycomb(HC), emphysema(EM) and consolidation(CON)) were quantified. The area percent of abnormal lung(ABN) and fibrosis(FIB) were calculated. The survival analyses and Cox proportional hazards regression were performed.

Results

Measured relative extents of ABN, HC, GGO, CON, EM, RO and FIB at thin section CT were as follows; ABN: $43 \pm 17\%$, HC: $7 \pm 7\%$, GGO: $12 \pm 12\%$, CON: $3 \pm 1\%$, EM: $4 \pm 5\%$, RO: $17 \pm 10\%$, FIB: $24 \pm 12\%$, respectively. Survival analysis indicate that disease-free survival of patients with higher extent of ABN, HC, RO, FIB(cut-off value 35%, 10%, 25%, 20%, respectively) were significantly shorter than in patients with lower extent of those regional patterns (all $p < 0.001$). Cox proportional hazards regression showed that ABN, HC, RO and FIB were predictive of survival(HR: 1.02, 1.04, 1.04, 1.04, respectively, all $p < 0.05$).

Conclusion

With the cut-off value of regional disease patterns at thin section CT, which is measured with texture-based automated quantification system, higher extent groups show shorter disease-free survival than lower extent groups.

Poster Session P5-2

Composite CT indices derived from texture-based disease patterns for physiologic parameters in patients with idiopathic pulmonary fibrosis

Soyeoun Lim, Joon Beom Seo, Sang Min Lee, Sang Min Lee, NamKug Kim, Hee Jun Park, Sang Young Oh, Jin Woo Song

Asan Medical Center, Korea

Purpose: To retrospectively evaluate the correlations between texture-based automated quantitative extents of regional disease patterns and physiologic parameters, and to develop composite CT indices reflecting physiologic status in patients with idiopathic pulmonary fibrosis (IPF)

Materials and Methods: 214 patients (M:F=168:46; mean age, 63.4 years \pm 7.6) with IPF were enrolled. A texture-based automated system using the in-house software, quantified six regional HRCT patterns: normal, NL; ground-glass opacity, GGO; reticular opacity, RO; honeycombing, HC; emphysema, EMPH; and consolidation, CONS. The correlations between quantified extents of regional disease patterns and physiologic parameters (forced vital capacity (FVC), diffusing capacity for carbon monoxide (DLCO), 6-minute walk distance (6MWD), oxyhemoglobin saturation (SpO₂) after 6MWD) were evaluated by using Pearson correlation coefficient. Composite CT indices were obtained for each physiologic parameter by using linear regression analysis.

Results: The mean extents of GGO, RO, HC, EMPH, and CONS were 12.7% \pm 12.2, 16.4% \pm 9.7, 6.7% \pm 6.6, 3.8% \pm 5.4, and 2.9% \pm 1.2. In terms of FVC, GGO, RO, CONS, and EMPH showed significant correlations ($P < 0.001$, $r = -0.330, -0.417, -0.314,$ and 0.360 , respectively). As for DLCO, HC, GGO, CONS, and RO showed significant correlations ($P < 0.05$, $r = -0.381, -0.306, -0.174,$ and -0.339 , respectively). There were significant correlations between age, HC, GGO, CONS, RO and 6MWD, respectively ($P < 0.05$, $r = -0.393, -0.150, -0.311, -0.248,$ and -0.194). With regard to SpO₂, HC, GGO, and RO showed significant correlations ($P < 0.05$, $r = -0.415, -0.225,$ and -0.513 , respectively).

Composite CT indices for FVC, DLCO, 6MWD, SpO₂ were $96.3-3.8 \times \text{CONS} + 0.4 \times \text{EMPH} - 0.6 \times \text{RO}$ ($r^2 = 0.298$), $95.7-2.2 \times \text{CONS} - 0.4 \times \text{RO} - 0.5 \times \text{GGO} - 1.4 \times \text{HC}$ ($r^2 = 0.373$), $834.7-4.9 \times \text{age} - 3.1 \times \text{GGO} - 3.5 \times \text{HC}$ ($r^2 = 0.299$), and $98.2-0.32 \times \text{RO} - 0.1 \times \text{GGO} - 0.4 \times \text{HC}$ ($r^2 = 0.428$), respectively

Conclusion: The automated quantitative assessment of regional HRCT patterns in IPF patients are well correlated with physiologic parameters and composite CT indices can explain physiologic status of IPF patients to a certain degree.

Poster Session P5-3

Enhancement of Classification Accuracy in Automated Lung Quantification for Diffuse Interstitial Lung Disease in HRCT with Ensemble Methods

Sanghoon Jun, Namkug Kim, Sangmin Lee, Joon Beom Seo

Asan Medical Center, Korea

We proposed the ensemble methods in order to improve classification performance of automated lung quantification which differentiates six regional patterns of diffuse interstitial lung disease (DILD) in high-resolution computerized tomography (HRCT) images. Two experienced radiologists marked 1200 rectangle regions of interest (ROIs) consisting of 200 ROIs representing six regional disease patterns (normal, ground-glass opacity, reticular opacity, honeycomb, emphysema and consolidation) in HRCT images. The 200 ROIs of a specific pattern were obtained from two scanners including each 100 ROIs from GE and Siemens, respectively. For evaluation, 92 HRCT images were randomly selected from patients' scans. Two radiologists independently and manually classified six patterns in the HRCT images. Twenty-eight texture and shape features were extracted to construct feature vectors for the ROIs. Using 1200 ROIs, individual classifiers including support vector machine, naive Bayesian, decision tree and k-nearest neighbor and various ensemble methods including boosting, bagging, voting, random forest and gradient tree boosting were trained. For selecting the relevant features for each individual classifier, sequential forward-selection was employed. In order to compare classification methods in the automated quantification system, agreements between the automated system and the readers were assessed. In the experiment, ensemble classifiers (bagging, 44.74 \pm 1.51 % and 42.05 \pm 1.66 % (mean \pm standard error), two radiologists respectively) shows significant better performance than the best of individual classifiers (i.e., support vector machine, 41.85 \pm 1.93 % and 41.46 \pm 1.96%; paired t test $p < 0.01$). We concluded that bagging ensemble method provides significantly better result in automated lung quantification system.

Poster Session P5-4

Six cases of unilateral upper-lung field pulmonary fibrosis

Akimasa Sekine¹, Tae Iwasawa², Takeshi Shinohara¹, Tomohisa Baba¹, Takashi Ogura¹

1. Department of Respiratory Medicine, Kanagawa Cardiovascular and Respiratory Center, Japan

2. Department of Radiology, Kanagawa Cardiovascular and Respiratory Center, Japan

We report six cases of unilateral upper-lung field pulmonary fibrosis. All lesions were present in the right lung. Five patients had a history of right thoracotomy whereas the remaining one patient had that of laparotomy for treating gastric cancer. In all patients, pulmonary function test revealed a remarkable decrease of vital capacity. Thoracic MRI evaluated in four patients showed an apparent impairment of thoracic motion of both lungs. Ventilation/perfusion analysis was performed in five patients, and blood and air flows drastically decreased in the right lung. Our results strongly indicate that right thoracotomy cause a impairment of thoracic motion and a decreased hypoventilation-hypoperfusion. These conditions may lead to the development of unilateral upper-lung field pulmonary fibrosis.

Poster Session P6-1-1

Direct evidence of airflow limitation at the intra-mediastinal airway in emphysema patients by the use of maximum forced expiratory 4D-CT images

Takashi Kijima¹, Haruhiko Hirata¹, Hiroko Kitaoka²

1. Department of Respiratory Medicine, Osaka University, Japan

2. Division of Engineering Technology, JSOL Corporation, Japan

Background: Functional disorder of the pulmonary emphysema has been believed due to dynamic compression of small airways. However, its direct evidences have never been shown. We hypothesized that overinflated lungs compressed the intra-mediastinal airway (IMA, intra-thoracic trachea, main bronchi, and right lobar bronchi) in emphysema at the beginning of forced expiration and would let IMA collapse due to fluid dynamical effect (Bernoulli's effect).

Objectives: We evaluated the morphological change of IMA during maximum forced expiration by 4D-CT, and investigated its relationship to the value of FEV1.0.

Method: Five emphysema patients and a normal subject underwent 4D-CT by multi-detector row CT during maximum forced expiration over six seconds at supine posture. Voxel size was 0.7 mm x 0.7 mm x 1.0 mm with the range of 16 cm, and time interval was 0.5 sec. Volumes of intra-thoracic trachea and bilateral main bronchi are measured for each frame.

Results: The IMA of all emphysema patients were extremely narrowed just after the beginning of forced expiration and slightly recovered later. The membranous part of IMA was invaginated inside. There was no apparent shape change in the normal subject. The relative volume after two seconds were highly correlation to FEV1.0 ($r^2=0.93$).

Conclusion: These 4D-CT images have revealed that low values of FEV1.0 in emphysema patients are caused by dynamic collapse of IMA due to the Bernoulli effect. Pneumodynamics should be urgently reconstructed based on dynamic imaging and fluid dynamics.

Poster Session P6-1-2

Dynamic change of airway in a patient with bronchial stenosis by ultra-low dose 4D-CT

Osamu Honda¹, Masahiro Yanagawa¹, Ken Ueda¹, Tomoko Gyobu¹, Akinori Hata¹, Yasushi Shintani², Masato Minami², Noriyuki Tomiyama¹

1. Osaka University Graduate School of Medicine, Department of Radiology, Japan

2. Osaka University Graduate School of Medicine, Department of General Thoracic Surgery, Japan

Purpose:

To evaluate the dynamic change of airway in bronchial stenosis.

Patient and methods:

The patient was 40's-year-old male with interstitial pneumonia (UIP), and right single-lung transplantation was performed in 2013. In 2015, he had dyspnea, and bronchial anastomotic stenosis was diagnosed by CT and bronchoscopy. Cine CT was performed for the evaluation of bronchial stenosis with spontaneous respiration and forced-expiratory respiration. The CT machine and the parameters for imaging was following: 320-row detector CT (Aquilion ONE, Toshiba, Japan), tube current of 10mA, 0.35 sec/rotation, 0.5 mm collimation, 0.5 mm slice thickness, reconstruction interval of 0.5 sec, reconstruction algorithm of FC 02. Iterative reconstruction (AIDR3D strong) was used. All images were transferred to the workstation, and 4D-CT images were reconstructed.

Results:

The diameter of the trachea and bronchus on forced-expiratory respiration was markedly decreased compared to that on spontaneous respiration. Trachea moved to the side of transplanted lung on forced-expiratory respiration, and the narrowing of bronchus was more severe especially in the side of bronchial stenosis on forced-expiratory respiration.

Conclusion:

Ultra-low dose 4D-CT with spontaneous and forced-expiratory respiration can reveal the different dynamic change of airway in a patient with bronchial stenosis.

Poster Session P6-1-3

Pleural sliding mapping derived for detecting pleural adhesions

Ryo Sakamoto¹, Takeshi Kubo², Koji Sakai³, Mitsugu Omasa⁴, Masatsugu Hamaji², Keita Nakagomi⁵, Hiroyuki Sekiguchi¹, Masahiro Yakami², Thai Akasaka¹, Yutaka Emoto⁶, Michael I Miller⁷, Susumu Mori⁷, Hiroyuki Yamamoto⁵, Kaori Togashi¹

1. Diagnostic Imaging and Nuclear Medicine, Graduate School of Medicine, Kyoto University, Japan

2. Kyoto University Hospital, Japan

3. Kyoto Prefectural University of Medicine, Japan

4. Nishikobe Medical Center, Japan

5. Canon Inc., Japan

6. Kyoto College of Medical Science, Japan

7. The Johns Hopkins University School of Medicine, USA

We propose a method for visualizing the amount of pleural sliding using 4DCT data to detect pleural adhesions. To visualize the sliding motion between the visceral and the parietal pleurae through a half breathing cycle, deformation field of the lungs and thoracic wall from an end-exhale phase (Te) to an end-inhale phase (Ti) was calculated using non-rigid image registration algorithm. All the phases between Te and Ti were used to achieve accurate registration from Te to Ti, and overall deformation was obtained as a composition of a series of small deformations. Based on the overall deformation field, the pleural sliding motion is calculated by subtracting pairs of moving vectors on the surface of lungs and inner thoracic wall. Three dimensional mapping was then created by plotting the norms of subtracted vectors on the surface of the lungs. Two thoracic surgeons rated the correlation between areas with decreased sliding value and actual locations of pleural adhesions in five-point scale with higher points given to stronger correlation. There were good correlations between decreased sliding areas and pleural adhesions site (3.9 in average), suggesting that our pleural sliding mapping has a potential to be a good predictor of the locations of pleural adhesions.

Poster Session P6-1-4

New developed motion imaging to evaluate the effect of bronchodilator on human bronchial ciliary movement using bronchoscopic sample

Toshiyuki Sawa¹, Tsutomu Yoshida¹, Takashi Ishiguro¹, Akane Horiba¹, Yohei Futamura¹, Takaaki Hasegawa¹, Takashi Nakahari²

1. Gifu Municipal Hospital, Japan

2. Kyoto Prefectural University of Medicine, Japan

Background: As mucociliary transport (MCT) of airway plays an important role as a defense mechanism in lower respiratory tract infection, evaluation of medicine on mucociliary function of individual patients is also useful clinically. To evaluate the effect of bronchodilator on human bronchial ciliary movement, the human bronchial ciliary movement and clinical applications was evaluated by a newly developed simple method using a bronchoscope sample before and after inhalation of bronchodilators.

Method: when the bronchoscopy was performed in the patients with respiratory disease, bronchial lavage to the transbronchial biopsy site was examined to collect peripheral bronchial epithelial cells.

After ciliary motion were observed to identify with microscopy, the ciliary beat were captured at 240 frames per second using a high-speed photographing function of the general-purpose digital video camera on the market. By software analysis, frequency and amplitude of the ciliary movement was measured.

Results: Human ciliary epithelium in the patients with respiratory disease was confirmed in the amplitude of 4 ~ 8µm and frequency of 5 ~ 20bps.

It was observed that ciliary movement is activated by oral and inhale bronchodilator (Tulobuterol, tiotropium, Fluticasone/ Formoterol) except external affixed medicine (Tulobuterol).

Conclusion. Even in general hospitals without specialized equipment, it is possible to observe easily and directly the movement of human airway ciliary epithelium using a bronchoscopic sample, to evaluate effect of medicine on the frequency of ciliary movement. It was suggested that the bronchodilators may improve the ciliary movement in the clinical dose.

Poster Session P6-2-1

Quantification of mucociliary function in murine lungs using magnetic particle imaging

Kohei Nishimoto¹, Kazuki Shimada², Yoshimi Inaoka², Kohei Enmeiji², Akiko Ohki², Mikiko Yamawaki², Kenya Murase¹

1. Department of Medical Physics and Engineering, Division of Medical Technology and Science, Faculty of Health Science, Graduate School of Medicine, Osaka University, Japan

2. Department of Medical Physics and Engineering, School of Allied Health Sciences, Osaka University, Japan

Mucociliary clearance is an important defense mechanism for clearing the lung by removing the inhaled aerocontaminants from the airways. In patients with chronic bronchitis or asthma, mucociliary function is impaired due to a decrease in ciliary epithelial cells and/or a change in mucus production. Thus, the development of a method to simply and quantitatively evaluate the mucociliary function is desired. Recently, a new imaging method called magnetic particle imaging (MPI) has been introduced, which allows imaging of the spatial distribution of magnetic nanoparticles (MNPs). This study was undertaken to investigate the feasibility of applying MPI to quantifying the mucociliary function.

To impair mucociliary function, emphysema was induced in seven-week-old male ICR mice (n=8) by injecting 4.5 U of porcine pancreas elastase (PPE) intratracheally using a microsyringe, whereas the mice of the control group (n=10) were not injected with PPE. Twenty-one days after the administration of PPE, 50 µL of nebulized MNPs (ResovistR) were administered intratracheally using a microsyringe and we imaged the lungs using our MPI scanner 2.5 hours, 1, 3, and 7 days after the administration of MNPs. We also calculated the average MPI values by drawing the region of interest on the lungs.

The average MPI values in the mice of the treated group were significantly higher than those in the control group at 3 and 7 days after the administration of MNPs. These results suggest that MPI can quantify the mucociliary clearance and will be useful for monitoring the mucociliary function in the lung.

Poster Session P6-2-2

Simulation study of inhaled gas imaging by the use of a 4D lung model and computational fluid dynamics

Hiroko Kitaoka

Division of Engineering Technology, JSOL Corporation, Japan

Background: Inhaled gas imaging techniques have been used for investigating ventilation distribution. Does the tracer concentration distribution accurately reflect the ventilation distribution? I simulated intra-pulmonary distribution of inhaled gas by the use of computational fluid dynamics with Kitaoka's 4D lung model (<http://www7b.biglobe.ne.jp/~lung4cer>).

Methods: I constructed a 4D finite element lung model in which one subacinus and its entire airway was included. Other lung regions were modeled as cubic sets whose side lengths were equal to their air-supplying bronchi. The lung model was deformed during two seconds so that the air went into the lung from the tracheal upper open end. By Solving incompressible Navier-Stokes equation and the tracer diffusion equation under the moving boundary condition, the tracer concentration distribution within the airway was computed (time step 0.00625 s).

Results: Intra-pulmonary tracer concentration was widely distributed even in the base-line condition. When the diffusion constant of the tracer was larger, the recurrent-pathway regions had higher concentration than the axial-pathway regions. The relationship between regional ventilated volume and the tracer concentration was not linear. When the bronchial stenosis was added, paradoxical increase of the concentration occurred because of the accelerated air velocity at the stenotic portion.

Conclusion: The simulation results suggested that the concentration distribution of inhaled gas tracer did not quantitatively reflect ventilation distribution. Although the tracer imaging technique is useful for basic investigation of respiratory physiology, clinical evaluation of the ventilation distribution should be directly obtained by image-based motion analysis technique.

Poster Session P6-2-3

A combinatory simulator of ventilation, diffusion, and perfusion in the human pulmonary subacinus

Hiroko Kitaoka

Division of Engineering Technology, JSOL Corporation, Japan

In order to utilize pulmonary functional images, it is the most important to understand physicochemical bases of ventilation, diffusion, and perfusion in the lung parenchyma.

I have constructed a 4D subacinar model based on a previously published 4D alveolar model. The model is a set of finite elements (tetras) so as to apply mechanical simulations containing about 7 million nodes per one subacinus. In the model, the alveolar wall contains capillary space connecting to the pulmonary arteriole and venule, and the air space is bordered by the alveolar membrane from the capillary space. The alveolar membrane consists of thin layers of type I alveolar cells, connective tissues, and the endothelial cells.

The model expands and contracts according to the respiratory cycle, and the airflow goes in and out according to the regional volume change. Oxygen in the air is transported by convection of airflow and diffusion in the air space. Oxygen is further transported into the blood space by diffusion through the alveolar membrane and by convection of the blood flow. All these processes can be computed with the 4D subacinar model by the use of computational fluid dynamics where Navier-Stokes equation and diffusion equation are directly coupled.

Preliminary simulations indicated that the blood oxygen concentration was almost linearly dependent of the effective surface area of the alveolar membrane under the same blood flow and the same oxygen supply by the airflow. This simulator is useful for investigating respiratory pathophysiology and for developing functional imaging techniques.

Poster Session P6-2-4

Procaterol-stimulated increases in ciliary bend amplitude and ciliary beat frequency in mouse bronchioles

Nobuyo Tamiya^{1,2}, Shigekuni Hosogi², Yoshizumi Takemura¹, Yoshinobu Iwasaki¹, Koichi Takayama¹, Takashi Nakahari², Yoshinori Marunaka²

1. Department of Respiriology, Graduate School of Medical Science, Kyoto Prefectural University of Medicine, Japan
2. Department of Molecular Cell Physiology, Graduate School of Medical Science, Kyoto Prefectural University of Medicine, Japan

The mucociliary transport of small airways is a host defense mechanism of the lung, and the beating cilia play a key role in the transport. The ciliary beating frequency (CBF) and ciliary bend amplitude (CBA) of isolated mouse bronchiolar ciliary cells were measured using a light microscope equipped with a high-speed camera (500 Hz). CBF is known to be a key factor in controlling the mucociliary transport rate. We examined the effects of a β 2-agonist (procaterol) on ciliary activities (CBA as well as CBF) in the small airways. Procaterol (β 2-agonist) increased CBA and CBF in a dose dependent manner. The time course of CBA increase is distinct from that of CBF increase: procaterol at 10 nM first increased CBA and then CBF. Moreover, 10 pM procaterol increased CBA, not CBF, whereas 10 nM procaterol increased both CBA and CBF. Concentration-response studies of procaterol demonstrated that the CBA curve was shifted to a lower concentration than the CBF curve, which suggests that CBA regulation is different from CBF regulation. Measurements of microbead movements on the bronchiole of lung slices revealed that 10 pM procaterol increased the rate of ciliary transport by 37% and 10 nM procaterol increased it by 70%. In conclusion, we have shown that increased CBA is of particular importance for increasing the bronchiolar ciliary transport rate, although CBF also plays a role in increasing it.

Poster Session P7-1-1

Computed tomography findings in 749 patients with pulmonary infection

Fumito Okada, Yumiko Ando, Asami Ono, Tomoko Nakayama, Haruka Sato, Shunro Matsumoto, Hiromu Mori

Department of Radiology, Oita University Faculty of Medicine, Japan

Purpose: Bacteriological evaluation may take time and thus delay diagnosis. Computed tomography (CT) may help in the differential diagnosis of infections and in the subsequent selection of appropriate antibiotics. The aim of this study was to assess CT findings in patients with acute pneumonia.

Materials and Methods: We retrospectively identified 1454 patients with acute pneumonia who had undergone chest CT. We excluded patients who had been diagnosed with concurrent infectious disease by serological and clinical findings. Consequently, our study group comprised 749 patients: 86 with *Streptococcus pneumoniae*, 211 with *Haemophilus influenzae*, 109 with *Moraxella catarrhalis*, 83 with *Staphylococcus aureus*, 80 with *Klebsiella pneumoniae*, 33 with *Streptococcus milleri*, 35 with *Pseudomonas aeruginosa*, 42 with *Mycoplasma pneumoniae*, 40 with *Chlamydia pneumoniae*, and 30 with seasonal influenza virus. CT examinations were performed within 1 to 6 days (mean, 4.8 days) after the onset of respiratory symptoms. Parenchymal abnormalities were evaluated along with enlarged lymph nodes and pleural effusions.

Results: CT findings of bronchial wall thickening and centrilobular nodules were significantly more frequent in patients with pneumonia caused by *Haemophilus influenzae*, *Moraxella catarrhalis*, *Staphylococcus aureus*, *Streptococcus milleri*, *Pseudomonas aeruginosa*, and *Mycoplasma pneumoniae*. Cavity formation and empyema were most frequently observed in patients with *Streptococcus milleri*. Consolidation could not be seen in patients with influenza viral pneumonia, unlike patients with other types of pneumonia.

Conclusion: CT findings including bronchial wall thickening, centrilobular nodules, cavity formation, and empyema in combination with clinical manifestations may be important to determine the causative pathogens in patients with pneumonia.

Poster Session P7-1-2

TYPICAL CT AND RADIOGRAFIC FINDINGS OF PULMONARY ECHINOCOCCOSIS

Esra Bilgi

Dresra Bilgi, Turkey

INTRODUCTION: The lung is the second most common site of involvement with echinococcosis granulosis in adults after the liver (10-30% of cases), and the most common site in children. The coexistence of liver and lung disease is present in only 6% of patients.

METHODS: 26 years old woman was admitted to our hospital with a two month history of chest pain. After normal axamination we were performed the plain chest radiograph and Computerised tomography (CT).

RESULTS:On chest radiographic we observed a more homogeneous round or oval masses with smooth borders surrounded by normal lung tissue and in enhanced CT we observed round or oval hypodens, enhancement after contrast injection well-defined borders range between 5 and 30 mm in diameter cystic masses and surrounded well-defined thick caviter lesion. We showed multiple well-defined homogenous cystic lesion in liver and soliter homogeneous cystic lesion left temporal lobes of the brain. With serologic tests were proved echinococcosis infestation.

DISCUSSION :Cystic echinococcosis is seen worldwide. Most patients are asymptomatic ,other symptoms of hydatid disease can result from the release of antigenic material and secondary immunological reactions that develop from cyst rupture. Patients with lung cysts,20-40% also have liver and others organs cysts [10, 11]. The most valuable diagnostic method in pulmonary hydatid disease is the plain chest radiograph and CT scan. In addition , CT scan is useful in showing complicasion and differential diagnosis.

Poster Session P7-1-3

Correlation of HRCT findings with pulmonary function test and immunologic diagnostic test of tuberculosis: Comparison interferon-gamma release assay[IGRA] and tuberculosis skin test[TST]

Do Hyung Lee, Ki Yeol Lee, Ji Yung Choo, Eun-young Kang, Yu Whan Oh, Seung Hwa Lee
Korea University Medical Center, Korea

Purpose:

Subclinical pulmonary tuberculosis has been shown to be associated with airflow obstruction. We investigated the relationship of IGRA and TST with high-resolution CT findings and airflow obstruction.

Methods:

From an ongoing, population-based, study of Korean adults aged 40-69 years (n=13,023), 688 subjects showed inactive TB on chest radiography. We randomly selected 97 subjects with chest radiographic findings that illustrated inactive TB, who also had no history of TB, but confirmed TB via IGRA or TST. And then, we performed HRCT and pulmonary function tests. HRCT was performed to calculate the extent of tuberculous sequelae using a CT scoring system. Scores were given by considering the volume decrease, as well as, the presence, severity, and extent of bronchiectasis, nodules, fibrosis, bullae, emphysema and mosaic perfusion in both lungs. We automatically obtained the scores for emphysema, ratio of emphysema, and total CT lung volume using software.

Results:

The positive rate of TST was 85.57%. The positive rate of IGRA was 84.54%. The prevalence of airflow obstruction in subclinical TB subjects was significantly higher after an adjustment was made for smoking status and age. IGRA is positively correlated with fibrosis, nodules, bronchiectasis, area of tuberculous sequelae, and total CT score.

Conclusion:

Airflow obstruction is more overt if the TB sequelae involve large areas of the lungs radiologically. The concentration of IGRA is positively correlated with fibrosis, nodules, bronchiectasis, and area of tuberculous sequelae on CT scans.

Poster Session P7-1-4

Bacteriological etiology in pneumonia patients with pulmonary emphysema using the clone library analysis of 16S rRNA gene in BALF

Keisuke Naito¹, Kei Yamasaki¹, Kazuhiro Yatera¹, Toshinori Kawanami¹, Kentaro Akata¹, Shingo Noguchi¹, Takashi Kido¹, Hiroshi Ishimoto¹, Kazumasa Hukuda², Takatoshi Aoki³, Hiroshi Mukae¹

1. Department of Respiratory Medicine, University of Occupational and Environmental Health, Japan

2. Department of Microbiology, University of Occupational and Environmental Health, Japan

3. Department of Radiology, University of Occupational and Environmental Health, Japan

Background: Pulmonary emphysema is an important radiological finding in chronic obstructive pulmonary disease (COPD) patients, but bacteriological differences in pneumonia patients according to severities of emphysematous changes have not been reported so far. Therefore, we evaluated the bacteriological differences according to the severity of pulmonary emphysema in Japanese pneumonia patients by both culture and the culture-independent molecular method using bronchoalveolar lavage fluid (BALF).

Patients and Methods: Japanese patients with community-acquired pneumonia (n=83) and healthcare-associated pneumonia (n=94) were retrospectively evaluated. The BALF specimens were evaluated using the clone library method of 16S rRNA gene in addition to cultivation. Partial bacterial 16S rRNA genes were amplified and clone libraries were constructed. Nucleotide sequences were determined and the homology was searched to determine the bacterial species. Qualitative radiological evaluation of pulmonary emphysema using Chest CT images was scored using Goddard classification.

Results: According to the severity of pulmonary emphysema, patients with the severity of pulmonary emphysema of none, mild, moderate, and severe were 47.4% (84/177), 36.2% (64/177), 10.2% (18/177), 6.2% (11/177), respectively. According to the molecular method, the severity of emphysema did not influence the incidence of *Haemophilus influenzae*, *Pseudomonas aeruginosa*, and *Streptococcus* spp. were the most detected phenotype as the first dominant phylotype, correlating with the severity of emphysema.

Conclusions: Our results of the molecular method revealed that the severity of pulmonary emphysema was not related to the detection of *H. influenzae* and, and *P. aeruginosa* was fewer than previously believed. In addition, *Streptococcus* spp. was the most detected bacterial phylotypes.

Poster Session P7-2-1

Fat Suppression Capabilities at Chest 3T MRI: Utilities of Two-point TSE-Dixon Technique in Comparison with SPAIR Technique

Yuji Kishida¹, Hisanobu Koyama¹, Yoshiharu Ohno², Katsusuke Kyotani³, Shinichiro Seki¹, Tomoyuki Okuaki⁴, Kazuro Sugimura¹

1. Division of Radiology, Department of Radiology, Kobe University Graduate School of Medicine, Japan

2. Advanced Biomedical Imaging Research Center, Kobe University Graduate School of Medicine / Division of Functional and Diagnostic Imaging Research, Department of Radiology, Kobe University Graduate School of Medicine, Japan

3. Center for Radiology and Radiation Oncology, Kobe University Hospital, Japan

4. Philips Healthcare Asia Pacific, Japan

Purpose: To evaluate the image qualities and the fat suppression capabilities of water images by two-point Turbo spin echo (TSE)-Dixon technique in comparison with fat suppression T2 weighted images (FS-T2WI) by spectral attenuated inversion recovery (SPAIR) technique at chest 3T MRI.

Materials and Methods: Twenty patients (mean age, 68.4 years) were enrolled and water images by two-point TSE-Dixon and FS-T2WIs by SPAIR were acquired by using 3T MR system. For the qualitative analysis, two radiologists visually and independently assessed the followings by five-point scale; lesion detection, the overall image qualities, and fat suppression capabilities. For the quantitative analysis, signal intensities (SIs) of muscle and fat were measured in both sequences by ROI placements, and the SI ratios (SIR) between muscle and fat were calculated. To evaluate the inter-observer agreements of visual assessments, kappa analysis were performed. To determine the utilities of TSE-Dixon technique, visual scores, SIRs and bilateral differences of SIR by TSE-Dixon technique were compared with those by SPAIR by using Wilcoxon signed-rank test.

Results: Kappa values between two observers were ranged from 0.499 to 0.760. There was no significant difference for lesion detection ($p > 0.05$). Qualitative overall image qualities and fat suppression capabilities of TSE-Dixon were significantly higher than those of SPAIR ($p < 0.0001$). In addition, both SIRs and the bilateral differences of SIR by TSE-Dixon were significantly lower than those by SPAIR ($p < 0.0001$).

Conclusions: The water images by TSE-Dixon technique had better image qualities and fat suppression capabilities rather than FS-T2WI by SPAIR at chest 3T MRI.

Poster Session P7-2-2

Anatomic and functional evaluation of central lymphatics with noninvasive MR lymphangiography

Eun Young Kim, Ho Yun Lee

Department of radiology, Samsung Medical Center, Korea

Objective: To investigate the clinical usefulness of noninvasive MR lymphangiography for differential diagnosis and treatment planning in lymphatic disease.

Methods: Ten patients (age range: 42-72 years) with suspected chylothorax (n=7) or lymphangioma (n=3) who underwent MR lymphangiography were included in this prospective study. The thoracic duct was evaluated using coronal and axial images of heavily T2-weighted sequences as well as reconstructed maximum intensity projection. Two radiologists documented visualization of the thoracic duct from the level of the diaphragm to the thoracic duct outlet, as well as an area of dispersion around the chyloma or direct continuity between the thoracic duct and mediastinal cystic mass.

Results: The entire thoracic duct was successfully delineated in all patients. Lymphangiographic findings played a critical role in identifying leakage sites in cases of postoperative chylothorax, and contributed to differential diagnosis and confirmation of continuity with the thoracic duct in cases of lymphangioma, as well as in diagnosing Gorham's disease, a rare disorder. In patients who underwent surgery, intraoperative findings were matched with lymphangiographic imaging findings.

Conclusions: Nonenhanced MR lymphangiography is a safe and effective method for imaging the central lymphatic system, and can contribute to differential diagnosis and appropriate preoperative evaluation of pathologic lymphatic problems.

Poster Session P7-2-3

Reproducibility of pulmonary blood flow measurements by phase-contrast MRI using two different MR scanners

Rin Iraha¹, Sadayuki Murayama¹, Nanae Tsuchiya¹, Tsuneo Yamashiro¹, Maho Tsubakimoto¹, Tae Iwasawa²

1. Department of Radiology, Graduate School of Medical Science, University of the Ryukyus, Japan

2. Department of Radiology, Kanagawa Cardiovascular and Respiratory Center, Japan

To determine the reproducibility of pulmonary blood flow measurements obtained with the PC method using two different 1.5-T systems (Magnetom Avanto: Siemens; Achieva: Philips) in 10 healthy subjects (5 male; age: 27-36 years). The region of interest (ROI) was set at the pulmonary artery (PA) truncus and bilateral PA. The measurements included mean and maximal blood flow rates, mean, maximal and minimal areas, mean blood flow volume, acceleration time and volume (AT and AV). The two scanners were in different institutions, and imaging was performed on different days within a one-month interval. Flow rate, area and flow were calculated automatically by software when we traced the ROI, and the time-flow curve was also obtained automatically. AT, AV were calculated by wave form analysis software. In order to calculate the reproducibility of the quantitative variables, intraclass correlation coefficients (ICC) were employed.

Results

In the PA truncus, ICC was almost perfect in the mean and maximal area, mean blood flow volume, and AV (r= 0.818-0.901), and substantial in the mean and maximal flow rates, and AT (r=0.66-0.795). In the right PA, ICC was almost perfect in the maximal area (r= 0.85), and substantial in the mean area, maximal flow rate and AT (r=0.657-0.793). In the left PA, ICC was almost perfect in AV (r= 0.85) and substantial in maximal area (r=0.63).

Conclusions

Some indices obtained from time-flow curves are highly reliable, even when they are obtained from different MR scanners, especially regarding pulmonary trunk.

Poster Session P7-2-4

Automatic bone of torso segmentation using contrast enhanced CT

Ahmed S. Maklad¹, Mikio Matsuhira¹, Hidenobu Suzuki¹, Yoshiki Kawata¹, Noboru Niki¹, Mitsuo Shimada², Gen Inuma³

1. Institute of Technology and Science, Tokushima University, Japan
2. Institute of Health Biosciences, University of Tokushima, Japan
3. National Cancer Center Hospital, Tokyo, Japan

Automatic bone segmentation from CT images is of high interest for surgeons and radiologists in analysis of bone fracture and planning surgical interventions. In Contrast enhanced CT phases, various organs are enhanced and overlaps in intensity with bone which makes segmentation of bones through contrast enhanced torso CT images a complicated task. In image processing, bone segmentation and elimination is important to analyze other organs using contrast enhanced CT images. To solve this problem in the literature, many techniques were proposed to segment bone from the native phase, then subtract result from the desired phase after applying a registration. In this paper, we propose a fully automatic method to segment bone of torso and classify it through any contrast enhanced torso CT images as well as native phase. This bone segmentation is achieved in four steps: bone candidates are segmented, cortical bone is classified, spongy bone is classified, and bone of the torso is classified. The method was examined using 15 torso CT scans in different phases from a local dataset. The results obtained by the method demonstrate that the method is promising in segmenting and classifying bones of torso from any phase of CT.

Poster Session P7-3-1

Accuracy of Narrow Band Imaging in Conjunction with White Light by Thoracoscopy for Detection of Disseminated Thoracic Endometriosis in Patients of Catamenial Pneumothorax

Teruaki Mizobuchi¹, Masatoshi Kurihara¹, Sumitaka Yamanaka¹, Hiroki Ebana²

1. Nissan Kohseikai Tamagawa Hospital, Japan
2. Division of Respiratory Medicine, Juntendo University, Faculty of Medicine and Graduate School of Medicine, Japan

Purpose: Thoracic endometriosis (TE) is defined as the presence of normal endometrial tissue abnormally implanted in the thoracic cavity. Clinical manifestations of TE syndrome include catamenial pneumothorax, which are synchronized with the menstrual cycle. The purpose of this study was to investigate the ability of narrow band imaging (NBI) in conjunction with standard white light imaging in detecting TE by thoracoscopy.

Methods: The clinical and pathological files of all patients who underwent surgery for spontaneous pneumothorax in Tamagawa Hospital between October 2014 and August 2015 were retrospectively reviewed. The patients pathologically diagnosed with TE were included. Signs of TE were observed with both NBI and white light imaging by careful examination of the visceral and parietal pleura, and the diaphragm was systemically inspected to search for holes and/or endometrial implants. Blebs, bullae and brown nodules of the visceral pleura were resected; lesions in the parietal pleura were removed by limited parietal pleurectomy; the diaphragm was partially resected and repaired.

Results: Twenty seven women were evaluated. TE was suspected at 29 lesions in 27 patients on the diaphragm, 28 lesions in 20 patients on the visceral pleura and 35 lesions in 24 patients on the parietal pleura. Endometrial tissue was pathologically confirmed in 29 of 29 (100 %) on the resected diaphragm, 17 of 28 (60.7 %) on the resected lung, 21 of 35 (60.0 %) on the resected parietal pleura.

Conclusions: The additional use of NBI with white light imaging seemed to be feasible; nevertheless, the prospective study was necessary.

Poster Session P7-3-2

A CASE PULMONARY ARTERIOVENOUS MALFORMATION

Mehmet Oncu

Dresra Bilgi, Turkey

Pulmonary arteriovenous malformations (PAVM's) are rare vascular anomalies of the lung in which abnormal dilated vessels provide a right -to- left shunt between the pulmonary arter and vein. There is recognized female predilection with F:M ratios ranging around 1.5 to 1.8. The estimated incidence is thought to be around 2-3 per 100.000.

METHOD

A 35 year old woman was admitted to hospital due to recurrent hemoptysis and dyspnea which last 21 days.

The Chest P-A revealed right lower lobe oval uniform opacity. The chest CT showed in right middle lobe PAVM diameter of 5 cm feeding artery was the branch of the right pulmonary arter and drainage veins were branches of right middle pulmonary vein.

RESULTS

Thorax ct angiography showed bilateral multiple oval uniform lesinons .The biggest lezyon was right middle lobe and diameter 5 cm. lesions revealed feeding artery and drainage veins. It was thought to be consisted with the lesions of pulmonary arteriovenous fistula.

DISCUSSION

PAVM's are 4 four main forms:

- A single fistula
 - Multiple discrete fistulas with one or a few predominant lesions
 - Multiple discrete fistulas of a similar size
 - Diffuse telengectasia -%50 of congenital cases have hereditary haemorrhagic (osler -weber-rendu disease)
- Treatment options include trans- catheter coil embolisation surgery once successfully treatment (embolotherapy , surgical resection) prognosis is generally good for an individual lesion. Possible imaging differential considerations includ abnormal systemic vessels. These are highly vascular parenchymal mass, other congenital or acquired pulmonary arterial or venous lesions (e.g. pulmonary varix)

Poster Session P7-3-3

Pulmonary Agenesis Diagnosed in mid-age

Cagatay Bolgen

Murat Gedikoglu, Turkey

Pulmonary aplasia,agenesis,hypoplasia is a rare bronchopulmonary malformation associated pulmonary or other organ anomalies. A certain confusion has arisen from the loose usage of terms. It would be advisable to use the term agenesis for a failure of development, aplasia for incomplete development. Scheneider has classified as; true agenesis with no trace of lung, bronchus, vessels on affected side; a type characterized by small outpocketing from the trachea with a rudimentary bronchus with no pulmonary tissue; a type in which fully formed bronchus is present ending in a mass of areolar tissue. Pulmonary agenesis is rarely seen in adults, the one with no associated additional anomalies live through delayed age. We present a case of pulmonary agenesis diagnosed in 48 years old.

A 48 year old women was admitted with 5 years dyspnea increasing with effort. She was asymptomatic in rest, has no comorbidities, family history, is non-smoker. Examination revealed decreased movement of right hemithorax, impaired percussion note in right basal lung and bronchial breath sound on right scapula, crackles on left lower lung. Chest X-ray showed homogeneous density in right hemithorax. Pulmonary function test revealed FEV1/FVC 54 %, FEV1 17% (0.42 L), PEF 22 %. CT scan showed absence of right lung, rudimentary airways and vessels, compensatuary hyperaeration in left lung, herniation to right, shifting of the mediastinal structures toward posterior of the left lung, 7mm pleural effusion in left, bronchiectasis in basal segments of the left lower lobe. Echocardiography showed right spaces in border limites, left ventricular wall thickness and function was normal, minimal decrease in right ventricular functions. No additional anomalies was detected. Patient was diagnosed as unilateral pulmonary agenesis depending on her present clinical and radiological findings.

Poster Session P7-3-4

Effects of weight loss therapy on respiratory system impedance in obese adults

Etsuhiro Nikkuni, Ritsuko Arakawa, Keita Kiuchi, Shinya Ookouchi, Toshiya Irokawa, Hiromasa Ogawa, Hajime Kurosawa

Department of Occupational Health Tohoku University Graduate School of Medicine, Japan

The obese subject has pulmonary functional decline with weight gain. In addition, it increases respiratory resistance. However, respiratory system resistance (Rrs) and reactance (Xrs) during weight loss therapy are not well known. A purpose of this study is to examine the influence that weight loss therapy gives to a pulmonary function on obese patient. R5 (Rrs at 5Hz), R20, and X5 were assessed in 21 obese patients (M:F=14:7, Age:39.4±13.2, BMI:45.7±10.8kg/m²) using a commercialized FOT apparatus (MostGraph-01, Chest MI, Inc, Tokyo, Japan). Vital capacity (VC) and expiratory reserve volume (ERV) were assessed using a conventional spirometry (HI-801, Chest MI, Inc, Tokyo, Japan). X5 before the weight loss therapy accepted significantly negative correlation with body weight and BMI, waist. By 4 weeks weight loss therapy, all subjects were retested (BMI:43.3 ±10.3kg/m²). The average value of R5 and R20 showed not significant. The average value of X5 showed significantly less negative than before weight loss therapy (before : -0.92±0.49 cmH₂O/L/s vs after: -0.75±0.44 cmH₂O/L/s, p<0.001). Although VC (before: 3.79±1.01 L vs after: 3.92±1.00 L, p<0.005) and ERV (before: 0.75±0.59 L vs after: 1.02±0.66 L, p<0.001) showed significant increasing by weight loss. These results suggest that the weight loss therapy for the obese patients showed a change to the lung volume and Xrs.

Poster Session P7-4-1

Long-term pulmonary complications of sulfur mustard exposure in former workers of poison gas factory

Yoshifumi Nishimura^{1,2}, Hiroshi Iwamoto¹, Nobuhisa Ishikawa³, Noboru Hattori¹, Hironobu Hamada⁴, Yasushi Horimasu¹, Shinichiro Ohshimo⁵, Kazunori Fujitaka¹, Keiichi Kondo², Kazuo Awai⁶, Nobuoki Kohno¹

1. Department of Molecular and Internal Medicine, Graduate School of Biomedical and Health Sciences, Hiroshima University, Japan

2. Tadanoumi Hospital, Japan

3. Department of Internal Medicine, Hiroshima Prefectural Hospital, Japan

4. Department of Physical Analysis and Therapeutic Sciences, Graduate School of Biomedical and Health Sciences, Hiroshima University, Japan

5. Department of Emergency and Critical Care Medicine, Hiroshima University, Japan

6. Department of Diagnostic Radiology, Institute of Biomedical Health and Sciences, Hiroshima University, Japan

Background Sulfur mustard (SM) is a vesicating chemical warfare agent, which can cause skin blistering and chronic lung complications. Chest CT findings have not been investigated among the long-term survivors of the former workers of the poison gas factory in Japan. The factory was in operation from 1929 to 1945, and SM was the main product. **Methods** Chest CT findings were evaluated in 317 long-term survivors of the poison gas workers from 2009 to 2012. We also investigated the associations between each CT finding and acute skin lesions. Skin lesions, such as blisters and erosions, were used to define significant exposure to SM. **Results** Of the 317 subjects, 45 (14%) had skin lesions in the poison gas factory. By the chest CT scan, 164 subjects (52%) had abnormal findings. Emphysema was the most common finding, occurring in 22% of all the subjects. Multivariate analyses showed significant associations between presence of emphysema and skin lesions ($p = 0.006$) independently of type of job and duration of work in the poison gas factory and background demographics. Moreover, never-smokers who had had skin lesions ($n = 21$) showed significantly higher rate of emphysema when compared with never-smokers without skin lesions ($n = 182$) (33% vs. 6%, $p = 0.001$). **Conclusions** In the long-term survivors of mustard gas workers, emphysema was common even in never smokers who had exposed to SM as defined by skin lesions in the poison gas factory. The present results indicate that SM exposure could cause late complication of emphysema.

Poster Session P7-4-2

Experience of IgG4-related thoracic diseases on F-18-FDG PET/CT in our institute

Kazuyoshi Suga, Yasuhiko Kawakami, Ayami Shimizu

Department of Radiology, St. Hill Hospital, Japan

Purpose: Systemic IgG4-related disease can occur in the thorax. FDG PET/CT may be a useful tool for detection and diagnosis of thoracic involvement of this FDG-avid disease.

Materials and Methods: The incidence and morphologic feature of thoracic involvement were evaluated in a total of 15 patients with IgG4-related disease, who had undergone FDG PET/CT during the past 5 years in our institute.

Results; Thoracic involvement with FDG uptake was seen in 10 (66.6%) of 15 patients. Radiographic manifestation of thoracic involvement was various, including lymphadenopathy, diffuse or focal reticular opacities in the lower lung field, nodular or mass lesions, thickening of bronchovascular bands or interlobular septa, pleural effusion or pleuritis, and consolidation of subpleural area or bronchovascular band. Thoracic involvement appeared to occur along lymphatic system.

Conclusion; The incidence of thoracic involvement seems to be rather high. Systemic FDG PET/CT scanning is useful for detecting multiple involved organs including the thorax, and may contribute to the comprehensive diagnosis of this disease. A wide variety of manifestation of thoracic involvement of this disease should be noted.

Poster Session P7-4-3

A case with rheumatoid arthritis who presented wheezes and methotrexate-associated lymphoproliferative disorder

Mariko Kinoshita¹, Hirokazu Sakasegawa¹, Takashi Esaki¹, Mika Ohsumi¹, Yuta Koizumi¹, Yusuke Tanaka¹, Shoki Ro¹, Naoya Sugimoto¹, Hisanao Yoshihara¹, Michio Kuramochi¹, Hidenori Arai¹, Hiroyuki Nagase¹, Masafumi Kawamura², Masao Yamaguchi¹, Ken Ohta^{1,3}

1. Division of Respiratory Medicine and Allergology, Department of Medicine, Teikyo University School of Medicine, Japan

2. Department of Surgery, Teikyo University School of Medicine, Japan

3. National Hospital Organization Tokyo National Hospital, Japan

A 70-year-old woman was admitted to our hospital for evaluation of wheezes and a nodular lesion in her left lung field. She was diagnosed with rheumatoid arthritis (RA) at 45 years old, and was treated with methotrexate (MTX) at 8 mg/week. Seven months before admission, dyspnea on exertion occurred and gradually worsened. Lung function test showed obstructive impairment (FEV1 0.77L, FEV1% 43.5%); airway reversibility using b2 agonist inhalation was absent. Chest X-ray and CT images demonstrated a left upper lobe tumor (2.5 cm in diameter), and bilateral hilar and mediastinal lymphadenopathy, all of which demonstrated obvious PET uptake. Bronchoscopy was performed, and aspiration cytology of a lymph node showed atypical lymphocytes (class 3). Serum sIL-2R was markedly increased (1898 U/ml). Since lymphoproliferative disorder (LPD) was suspected, MTX was discontinued. Thereafter, lung tumor got smaller, and finally disappeared, indicating the diagnosis of MTX-associated LPD. Wheezes also disappeared, in parallel with improvement of thickening of bronchial walls on CT images; thus, wheezes were thought as a manifestation of her LPD. In patients with lung tumor(s) plus RA treated with MTX, MTX-associated LPD should be carefully differentiated from other malignancies since it is usually self-limited and needs watching for diagnosis with caution.

IgG4-related thoracic disease: report of two cases

Fumiyasu Tsushima, Ono Shuichi, Tamaki Fujita, Hiromasa Fujita, Shinya Kakehata, Hiroko Seino, Hiroyuki Miura, Yoshihiro Takai

Department of Radiology, Hirosaki University School of Medicine, Japan

We report 2 cases with IgG4-related thoracic disease that were difficult to diagnose with diagnostic imaging. Case 1: A 60-year-old man consulted our hospital with chief complaints of dry mouth and fatigability. His CT images showed multiple ground glass opacities and consolidation in both lungs. High RI uptake was noted for both lesions on exploration by FDG-PET/CT. A VATS biopsy was performed and the lesion was diagnosed as IgG4-related lung disease.

Case 2: A 70-year-old man had cough. His chest CT revealed diffuse reticulonodular shadow and lymph node(LN) swelling. A soft tissue mass was showed in the right posterior mediastinum. With high RI uptake on FDG-PET/CT, LN biopsy was performed and it was diagnosed as IgG4-related disease.

As for imaging features of pulmonary lesions on CT, the following types are reported : 1) solid nodular type presenting as solitary nodular opacities, 2) round ground glass opacity type presenting as ground glass-like opacities with relatively discrete margins, 3) alveolar interstitial type presenting as honeycomb lung opacities reminiscent of so-called pulmonary fibrosis, and 4) bronchovascular type presenting as lesions extending along bronchial vascular bundles. In this presentation, we will report these two cases in detail and discuss with previous literature.